

A STUDY OF FLAME SPREAD OVER
CELLULOSIC SURFACES.

A THESIS SUBMITTED FOR THE DEGREE OF
DOCTOR OF PHILOSOPHY.

By J. B. Stott.
Under the direction of
J. E. Garside Ph. D.

June 1949.

TABLE of CONTENTS

	Page No.
List of Diagrams	
Preface	1
The Object of the Work and the Results achieved	4
Part I The Effect of Specific Surface on the rate of Spread of Flame over Solids	6
(A) Unsupported Combustion	6
(B) Supported Combustion	16
Appendix I	25
Appendix II	32
<hr/>	
Part II Flame Spread over a Single Solid Surface - Introduction	37
(A) Preliminary Experiments	42
a Physical Constants	50
(B) Heat Transfer During Circular Spread - Apparatus	58
Experimental procedure	78
The final calculation of the heat Transfers taking place as the wood is burnt	96
Experimental Conditions	124
Results and Observations	127
Discussion	136
Conclusions and Suggestions for Further work	142
Acknowledgments	
Bibliography	

LIST OF DIAGRAMS

<u>Figure No.</u>		<u>Opposite Page No.</u>
1.	Shape of standard test piece	11
2.	Normal type of burning	11
3.	The distance covered by the flame in a given time.	13
4.	Abnormal type of burning	13
5.	Variation of rate of spread with reciprocal thickness.	16
6.	Variation of rate of spread with specific surface.	18
7.	Effect of specific surface of Kraft papers on the rate of spread.	17
8.	Construction of electric radiator	17
9.	Effect of radiation intensity on rate of spread.	20
10.	Effect of specific surface on the rate of spread at a constant radiation intensity.	20
11.	Construction of the black body calibration furnace.	25
12.	Response of thermopile to black body radiation.	25
13.	The variation with distance from the radiator of the radiation.	29
14.	The thermopile response at different distances from the radiator.	29
15.	Thermopile calibration curves.	30
16.	The radiation from a bar to a small element of area.	30
17.	Angle subtended by radiator element	33
18.	Angle subtended by refractory	33

<u>Figure No.</u>		<u>Opposite Page No.</u>
19.	The effect of prolonged radiation intensity on the rate of spread.	44
20.	The effect of radiation on the rate of spread over four timbers.	44
21.	The relative positions of the camera, radiator and wood.	45
22.	A typical trace of the burnt area of wood.	48
23.	Photograph of the burning wood.	48
24.	The average radius of the burning area at different times.	49
25.	The variation of the circular rate of spread with varying radiation intensity.	49
26.	The construction of the radiator and the support for the wood.	59
27.	The construction of the bolometer housing.	64
28.	The bolometer sweep mechanism.	65
29.	The load line diagram.	65
30.	Amplification circuit with cathode resistance.	71
31.	Push-pull amplification circuit.	71
32.	Two stage amplifier circuit.	72
33.	The amplifier power pack.	73
34.	General wiring diagram.	75
35.	Bolometer bridge circuit.	76
36.	The gearing of the bolometer sweep and rotary switch.	77
37.	Plan of rotating drum camera and drive	78
38.	General View of rotating drum camera	79

<u>Figure No.</u>		<u>Opposite Page No.</u>
39.	Print of a typical cathode ray trace.	80
40.	The input and calibration circuit to the amplifier.	81
41.	Response curve of the amplifier and cathode ray tube.	81
42.	The bolometer response to black body radiation.	86
43.	The bolometer response at high radiation intensities.	86
44.	Calculated radiation intensity from the three bar radiator.	91
45.	Integration over the hemispherical surface.	91
46.	Cathode ray trace of extraneous radiation.	95
47.	The extraneous radiation as a function of the bolometer angle.	95
48.	The variation of radiation intensity from burning wood as measured by the bolometer.	97
49.	The variation of radiation intensity from burning wood at a constant bolometer angle with time.	97
50.	Graphical integration of the radiation over a hemispherical surface.	99
51.	Temperatures in burning birch	99
52.	Temperature gradients in wood heated by radiation.	105
53.	Temperature gradients in burning birch.	105
54.	Temperature gradients used to find the heat content of a birch specimen.	111
55.	Summation of the heat conducted into a birch specimen.	111

<u>Figure No.</u>		<u>Opposite Page No.</u>
56.	Summary of the heat transfers in burning birch timber.	128
57.	The differential thermal analysis of birch wood.	128
58.	Temperatures in burning air dried birch.	131
59.	The radiation from a piece of burning birch presented as a polar diagram.	132
60.	The rates of spread at different radiation intensities.	133
61.	The rates of spread as a function of radiation intensity x the initial surface temperature.	133
62.	The heat evolved per unit area of surface during the burning time at different rates of spread.	134
63.	The relationship between the average length of burning zone, depth of combustion and the average amount of reactant.	140
64.	Suggested further experiments.	140

PREFACE

The profound changes which take place when the temperature of cellulose is raised have been the subject of extensive researches over a considerable period. Much of this work has been concerned with the products of distillation when wood is heated in the absence of air, and in view of the importance of wood as building material, its physical constants pertaining to heat transfer have been determined for many species. Later, for similar reasons, the results of the above researches were examined in order to determine how far they could be used to assess the risk of fire arising in structures containing wood and other cellulosic materials, and tests were developed to determine the susceptibility to continued heating of woods of different species subjected to various forms of chemical treatment. Other tests were also devised to measure their relative tendency to ignition by various sources and as a result of these tests effective methods of reducing the ignition tendency were developed in which the wood was impregnated with various chemical solutions.

The mechanism of prolonged burning originating on a plane wooden surface of infinite extent has been thoroughly investigated by Bamford and his collaborators. By correlating the dependence

on temperature of the rate of destruction of wood and the heat transfer at the burning surface, these authors developed an equation which describes the progress of the burning reaction into the body of the wood.

Much of the data accumulated in the above researches bear directly on calculations of the rate at which flame spreads over the surface of wood, and this rate is of great importance both in the initial stages and also during the further growth of fires.

That the linear rate of spread of flame over the surface of wood was constant under fixed conditions was pointed out by Professor G.I. Finch, who introduced the concept of the fire growth constant as a measure of the area rate of spread which was said to be proportional to the square of time. From 11.12. previous experiments it appeared that many factors influenced the rate of fire growth, the more obvious ones being moisture content, configuration, disposition, temperature and species. When the problem is approached from a more fundamental standpoint, it is clear that for a given rate of flame travel, the heat from the flame together with any supporting heat must be capable of distilling sufficient volatiles from the wood to maintain the flame at its original size. Thus the factors determining the rate of spread will be (a) the heat transfer coefficients from the flame to the surface of the wood and into the body of the wood, and (b) the constants which determine the rate of

decomposition of wood at different temperatures. It was held by Professor Finch that at a constant moisture content the rate of spread was largely determined by the quantity "specific surface" defined as the area of surface effectively exposed to the air and flame per unit weight of wood. It was further pointed out that the effective surface would be different for different modes of heat transfer from the flame to the wood.

Using this concept it was possible to assign numerical values of specific surface to three main groups of inflammable materials - tinder, kindling and bulk fuel assuming that the surface exposed to the air had no micro-structure. Thus, for flame propagation, the specific surface of tinder such as wood shavings, paper etc. must be greater than 20 sq.cms.per gram, whilst with some materials such as petrol/air mixtures, much higher values of effective specific surface are realised.

Kindling being small wooden chips, light furniture etc., has a specific surface of between 20 and 2 sq.cms./gram, and can be ignited by tinder but not by a match flame.

Bulk fuel comprises the rest of the heavier inflammable material with a specific surface of less than 2 sq.cms/gram, but is capable of ignition by a quantity of kindling.

Largely as a result of deliberations on the above arguments during meetings of the Incendiary Bomb Test Panel from 1943/45, work was initiated at Leeds in order to determine the fire

growth constant mentioned above under the fixed conditions which might apply in full scale buildings. Preliminary experiments were made by Garside and Whitehead during 1944 and this thesis is based upon work carried out by the author after that time.

The object of the work and the results achieved.

The initial object was to determine the fire growth constant for cellulose sheets of various specific surface under controlled conditions of other variables. This was achieved, the effect of supporting radiation observed, and practical evidence produced that the area rate of growth was proportional to T^2 .

As a result of considerations of this work it became apparent that the term "effectively exposed surface" was so loose as to have little practical value unless some measure was found of what was and was not effective. In other words it was necessary to determine exactly what proportion of the heat evolved was transferred into the body of the wood, and also what part of that heat was effective in the further distillation of volatiles from the surface. Consequently further work was directed towards determining the nature of the dynamic heat balance obtaining when flame spreads over a wooden surface. There are a great many factors involved in the heat transfer from flames to solids, some of which cannot be measured under conditions such as are being discussed. Theoretically if the

shape, temperature and composition of the flame are known, it should be possible to calculate the heat transferred to the wooden surface. Unfortunately the shape of the flame does not compare approximately to the configurations quoted in the standard literature on the subject, whilst both the temperature and composition of the flame vary from place to place, in a manner not known.

However, by measuring certain quantities more amenable to experimentation, it has been found possible to deduce

- a) the amount of heat absorbed by the body of the wood,
- b) the amount of heat radiated by the flame and hot burning wood, and
- c) a relationship which describes the rate of spread of flame in terms of the physical constants of the material in question, the rate constants of the chemical reactions taking place in the wood during distillation and certain other factors determined from the results.

It is hoped that relationship (c) will eventually make possible the calculation of the rate of spread of flame over any dry wooden surface exposed to air, from a knowledge of the appropriate physical and chemical constants involved.

THE EFFECT OF SPECIFIC SURFACE ON THE RATE OF
SPREAD OF FLAME OVER SOLIDS

Part 1.

INTRODUCTION

In order that a flame may continue as such in any medium it must satisfy a condition which applies to all sustained chemical reactions, namely that the energy liberated by the reaction plus any external energy received from the surroundings must be sufficient to maintain the reaction at its normal rate. In the case of a flame burning upon the surface of a solid, the heat generated both by the burning gases originally evolved from the surface of the material and by any reactions taking place in the body of the wood would be sufficient, under the prevailing conditions of heat transfer, to distil the volatiles from the solid surface at a rate sufficient to maintain the supply of inflammable gases. For cellulosic material burning upon an upper horizontal face, the above condition does not always hold, in which case energy must be supplied from an additional source if the flame is to propagate. If the material be sufficiently thin, however, flames burning upon both upper and lower horizontal surfaces will in general supply enough heat to one another to maintain combustion, provided that the surfaces are not separated by too great a thickness of material. The critical thickness at which a flame will only

just propagate by itself has been termed the limiting thickness.

From the above it should follow that energy applied from an external source to a flame should increase its rate of travel and it was originally suggested by Professor Finch that the rate of spread should be measured first without and then with a supporting source of heat. In both cases it was decided to investigate only those flames capable of self propagation, so that hence it was necessary that the material employed should not exceed a certain limiting thickness, and paper was chosen as a representative cellulosic material obtainable in sheet form over a wide range of suitable thicknesses.

Since the investigation was concerned in the main with the effect of specific surface upon flame spread, other contributory variables had to be kept as nearly as possible constant. Amongst several factors which might introduce alterations in the rate of spread, may be mentioned moisture content, variable char formation, and changing heat transfer coefficients caused largely by draughts. Furthermore, a choice had to be made between the two possible directions of flame propagation, horizontal or vertical. Preliminary experiments carried out by J.F.Garside and A.B.Whitehead at Leeds, had shown that the technique of measuring vertical flame speed was much more difficult than horizontal methods because of the high rates and ill defined flame fronts of upward spread and the extremely low

rates of spread downwards. The present investigation has therefore been carried out entirely on horizontal surfaces.

It was also necessary to decide whether the flame front should be made to advance as a straight line or as the circumference of a circle. Measurements of the rate of circular flame spread from a point source were found to be complicated by the contraction and breaking of the ash behind and within the flame front as well as by changes in heat transfer coefficients with increasing radius of the flame - an effect which seemed to be mainly due to convection currents. For, considering the small length s of circular flame front of radius r and a strip of unburnt material of width r directly in front of s , it will be seen that as r increases the constant length of flame has to heat up a smaller area of unburnt material equal to

$$\left[\pi (r + \delta r)^2 - \pi r^2 \right] \times \frac{\delta s}{2\pi r} = \frac{\delta s \delta r}{2} \left(2 + \frac{\delta r}{r} \right)$$

hence this effect should show itself only when δr is comparable with r . Considering however, the radiation received by a small length of flame front δl from another small length of flame front dl on the circumference of the circle, this is equal to

$$\frac{I dl \delta l \cos^2 \theta}{2D^2}$$

where $2D$ is the distance between the small elements dl and δl and θ is the angle between their normals and the line joining them. Now since $\frac{dl}{dr} = d\theta$ and $\frac{D}{r} = \cos \theta$ the radiation from dl

to δl is given by $\frac{I \delta l}{4r} d\theta$ and on integrating between

$-\frac{\pi}{2}$ to $+\frac{\pi}{2}$ this becomes $\frac{\pi I \delta l}{4r}$, from which it will be

seen that the supporting radiation decreases as r increases.

The above two effects are in opposition. A small number of experiments were made using sheets of paper about 25 cm square held horizontally along opposite edges by two metal clamps.

Ignition was effected by a small pilot flame applied to a 1 cm hole at the centre of the paper. Before ignition the glass tube maintaining the flame passed vertically through the hole in the paper with its open end 3 cm above the surface of the paper and the paper was lit by dropping the end of the tube $\frac{1}{4}$ " below the paper. The rate of spread was measured between a number of concentric circles previously drawn on the paper. In two cases tried as preliminary experiments however, it was found that the circular rate of spread was considerably greater than the linear rate of spread over the distance measured, i.e. up to approximately 7 cm.

	<u>Linear rate of spread</u>	<u>Circular rate = of spread</u>
Ellam's duplicating paper	0.50	0.86
Whatman's B Cap 15	0.32	0.39

which seemed to suggest that either the supporting radiation effect was considerable or else that there was a chimney effect due to the hole burnt in the centre of the paper, air coming up through this hole expanding and sweeping the flame forward.

Hence it was decided to restrict the experiments to those in which the flame advanced over the surface of the paper as an approximate straight line, precautions being taken to avoid draughts.

Apparatus and Procedure: (Part A)

The materials used were selected from a wide range of Whatman filter papers and some Kraft papers kindly supplied by the Printing and Allied Trades Research Association; in one case sheet balsa wood was used and all the samples had been stored for several months before use in a room of reasonably constant temperature and humidity.

A standard test piece of the shape and size shown in Figure 1 was used throughout this work and had the following advantages:-

(1) it could be held horizontally, whatever the thickness of the sample, if supported at one end and given a slight upward concavity (v. Figures 2 and 3);

(11) when the paper was ignited at the point the resultant flame front always advanced linearly;

and

(111) edge effects were negligible, increasing the width of the test-piece from 4 cm to 8 cm having no effect upon the rate of flame spread. Therefore it seemed unlikely that any variation in heat transfer at the edges of the strip with different papers would have an appreciable effect.

The test-piece was clamped horizontally 4.5 cm. above bench

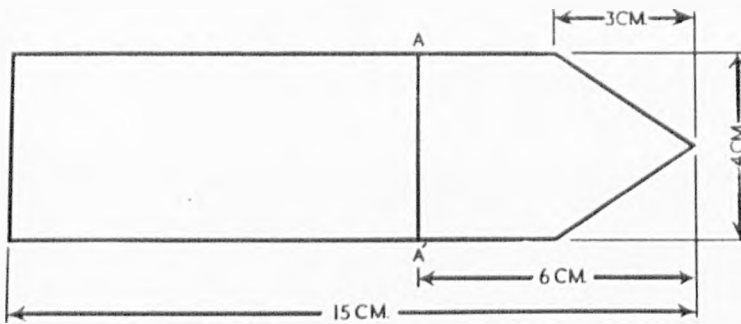


Figure 1.
Shape of standard test piece.

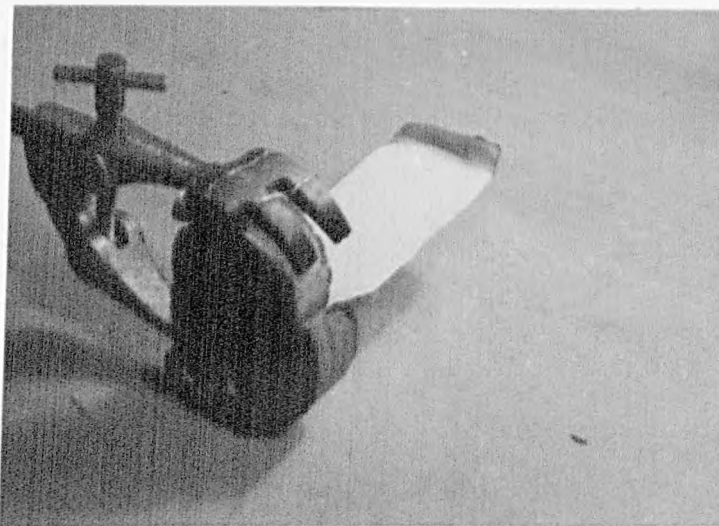


Figure 2.
Normal type of burning

level, as shown in Figure 2, and was ignited at the pointed end. The time taken for the flame to travel between the datum line AA' (Figure 1) and a parallel line drawn a known distance from AA' was measured with a stop-watch reading to one-fifth of a second. In this way, readings were obtained in respect of four distances of flame travel, namely 1.5, 3.0, 4.5 and 6.0 cm. respectively, the results pertaining to any one distance being obtained in triplicate.

Table 1

Rate of linear flame spread on Kraft 009 W papers.

Distance travelled by flame (cms.)	Time (seconds)	Average time (seconds)	Thickness (cms.)
	5.9		0.0218
1.5	6.0	6.5	.0213
	7.6		0.0216
	12.2		0 .0216
3.0	14.6	13.3	.0223
	13.1		.0221
	20.4		.0213
4.5	18.0	19.1	.0221
	19.0		.0221
	24.6		.0221
6.0	23.3	24.2	.0223
	24.8		.0218

Thus, for each sample of paper, twelve readings were taken altogether, which were plotted subsequently as a distance-time graph, the slope of which was a measure of the rate of flame spread. Such graphs as the typical example shown in Figure 3 always took the form of good straight lines passing through the origin, thus confirming that a constant rate of flame spread was in fact obtained.

The average thickness of each test-piece was measured using a micrometer, and the apparent density found from the actual weight and calculated volume. Specific surface was then calculated as surface area of the test-piece per unit weight (neglecting edges).

The investigation as a whole covered a range of specific surfaces between 6 and 250 $\frac{\text{cm.}^2}{\text{gram}}$. The lower values of specific surface were achieved by bonding together, with starch solution, several sheets of Kraft paper and pressing until dry.

Observations

In general the several papers burnt with a flame of apparently identical characteristics; it was semi-luminous, almost smokeless, and some 3 cm. high. In most instances flame movement caused the paper to bend upwards slightly behind the flame front, the actual area of combustion occupying a strip about 0.5 cm. wide across the test-piece, the position of the flame front itself being clearly marked by a sharp line of discoloration. The latter was not perfectly linear, but bow-

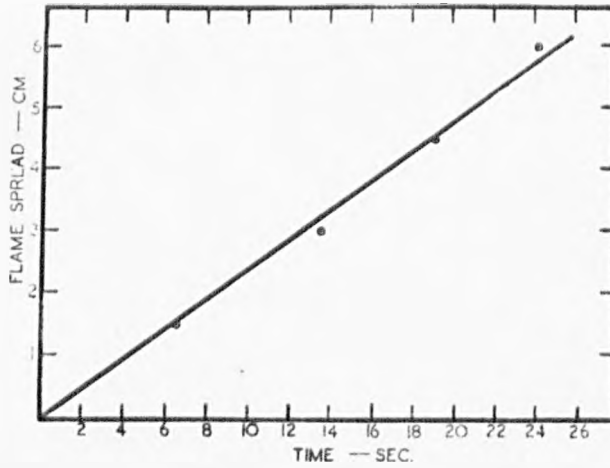


Figure B .
The distance covered by the flame
in a given time.

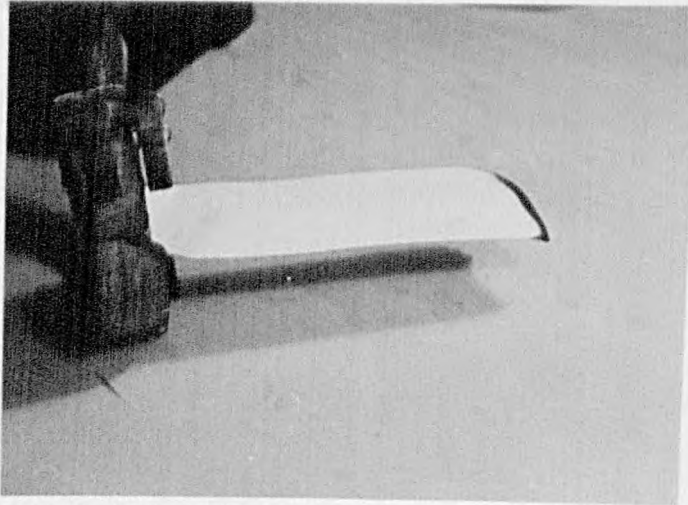


Figure 4.
Abnormal type of burning.

shaped, being advanced approximately 3 mm. at its centre and edges. In practice the speed of the central protusion was that measured.

With some of the thinner paper, however, there occurred what appeared to be a contraction of the partly-burnt paper or ash in the vicinity of the flame front, which produced curvature in the longitudinal plane of the paper, and the sign of the curvature was dependent apparently upon that of the tip itself at the instant of its ignition. Generally the tip was bent slightly upwards before ignition, and the subsequent contraction upon ignition resulted in an upward curvature which produced the type of flame described in the preceding paragraph. On the other hand, if ignition induced a downward curvature, the area of combustion was widened appreciably, the flame itself was larger, and the rate of spread was increased, effects which may be attributed to the fact that under such circumstances the flame was travelling uphill with consequent greater heat transfer from it to the unburnt paper. It was possible always to avoid such anomalous results, however, by bending the tip of the test-piece upwards slightly at the start of each experiment when the more usual type of combustion and a constant rate of flame travel ensued.

The surface characteristics of the Whatman filter papers varied greatly. Thus whereas some papers possessed a smooth surface, even to the extent of a slight glaze in extreme cases, others were rough, their surfaces being characterized by small

hillocks some 0.1 cm. across and a few thousandths of a cm. high. Yet again, certain papers exhibited a hairy appearance, due to the projection of many fibres from the surface. An attempt to correlate surface characteristics with the rates of flame spread was unsuccessful, largely because gradual variation in the characteristics of the papers used prevented their strict classification.

Finally it might be supposed that the rate of spread of flame over the surface of paper would be affected to some extent by the direction of the grain of the latter. Experiments in which samples were burnt along and across the grain however, showed no measurable difference in rate of flame travel.

Results

Results were obtained in respect of 34 different papers and one species of wood, namely balsa, and are tabulated below.

TABLE 2

Type of Paper	Rate of Flame Spread	Specific Surface	Reciprocal Thickness
	cm/sec.	cm. ² /gm.	cm. ⁻¹
Kraft 030W	0.10	30	14
" 016W	0.14	39	24
" 009W	0.23	65	46
" 36 lb/D.C	0.40	114	69
" 26½lb/D.C.	0.53	161	94
" 16 lb/D.C	0.91	255	196

Table 2 (Contd.)

Type of Paper	Rate of Flame Spread	Specific Surface	Reciprocal Thickness
Whatman B Imp.140	0.09	30	23
" B Imp.90	0.15	51	35
" B Imp.72	0.16	55	42
" 15	0.21	70	34
" B Med. 34	0.24	74	45
" 5	0.28	94	49
" 2	0.28	107	64
" 541	0.29	127	59
" 52	0.29	99	65
" 32	0.29	103	56
" 540	0.30	102	69
" 1	0.30	113	61
" B Cap.15	0.32	100	66
" 531	0.33	124	63
" 530	0.34	111	71
" 542	0.34	96	66
" 4	0.36	91	50
" 31	0.37	115	44
" 7	0.37	123	49
" 54	0.37	97	58
" 50	0.37	102	92
" 30	0.38	123	49
" 42	0.38	98	51

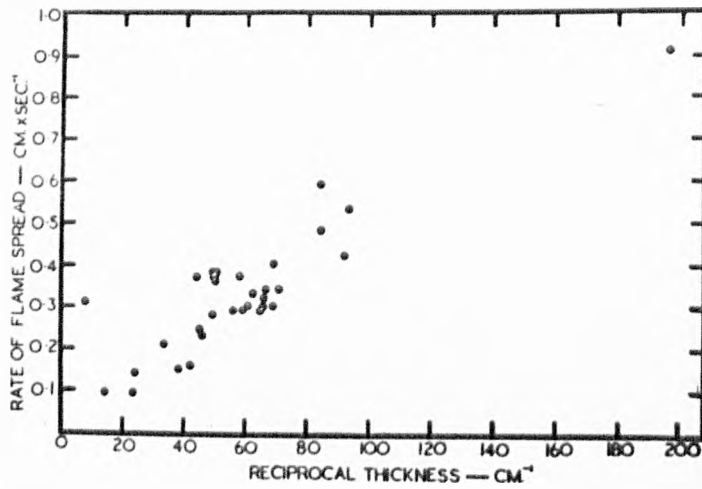


Figure 5.
Variation of rate of spread with
reciprocal thickness

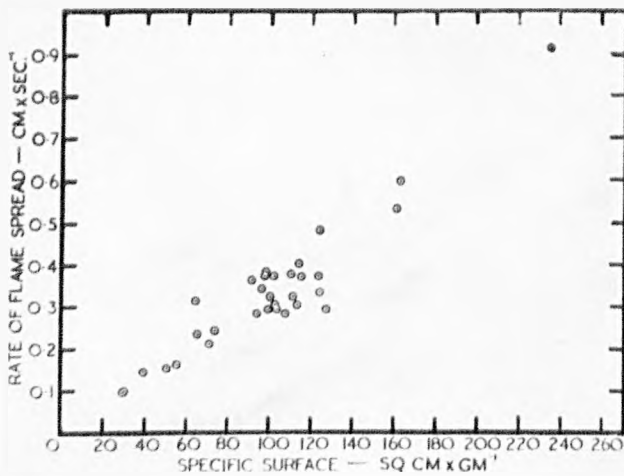


Figure 6.
Variation of rate of spread with
specific surface.

Table 2 (Contd.)

Type of Paper	Rate of Flame Spread	Specific Surface	Reciprocal Thickness
Whatman 544	0.48	124	84
" 11	0.58	163	84
Balsa Wood	0.31	64	7.1
Kraft 030W(2 sheets)	0.055	15.1	7.0
" (3 ")	0.043	10.0	4.7
" (4 ")	0.023	7.5	3.5

The results are presented graphically in Figure 5, in which the reciprocal thickness of the material has been plotted against the rate of flame spread, and also in Figure 6 as specific surface v. rate of flame spread. Figure 7 represents the results obtained with the Kraft papers alone and emphasises that the rate of flame spread and specific surface are almost exactly proportional when papers all of similar characteristics such as the range of Kraft papers are considered.

B. SUPPORTED COMBUSTION

The previous results in respect of materials burning freely in air, support the view that an important factor in surface flame spread is the ratio of the exposed combustible surface to the quantity of combustible associated with that surface. Further consideration suggests that if the heat transfer from the flame

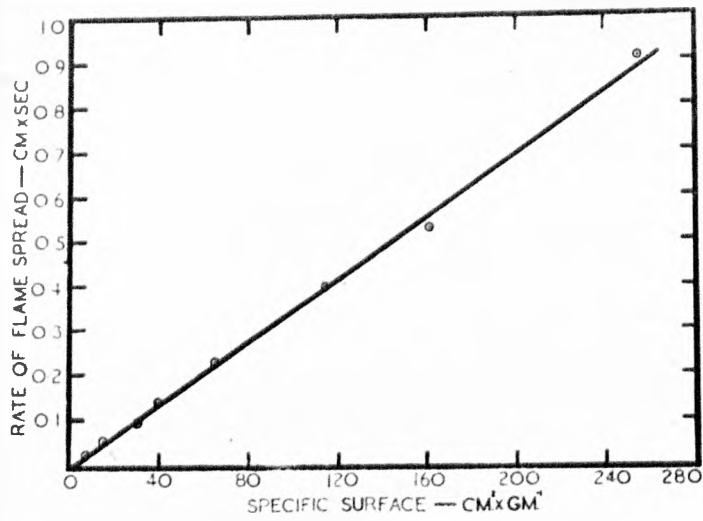


Figure 7.
Effect of specific surface of Kraft papers
on the rate of spread.

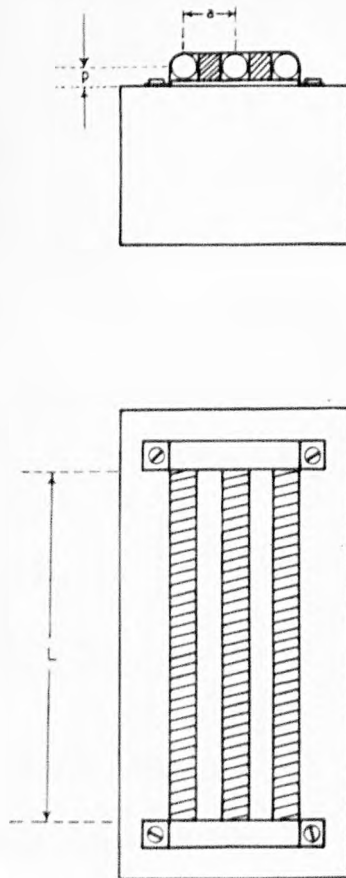


Figure 8.
Construction of electric radiator.

to the unburnt material be increased or decreased, the rate of flame spread should be changed accordingly. Hence, an investigation was commenced in which the combustible surfaces were exposed to external radiation, so as to assess

- (1) the effect of varying irradiation upon the rate of flame travel over the surface of one particular material

and

- (11) the difference in rate of flame travel over a range of materials of varying specific surface when exposed to a constant intensity of external radiation.

Apparatus and Procedure

The source of external radiation was the electric heater shown in Figure 8, consisting of three 600-watt elements backed with firebrick, which gave almost uniform intensity of radiation over the area of the test-piece. The actual radiation was measured by means of a Moll thermopile, calibrated against a black-body furnace. The latter could not be operated at the temperatures necessary to obtain the higher intensities of radiation furnished by the radiator, however; and, as there was some doubt whether the thermopile would register those high values accurately, a direct calculation was made of the radiation intensity at any distance from the radiator, full details of which are given in Appendix I.

The intensity of incident radiation was varied by adjusting the vertical distance between the radiator and the test-piece, which was placed parallel to, and a known distance directly beneath the radiator, precautions being taken to ensure that it received direct radiation only and none reflected from the surroundings. The test-piece was irradiated for 30 seconds before being ignited, after which the rate of flame travel was measured as described above.

Observations

Using paper, the flames appeared to have the same characteristics as before, and advanced almost linearly in most instances. At the higher radiation intensities, however, there was a tendency for 'flash-over' to occur on isolated occasions, i.e. the flame became enlarged suddenly and spread rapidly over a limited zone of the paper, as though distillation of inflammable gases had occurred preferentially there. The phenomenon was restricted to a few experiments only, and the results were abnormal. It would seem that if the rate of travel were measured over a sufficient length of material, these isolated flash-overs would increase the average rate of spread.

It was difficult to assess accurately the time required by the various papers to reach equilibrium temperature under any particular intensity of radiation. In general it appeared that the effects of varying exposures prior to ignition were absorbed in the experimental error, but protracted irradiation caused severe distortion, as well as drying, of the test-piece. The

accepted exposure of 30 seconds was the maximum time compatible with accurate measurement of flame travel.

Results

In the first instance, measurements were made of the fraction of the incident radiation which was transmitted by several Kraft papers. Each paper in turn was interposed between the radiator and the calibrated thermopile, yielding the results given in Table 3.

TABLE 3

Radiation absorbed and reflected by the Papers.

Type of Paper	Percentage Radiation Absorbed and Reflected
Kraft 16 lb/D.C.	71.3
" 26½ lb/D.C.	86.8
" 36 lb/D.C.	91.8
" 009 W	95.8
" 016 W	96.9
" 030 W	98.0

The difference between the incident radiation and that transmitted was taken as the 'radiation absorbed', no correction being applied for the radiation reflected from the paper since it was likely to be constant for the Kraft papers, all of which possessed similar characteristics.

The papers were then subjected to radiation intensities varying between zero and 890 B.Th.U./sq.ft./hr. and the rates of

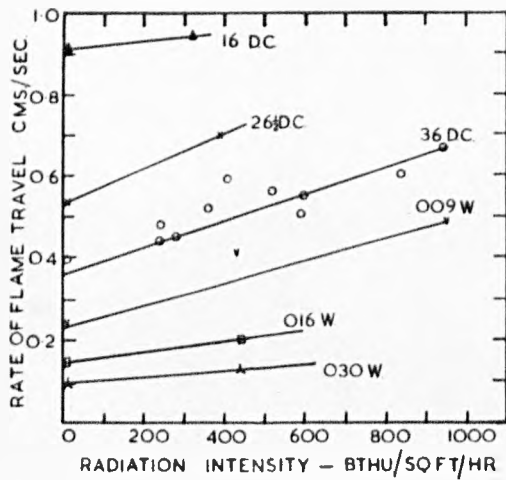


Figure 9.
Effect of radiation intensity on the rate of spread.

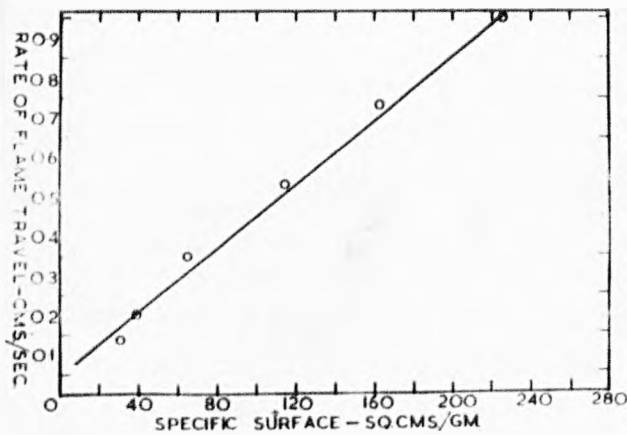


Figure 10.
Effect of specific surface on the rate of spread at a constant radiation intensity.

flame travel over their surfaces were measured. The results are shown in Tables 4 and 5 and also graphically in Figure 9, in which the rate of flame travel has been plotted against 'absorbed radiation'.

TABLE 4

Rate of spread of Kraft 36 D.C. with varying radiation intensities	
Rate cm/sec	Incident Radiation (BTHU/sq.ft./hr.)
0.44	260
0.45	310
0.48	260
0.51	640
0.52	390
0.55	650
0.56	570
0.59	450
0.60	910
0.67	970

TABLE 5

Name of Paper	Rate (cm/sec.)	Absorbed and Reflected Radiation
Kraft 009 W	0.93	2010
" 009 W	0.42	430
" 016 W	0.20	440
" 16 lbs D.C.	0.94	320

Table 5 (contd.)

Name of Paper	Rate (cm/sec.)	Absorbed and Reflected Radiation
Kraft 26½ lbs D.C.	0.70	390
" 030 W	0.13	440

It will be noted that over the range of intensities of radiation covered, the rate of flame travel over Kraft paper 36 lb./D.C. varies proportionately with the quantity of radiation 'absorbed'. Thus it is reasonable to assume a similar proportionality for the other Kraft papers, and straight lines have been drawn between the two experimental points. The constants involved in the relationship between rate of flame travel and 'absorbed' radiation for all papers other than 36 lb/D.C. will, of course, be known with less accuracy.

Finally, Figure 10 has been drawn, using values interpolated from Figure 9 to illustrate the variation of rate of flame travel with specific surface at one particular intensity of radiation.

DISCUSSION

The above results confirm three of the original postulates about which practical confirmation was required

- (I) For all cases the linear rate of spread of flame was found to be constant
- (II) the area rate of flame spread was found to be proportional to T^2 at least over the area measured

and

- (III) the rate of flame spread was found to vary roughly in proportion to specific surface using a wide range of papers (Figure 6) and accurately when using same material in different thicknesses (Figure 7).

In addition the effect of supporting radiation has been

found to increase the rate of fire growth to a considerable degree. When the application of these results to practical problems is considered however, certain anomalies arise which are largely the result of differences in the reaction taking place when wood burns, and these reactions in which specific surface has previously been found to be a determining factor.

In most of the later types of problem such as the catalysis of the reaction of two gases at the surface of a solid, the specific surface is satisfactorily defined as the area of solid in contact with the mixture of the two gases, as here reaction takes place over the whole of the surface. In the case of burning wood however, reaction is localised within definite areas which are bound to alter in both position and size with time if there is a measurable rate of spread. Now it is well known that flame does not spread at the same rate when travelling upwards as when travelling downwards and thus the position of the reaction zone has a very large effect on the rate of spread even though the specific surface as defined above is the same in both cases.

This is obviously due to the more efficient heat transfer when the flame spreads in an upward direction because of convection currents which carry the hot burning gases over the unburnt wood.

From this it becomes apparent that the heat transfer coefficients are very important in themselves, quite apart from the specific surface in question, their importance being emphasised by the large effect which supporting radiation has previously been shown to have. Moreover it has often been pointed out that two fires

adjacent to each other may exhibit considerable mutual support, the radiation from each increasing the rate of spread of flame above that which obtains when each fire is burning singly, although the specific surface of each fire is not altered by its approach to the other.

It is evident from the above that specific surface cannot be used as an accurate numerical estimate of the fire risk of different structures although it still remains a good qualitative measure of the rate at which flame will spread through structures.

It was concluded that before the rate of the spread over a surface could be predicted from its physical constants and those of its surroundings it would be necessary to measure the heat transfer from the flame on such a burning surface, to the surface itself and also to take into account the effect of this transferred heat in the distillation of volatiles from the burning material.

It would seem that in burning the flame is not actually in contact with the associated surface but is separated from it by a small vertical distance which may be regarded as a thermal gradient between the inflamed gaseous mixture and the colder solid surface. If such a gradient exists, then the heat transfer from the flame to the surface must be almost exclusively by radiation, and if the dimensions of the gradient were known, it should be possible to estimate the intensity of that radiation, taking into account the temperature and shape of the flame.

It now became obvious that further experimentation was required, and in particular it seemed desirable to make an estimate of the surface temperature of the material as and when the flame reached it. The measurement of surface temperature is very difficult under most circumstances, and in the case of burning cellulose the best way seemed to be to deduce it from the variations of the temperatures in a body of material of appreciable thickness. This would have the advantage of allowing measurements to be made on a single burning surface rather than on two supporting ones. These two conclusions lead naturally to the choice of wood for further experiments which are described in Part II of the Thesis.

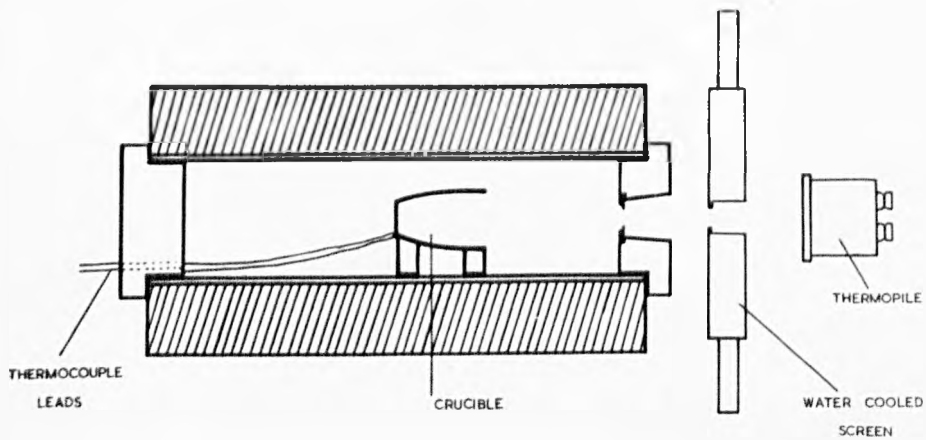


Figure 11.
Construction of the black body calibration furnace.

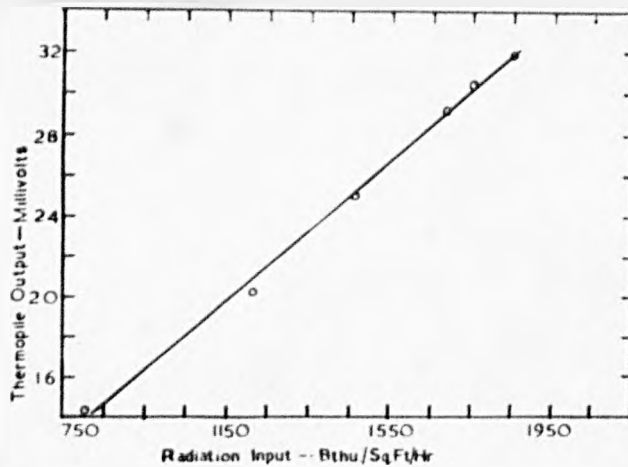


Figure. 12.
Response of thermopile to black body radiation.

APPENDIX IThermopile Calibration

The instrument employed was a 17-element Moll Thermopile, connected to a millivoltmeter of 2000 ohms resistance. For purposes of calibration the thermopile had to be exposed to a range of known intensities of black-body radiation. The radiation was supplied by a furnace, shown in Figure 11, consisting of a nichrome wire wound refractory tube, heat insulated with diatomaceous earth. An aperture was provided in the 1/16" thick stainless steel plate of diameter slightly less than that of the fluorite window of the thermopile. A silica crucible was placed within the furnace tube directly opposite the aperture to serve as a black-body cavity, the temperature of which was measured by means of a thermocouple, and also by a disappearing filament optical pyrometer; the two temperatures always agreed to within 5°c. The thermopile was shielded from radiation from the external walls of the furnace by means of the water-cooled screen shown in Figure 11, and was so mounted as to permit fine adjustment of its position in both vertical and horizontal directions.

The total radiation incident upon the thermopile window is then given by the following equations:-

$$q = \sigma T^4 A_1 \left[\frac{1 + \frac{a_2^2}{b} + \frac{k^2}{b^2} - \sqrt{\left(1 + \frac{a_2^2}{b} + \frac{k^2}{b^2}\right)} - \frac{4a_2^2}{b}}{2} \right]$$

where T is the absolute temperature of the crucible,

A is the area of the thermopile window,

a is the radius of the furnace aperture at a temperature T ,

b is the radius of the thermopile window,

k is the distance between the thermopile window and the furnace aperture, and

is the Stefan-Boltzmann constant.

The shape factor within the square brackets has been given previously by Hottel¹⁴.

Now if k be large compared with a and b , and if a and b are nearly equal, the expression $1 + \frac{a^2}{b^2} + \frac{k^2}{b^2}$ is very nearly equal

to the expression $\sqrt{\left(1 + \frac{a^2}{b^2} + \frac{k^2}{b^2}\right)^2 - 4 \frac{a^2}{b^2}}$; consequently

the numerical value of the ^{above} shape factor is given by the difference between two nearly equal numbers, which must be determined with great accuracy if even a moderately accurate shape factor is to be obtained.

It was found impossible to measure a , b and k with the required accuracy, but the difficulty was overcome by re-arranging the terms in the expression given by Hottel, as follows:-

$$\text{Let } N = 1 + \frac{a^2}{b^2} + \frac{k^2}{b^2}$$

Then the shape factor may be re-written as

$$\frac{A_1}{2} \left(N - \sqrt{N^2 - 4 \frac{a^2}{b^2}} \right)$$

which in turn equals $\frac{A_1}{2} (N - \sqrt{N^2 - \frac{4a^2}{b^2}}) \times \frac{(N + \sqrt{N^2 - \frac{4a^2}{b^2}})}{(N + \sqrt{N^2 - \frac{4a^2}{b^2}})$

and simplifies to $\frac{A_1}{2} \frac{N^2 - (N^2 - \frac{4a^2}{b^2})}{N + \sqrt{N^2 - \frac{4a^2}{b^2}}}$

or

$$\frac{2A_1 \cdot \frac{a^2}{b^2}}{N + \sqrt{N^2 - \frac{4a^2}{b^2}}}$$

In this way, the objectionable difference between two almost equal numbers is eliminated and the shape factor can be determined with a good degree of accuracy. A similar difficulties occur with many other shape factors and in some cases may be resolved in the same way if the terms can be arranged in the general form of $x - \sqrt{a - x^2}$.

Thus the radiation between rectangles of equal size in parallel planes and with one side large enough to be considered infinite is given by

$$q = \sigma (T_1^4 - T_2^4) A \left(\sqrt{1 + \frac{1}{x^2}} - \frac{1}{x} \right)$$

where x is the ratio between the width of the strips to the distance between them. Thus if

$$\frac{1}{x^2} \gg 1$$

the difference in the bracket becomes very small. By

multiplying by

$$\frac{\sqrt{1 + \frac{1}{x^2}} + \frac{1}{x}}{\sqrt{1 + \frac{1}{x^2}} + \frac{1}{x}}$$

The expression becomes

$$q = \sigma (T_1^4 - T_2^4) A \frac{\left(1 + \frac{1}{x^2} - \frac{1}{x^2}\right)}{\sqrt{1 + \frac{1}{x^2} + \frac{1}{x}}}$$

which reduces to a form which does not involve the difference of two terms, i.e.

$$= \frac{\sigma (T_1^4 - T_2^4) A}{\sqrt{1 + \frac{1}{x^2} + \frac{1}{x}}}$$

By this device shape factors which would otherwise be unmanageable can be applied over much wider ranges of the variables.

Unfortunately the maximum intensity of radiation obtainable from the calibration furnace was 1740 B.Th.U./ft.²/hr. and this was achieved only by running the furnace at its maximum safe temperature and by decreasing the distance k to the minimum value imposed by the physical dimension of the apparatus. The results showed that the thermopile output varied in direct proportion to the incident radiation, as shown in Figure 12, but it appeared unlikely that the linear relationship would continue to hold over the higher radiant intensities obtainable with the experimental radiator, especially as it was noted that the nearer the thermopile was to the radiator the greater the angle at which some of the radiation approached the former. It seemed reasonable to suppose that radiation which deviated appreciably

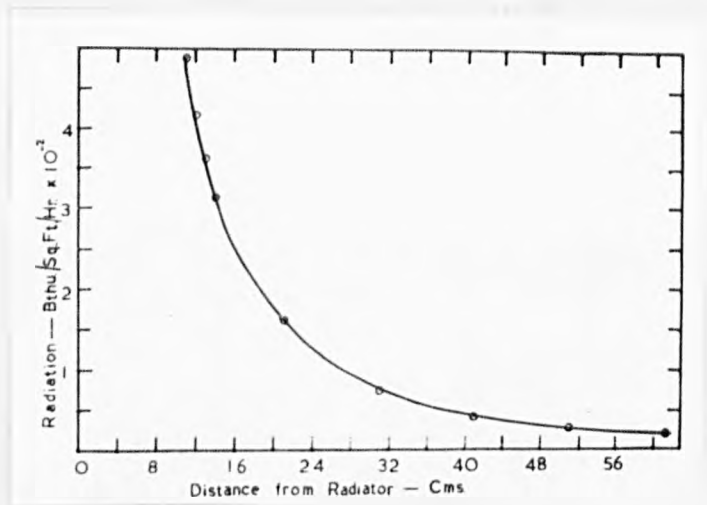


Figure 13.
The variation with distance from the radiator
of the radiation.

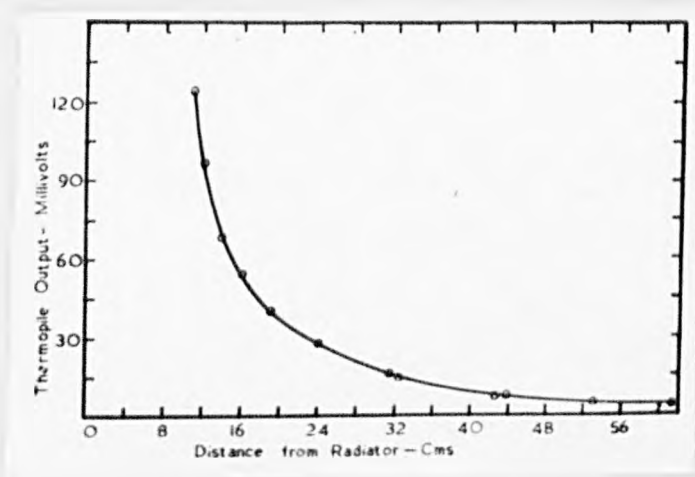


Figure 14.
The thermopile response at different distances
from the radiator

from the normal would not be intercepted completely by the thermopile elements, and would not therefore necessarily obey the cosine law. It may be mentioned here that all measurements of radiation from the experimental radiator were made along the mid-normal to its refractory back, unless otherwise stated.

It was deemed essential therefore, to calculate the variation with distance of the radiation from the refractory of the radiator to the thermopile, taking into account the shape and temperature of the heater elements and of the refractory itself. The full calculation is given in Appendix II, while the results are shown in Table 6 and in Figure 13.

TABLE 6

Distance from Radiator Backing (cms)	Calculated Radiation Intensity B.T.H.U./sq.ft./hr.
11	6300
12	5430
13	4720
14	4110
21	2080
31	970
41	540
51	360
61	250

Simultaneous measurements were made of the variation with distance

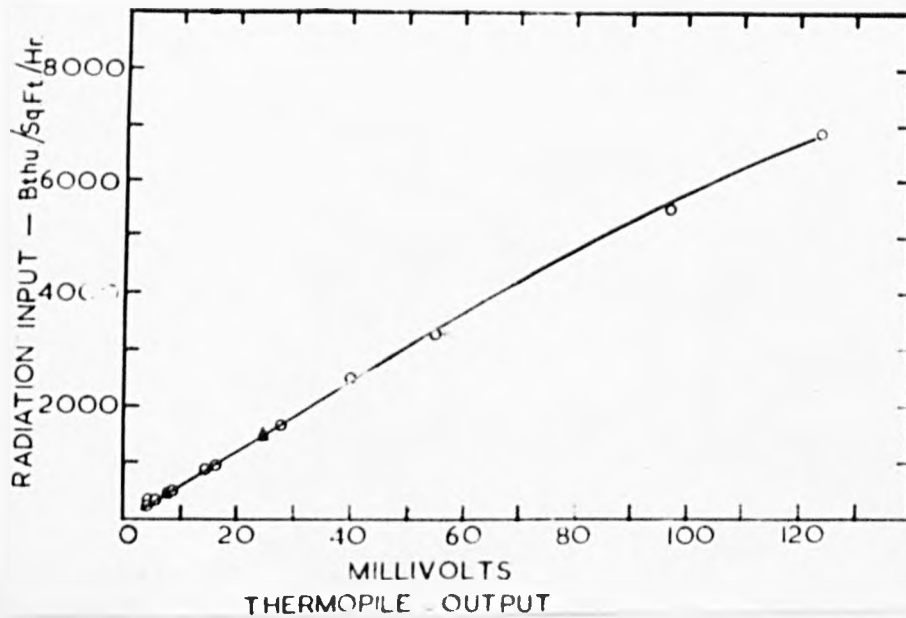


Figure 15.
Thermopile calibration curve.

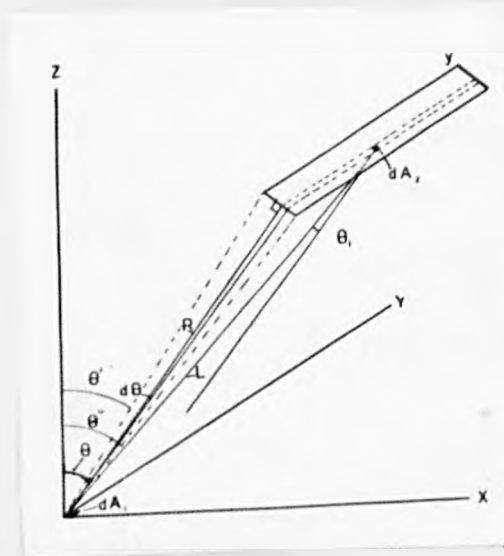


Figure 16.
The radiation from a bar to a small
element of area.

from the radiator of the thermopile output, and the results are plotted in Figure 14. The curve is very similar in form to that of Figure 13. Now from the thermopile calibration against black-body emission, a radiant intensity of 1463 B.Th.U./ft.²/hr. corresponds to an e.m.f. of 24.9 millivolts, which from Figure 14 corresponds in turn to a distance of 25.4 cm. from the radiator. But the calculated intensity of radiation at this distance was only 1130 B.Th.U./ft.²/hr; hence all calculated intensities were assumed to be in error by a factor of 1.295. The above reasoning is based on the assumption that the radiation incident upon the thermopile at any distance from the radiator was measured with the same efficiency as that received from the calibration furnace at that distance, and would seem to be justified by the relationship which exists between the measured thermopile e.m.f. and the calculated radiation. Thus, at any distance from the radiator the thermopile registered a certain voltage, and the corresponding intensity of radiation was taken as the calculated radiation multiplied by 1.295. In this way Figure 15 and Table 7 were constructed, from which it will be seen that the thermopile response is almost linear at distances beyond approximately 15 cm. from the radiator, and as the instrument should attain its maximum efficiency at an infinite distance from the radiator, the linear response obtained at a distance of 25.4 cm. would appear a close approximation to that

maximum. Also, as the calibration furnace aperture was slightly less than that of the thermopile, the same efficiency should obtain there. Hence, Figure 15 was used to determine the radiation incident upon the test-pieces in all subsequent experiments.

Finally, an investigation was made of the uniformity of radiation over the area occupied by the test-piece, and although the intensity diminished slightly with distance from the mid-normal to the radiator, it was insufficient to affect the accuracy of the results.

TABLE 7

<u>Output from Thermopile (millivolts)</u>	<u>Incident Radiation Intensity B.T.H.U./sq.ft./hr.</u>
31.9	1849
30.4	1744
39.2	1686
23.2	1515
20.2	1215
14.3	767

APPENDIX II

A Calculation of the Intensity of Radiation Incident upon a Small Element of Area dA_1 , Situated on and Perpendicular to the Mid-normal to the Plane of the Radiator.

Five distinct sources of radiation are considered to be of sufficient size and temperature to influence appreciably the variation in the total radiation incident upon the small element of area dA_1 , namely the three 600 watt radiator bars and the two strips of refractory between the bars. Radiation emitted and reflected from the refractory outside the two outer bars was neglected, because of its low temperature and unfavourable position to reflect radiation on to the thermopile.

Primarily, consideration was given to the radiator bars, and it was decided to treat them as flat strips of uniform temperature. A similar treatment was afforded by H.C.Hottel¹⁹ to boiler tubes of infinite length, but his shape factor could not be applied in the present case since the bars were too short to be considered infinite compared to their distance from dA_1 . Hence it is necessary to consider the radiation from a strip of finite length received by dA_1 . Half of such a strip is shown in Figure 16, orientated parallel to the y-axis of three rectangular co-ordinates, with its plane normal to the line joining the centre of one end of the strip to the origin. Now the radiation incident upon dA_1 from dA_2 is

$$q = E \frac{\sigma}{\pi} T^4 dA_1 dA_2 \frac{\cos \theta_1 \cos \theta_2}{L^2}$$

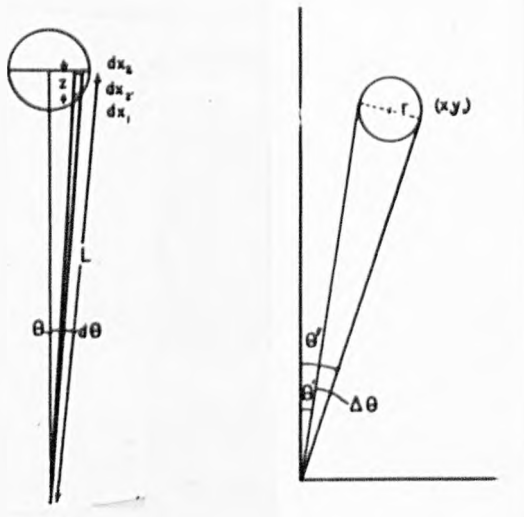


Figure 17.
Angle subtended by radiator element.

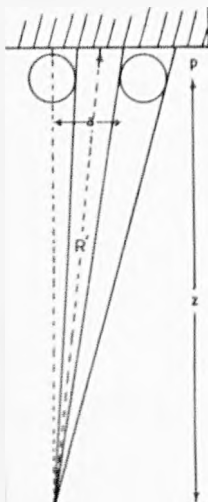


Figure 18.
Angle subtended by refractory.

where E is the emissivity of dA_2 .

T is the temperature of dA_2 , and

σ is the Stefan-Boltzmann constant.

But $\cos \theta_0 = \frac{z}{L}$ and $\cos \theta_1 = \frac{R}{L}$.

Therefore $q = E \frac{\sigma}{\pi} T^4 dA_1 dA_2 \frac{Rz}{L}$

again $dA_2 = R d\theta dy$.

Hence $q = E \frac{\sigma}{\pi} T^4 dA_1 \frac{R^2 z}{L^2} d\theta dy$.

Now $\cos \theta = \frac{z}{R}$, and as R is very nearly constant provided that dA does not approach too closely to the bar, the total radiation from the bar to dA_1 is given by

$$\begin{aligned} Q &= E \frac{\sigma}{\pi} T^4 dA_1 \int_{-y}^y \int_{\theta'}^{\theta''} \frac{R^3 \cos \theta}{(R^2 + y^2)^{3/2}} dy d\theta \\ &= E \frac{\sigma}{\pi} T^4 dA_1 (\sin \theta'' - \sin \theta') \int_{-y}^y \frac{R^3}{(R^2 + y^2)^2} dy \\ &= E \frac{\sigma}{\pi} T^4 dA_1 (\sin \theta'' - \sin \theta') \left[\tan^{-1} \frac{y}{R} \cdot \frac{Ry}{R^2 + y^2} \right]_{-y}^y \\ &= E \frac{\sigma}{\pi} T^4 dA_1 (\sin \theta'' - \sin \theta') \left(\tan^{-1} \frac{y}{R} \right) + \frac{Ry}{R^2 + y^2} \end{aligned}$$

Now from Figure 17

$$\sin \theta' = \sin (\theta - \Delta\theta) = \sin \theta \cos \Delta\theta - \cos \theta \sin \Delta\theta$$

$$\text{and } \sin \theta'' = \sin (\theta + \Delta\theta) = \sin \theta \cos \Delta\theta + \cos \theta \sin \Delta\theta$$

$$\text{Therefore } \sin \theta'' - \sin \theta' = 2 \cos \theta \sin \Delta\theta$$

$$= 2 \frac{z}{R} \frac{r}{R}$$

$$= 2 \frac{zr}{R^2}$$

$$= \frac{2}{z^2 + x^2} zr$$

Hence the total radiation from a radiator bar to a small element of area dA_1 becomes

$$Q = E \frac{\sigma}{\pi} T^4 dA_1 \frac{2zr}{z^2 + r^2} \left[\left(\tan^{-1} \frac{y}{\sqrt{x^2 + z^2}} \right) + \frac{y \sqrt{x^2 + z^2}}{z^2 + x^2 + y^2} \right]$$

Turning now to the refractory between the bars, the radiation can be estimated similarly by regarding each strip of refractory, XX^1 in Figure 18, as a strip of width $xx^1 \cos \phi$ normal to the line from the centre of the strip to the small area dA_1 .

The shape factor for the strip then is

$$dA_1 (\sin \theta' - \sin \theta'') \left[\left(\tan^{-1} \frac{y_1}{R} \right) + \frac{R^1 y}{R^1 z + y^2} \right] \cos \phi$$

where $\sin \theta' = \frac{a}{R_1}$, $\sin \theta'' = \frac{r}{R_1}$, $\cos \phi = \frac{z}{\frac{a+r}{2}}$ and $R^1 z = (z+p)^2 + \dots$
 $\dots \frac{(a+r)^2}{2}$

Thus for each strip of refractory

$$Q = E \frac{\sigma}{\pi} T^4 dA_1 \left(\frac{a-r}{R^1} \right) \left[\left(\tan^{-1} \frac{y_1}{R} \right) + \frac{R^1 y}{R^1 z + y^2} \right] \frac{2z}{a+r}$$

It now became possible to evaluate the shape factors for the radiator bars and the refractory backing by using the linear dimensions of the radiator, and specimen calculations are appended below.

(1) Shape Factor for Central Bar

The shape factor is $\frac{2zr}{z^2 + x^2} \left[\left(\tan^{-1} \frac{y}{\sqrt{x^2 + z^2}} \right) + \frac{y \sqrt{x^2 + z^2}}{z^2 + x^2 + y^2} \right]$

Now $x = 0$, $y = 6.9$ cm, $r = 0.59$ cm. and z is the vertical height from dA_1 to the centre of the bar; the shape factor therefore

35

becomes $\frac{1.18}{z} \left[\left(\tan^{-1} \frac{6.9}{z} \right) + \frac{6.9z}{z^2 + 47.7} \right]$

Thus when $z = 50$ cm. the shape factor is 0.00645.

(ii) Shape Factor of the Outside Bars

Here $x = 2.4$ cms. $y = 6.9$ cms. and $r = 0.59$ cms.

Therefore the shape factor is

$$\frac{1.182}{z^2 + 5.8} \left[\left(\tan^{-1} \frac{6.9}{\sqrt{z^2 + 5.8}} \right) + \frac{6.9 \sqrt{5.8 + z^2}}{z^2 + 53.5} \right]$$

Again when $z = 50$ cm. the shape factor is 0.00642.

Hence for the two bars the shape factor is 2×0.00642 or 0.00128.

(iii) Shape Factor for the Refractory Strips

The shape factor is $(\sin \theta' - \sin \theta) \left(\tan^{-1} \frac{y}{R'} + \frac{R'y}{R'^2 + y^2} \right) \cos \phi$

where $\sin \theta' = \frac{a}{\sqrt{a^2 + z^2}}$ $\sin \theta = \frac{r}{\sqrt{r^2 + z^2}}$, and

$$R'^2 = (z+p)^2 + \left(\frac{a+r}{2} \right)^2$$

Now $a = 1.8$ cm, $y = 7.0$ cm. and $p = 0.88$ cm..

Therefore the shape factor becomes

$$\left(\frac{1.8}{\sqrt{3.2 + z^2}} - \frac{0.59}{\sqrt{0.35 + z^2}} \right) \left(\tan^{-1} \frac{7.0}{\sqrt{(z+0.88)^2 + 1.44}} + \frac{7.0 \sqrt{(z+0.88)^2 + 1.44}}{(z+0.88)^2 + 50.4} \right) \times \frac{z}{\sqrt{z^2 + 1.44}}$$

When $z = 50$ cm. the factor is 0.00670.

Therefore, for both strips the shape factor is 2×0.00670 or 0.0134.

In order to obtain the variation in total radiation from the radiator, the proportions originating on the refractory and

in the bars had to be calculated separately, since the two sources had slightly different shape factors. As the latter difference was small it was unnecessary that the proportions should be known exactly, and a fairly large discrepancy between the calculated and observed radiation did not necessarily mean that the variation of radiant intensity with distance from the radiator was greatly in error.

Before the radiation from the bars and the refractory could be calculated, the respective emissivities and temperatures must be known. The temperature of the bars was measured at several places with an optical pyrometer situated upon the mid-normal to the plane of the radiator, giving an average figure of 1243°K. Similarly, the average temperature of the refractory was 923°K, although the latter figure was less accurate being measured by thermocouples inserted in the face. The emissivities of the bars and refractory were taken from relevant tables as 0.9 and 0.7 respectively.

Then the total radiation per unit area is given by

$$Q = E_1 \frac{\sigma}{\pi} T_1^4 S_1 + E_2 \frac{\sigma}{\pi} T_2^4 S_2,$$

where E is the emissivity, T the temperature and S the shape factor, the subscripts 1 and 2 referring to the bars and refractory respectively.

$$\begin{aligned} \text{Thus at 50 cm. distance, } Q &= (0.578 \times 10^{-8} \times (1243)^4 \times 0.0193) \\ &\quad + (0.7 \times 0.578 \times 10^{-8} \times (923)^4 \times 0.0134) \\ &= 305 \text{ B.Th.U./sq.ft/hr.} \end{aligned}$$

Part 11FLAME SPREAD OVER A SINGLE SOLID SURFACEINTRODUCTION

This section of the Thesis is a description of some of the energy transfers at a single solid burning surface. In particular the emphasis has been laid on the form in which heat arising in the combustion of the wood is dissipated into the surroundings. Here two fundamental problems arise. It is first necessary to correlate the effect of all variables on the passage of flame over a single surface so that the change in the rate of spread of flame caused by a change of any one variable can be predicted. Secondly there is the problem of determining rates of flame spread over the surface of combustible materials of different shapes.

The first of these is the more fundamental and would have to be solved before the second problem could be fully elucidated. On the other hand, the second problem is of more interest in the practical aspects of fire prevention and in the combustion of solid fuel beds, and data relating to such problems could be used in general calculations without having fully solved the first problem. During the preceding five years, the various effects on fire spread of the three different modes of heat transfer, namely - conduction, radiation and convection, have been widely discussed and some of the conclusions are summarised below.

In the most outbreaks of fire, convected and radiated heat are nearly always more important than conducted heat₁₁, largely because of the low conductivity of the normal combustible materials encountered in practice. Conduction of course, does become important when large masses of metal are part of the burning structure, but even here the original heat transfer to the metal is largely by convection and radiation from the flames of the burning volatiles.

Radiation plays its largest part in heat transfer between adjacent areas of material and is of particular importance in the spread of flame in directions deviating from the vertically upwards. Thus, as has been pointed out before, the heat transfer from the side of one building to an adjacent building is mainly by radiation if there is no large convection effect from the side due to fire wind. Also as the intensity of the radiation varies approximately with the square of the distance from the source in most cases, it tends to have its greatest effect in short range heat transfer, particularly as it is efficiently stopped by most intervening partitions.

If the radiation intensity from the flame burning under a given set of conditions were known, it would be possible to calculate the size of flames on adjacent faces of wood which would be necessary for supported combustion to proceed, taking into account that each shall supply the other with sufficient heat to maintain the same or a greater rate of burning, and thus each flame must be of a certain critical size before

either will spread.

Convection on the other hand, plays a larger role in the spread of flame vertically upwards. It is of especial effect under conditions which tend to canalise the flow of burnt gases on to unburnt materials, and is probably the main agent in the upward spread of fire from the lower stories of buildings, thus a lift shaft or staircase can effectively direct the heat evolved from a fire in a lower room into the upper stories which may, in some cases, be a considerable distance away, and where heat transfer by radiation would have been stopped by intervening floors. Such heat transfer preheats the combustible material, making it particularly amenable to further flame spread.

From the above, the importance of the proportions of heat evolved by radiation conduction and convection by a burning surface is apparent.

Experiments were confined to flames spreading over the surface of the material as opposed to sustained burning, that is, measurements were only made until the flame spread to the boundaries of the material under consideration. It has been found by several previous workers that the depth of charring and indeed, the obtaining of any flame at all, is dependent on the intensity of the supporting heat. In the present case flame was sustained on the surface of the wood by comparatively low intensities of radiation and from figures quoted by Bamford¹⁰ and Summersgill⁸ the wood should never have charred to a depth

of greater than 5 mm.. These are the conditions obtaining during the initial stages of the spread of flame and the results quoted later will be of most use under such conditions. Much work has previously been done on the sustained combustion and distillation of wood and some of the results obtained under these conditions are of use in research into the rates of spread of flame. In particular the temperature during the time that the wood is charring, and the effects of moisture on the internal temperature of the wood are important, especially when considering the mechanism of flame travel over a single surface. Here the rate of distillation of volatiles decides how quickly the flame travels, and as the temperature of the wood is a function of the size and temperature of the flame, so the rate of flame spread is determined by the equilibrium conditions arising when the rate of distillation of volatiles is sufficient to maintain a flame of the same size and temperature as that already distilling the volatiles, thus equilibrium largely depends on the heat transfer coefficient between the flame and the burning wood.

The experiments were therefore designed to measure the various heat transfers which take place when wood is burned and in particular the amount of conducted and radiated heat are measured and the convected heat deduced. This necessitated measurements of both the temperature distribution in the wood and of the radiation intensities over a hemisphere with a

symmetrical flame at the centre of its base, making it necessary to study flame spreading as a circle from a point source. This is not quite such a simple case as the linear spread of flame, but many of the results calculated under conditions of circular spread can be generally applied. This part of the Thesis has been divided into two main sections. The first of these describes preliminary experiments made to decide which timbers and thicknesses were most suitable for the final calculations of the heat balance, and as a result of these experiments the choice of test material was restricted to birch timber of 1" thickness, as described in the second section. In most cases the timber was oven dried, but one or two experiments were carried out on air dried specimens.

Part APRELIMINARY EXPERIMENTS

The purpose of these experiments was to obtain values of the physical constants of four timbers and to discover the characteristics of flame spread over their surface in order to decide which was the most suitable for the detailed investigations described in the introduction. The four species investigated were: -

- (1) Pine: - a resinous soft wood which cracks easily along the grain and exudes resin when heated.
- (2) Birch: - a soft white wood apparently containing no resin.
- (3) English Oak: - a hard dense wood well known for its fire resistant properties.
- (4) Gurjon: - a hard wood found chiefly in Burma, having an even grain and containing resin.

The wood was obtained in the form of 1" thick, planed planks and under the conditions of storage reached a moisture content of about 8%. Experiments were made to determine

- (1) The rate of spread of flame without supporting radiation along 1/8" thick specimens, cut and burnt along the grain in the same manner as in the experiments with paper.
- (2) The rates of linear spread along a single upper horizontal surface at various radiation intensities.
- (3) The rates of circular spread along a single upper

horizontal surface at various radiation intensities.

In the above cases the source of supporting radiation and its method of measurement were the same as in the paper experiments.

Experiment 1

Flames spread in much the same manner as in the paper experiments but were distinctly slower and the results (Table 8) were not as uniform.

TABLE 8

Rates on linear spread for 1/8" thick specimens without supporting Radiation	
Species	Rate of spread (cms./sec.)
Birch	0.038
Oak	0.040
Pine	0.036
Gurjon	0.038

Experiment 2

The specimens used for the supported linear spread experiments were 4 cm. wide, 15 cm. long and 2.5 cm. thick in all cases except one, where a specimen of half the normal thickness was used.

The wood was held vertically underneath the radiator by a clamp at one end and ignited at the other. It was not found necessary to cut the ends to a point in order to ensure even flame fronts but a preliminary travel of 6 cm. was allowed before

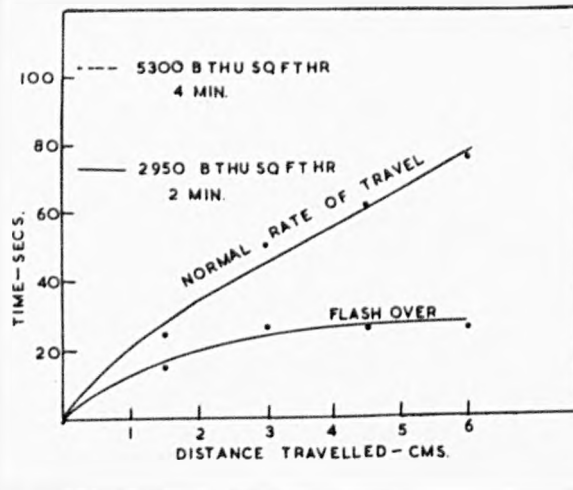


Figure 19.
The effect of prolonged radiation intensity on the rate of spread.

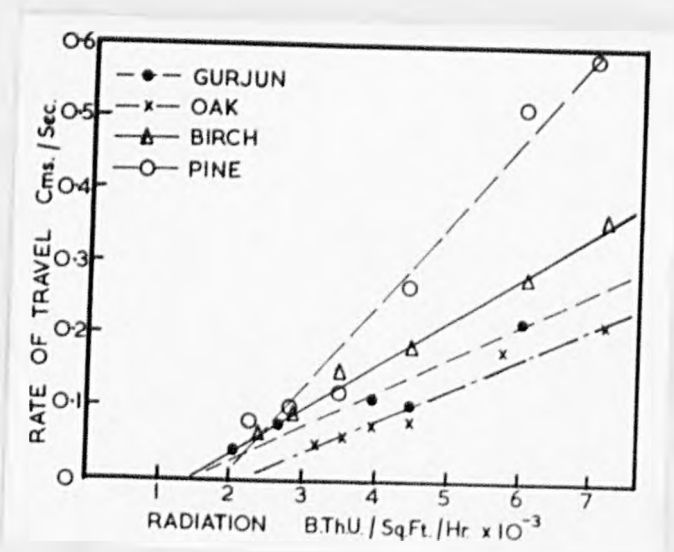


Figure 20.
The effect of radiation on the rate of spread over four timbers.

measurements were taken. In all cases the length of block was parallel to the grain. In order to decide what circumstances gave the most constant speed, in the first few experiments the accepted rate of spread was the average of twelve tests carried out over different distances and timed in the usual manner with stop watch reading to $1/5$ second. Using Gurjon, it was found that if the radiation before ignition was prolonged, i.e. for periods of over 3 minutes, at a radiation of 6.000 B.Th.U./sq.ft./hour, 'flash-over' occurred soon after ignition, i.e. a sudden rise in the rate of spread occurred and the top surface of the wood became covered with flame almost immediately. The same effect was observed with all the other woods but to a less degree.

If however, the wood was ignited as soon as it would propagate flame, a period which depended on the radiation intensity, a much more constant rate of spread was obtained. The effect of prolonged radiation intensity is shown in Table 9 and Figure 19.

In all further cases the wood was ignited as soon as it would propagate and the accepted rate of spread was taken as the average of six results measured over a distance of 6 cms. The radiation intensity was altered in the usual way by varying the height of the specimen beneath the radiator. The results are tabulated in Table 10 and Figure 20. The figures obtained from the non-resinous woods were more constant than those of pine and gurjon.

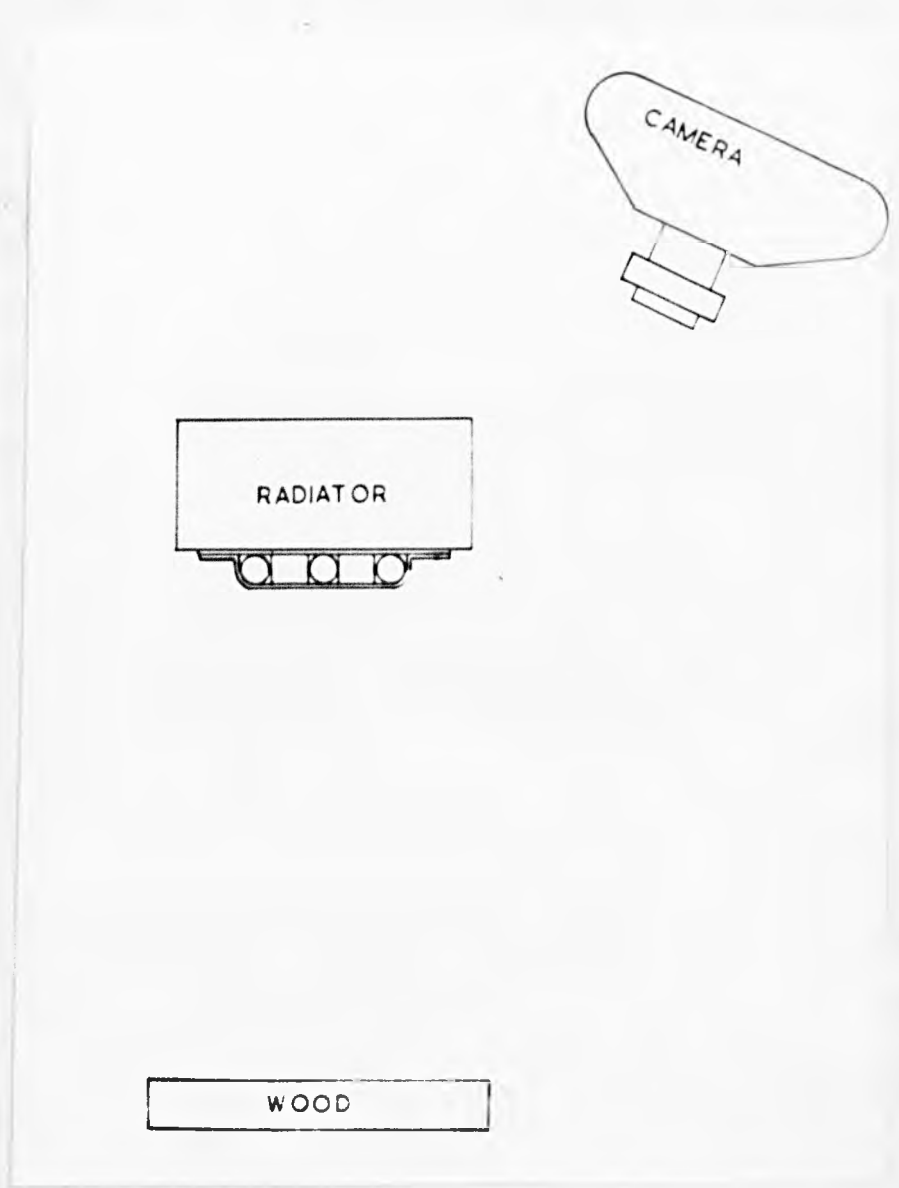


Figure 21.
The relative positions of the camera , radiator
and wood.

Experiment 3

Attention was next turned to the circular spread of flame and for this purpose 6" square by 1" thick blocks were held horizontally underneath the radiator. Only gurjon and birch were used in these experiments, birch because it seemed to give the most uniform results and gurjon because any difficulties in technique should show up more easily in the most difficult specimen to handle. Because of the unsymmetrical nature of the radiator, it was not possible to maintain a uniform field of radiation over the wood, and at the closest distance of the radiator, the radiation at the edges was 6% lower than at the centre. In all cases the centre intensity was the one tabulated. The wood was ignited at the centre by a small pilot flame and flame spread radially from that point but the irregularities in the flame front made it impossible to decide at what instant it crossed the circumferences of concentric circles drawn on the wood. In general however, the burnt area was placed symmetrically about the centre of the block and it was decided to measure the area photographically at various instants during the burning. This was achieved by supporting a 35 mm. camera as near directly above the wood as was possible without the radiator obscuring the field of view, as shown in Figure 21. Exposures were then made at 5 second intervals during the burning time, each frame included the stop watch which was started at the beginning of the experiments. The negative images were projected onto sheets of

TABLE 9LINEAR SPREAD OF 1" GURJON UNDER RADIATION

Normal rate of Spread			Flash-over		
Distance travelled (cms)	Time taken (secs.)	Average time (secs.)	Distance travelled (cms.)	Time taken (secs.)	Average time (secs.)
	20.0)			27.0)	
1.5) 12.8)	14.5	1.5) 19.4)	22.1
) 10.8)) 20.0)	
	33.0)			44.5)	
3.0) 28.4)	26.0	3.0) 46.8)	45.0
) 16.6)) 43.6)	
	20.4)			66.2)	
4.5) 33.2)	26.3	4.5) 56.0)	61.1
) 24.8)) 61.1)	
	19.2)			68.5)	
6.0) 20.0)	21.2	6.0) 63.6)	74.0
) 24.6)) 90.0)	
Pre Radiation of 2950 B.Th.U./sq.ft./hr. for 2 mins.			Pre Radiation of 5300 B.Th.U./sq.ft./hr. for 4 mins.		

TABLE 10Preliminary results for Flame Spread over Wood.Linear Spread under Radiation

Species of wood	Radiation B.Th.U./sq.ft./hr.	Rate (cms./sec.)
1" Gurjon Moisture content = 7.7%	2020	0.041
	2540	0.041
	3990	0.110
	4510	0.100
	6070	0.220
1" Moisture content = 8.9%	3180	0.044
	3520	0.058
	3990	0.075
	4510	0.081
	5780	0.183
	7160	0.215
1" Birch Moisture content = 8.0%	2310	0.063
	2830	0.096
	3510	0.141
	4510	0.186
	6070	0.279
	7160	0.360
1" Pine Moisture content = 8.8%	2310	0.080
	2830	0.107
	3510	0.121
	4510	0.298
	6070	0.521
	7160	0.608
$\frac{1}{2}$ " Gurjon	2600	0.047

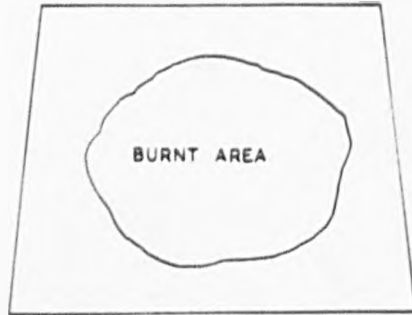


Figure 22.
A typical trace of the burnt area of wood.

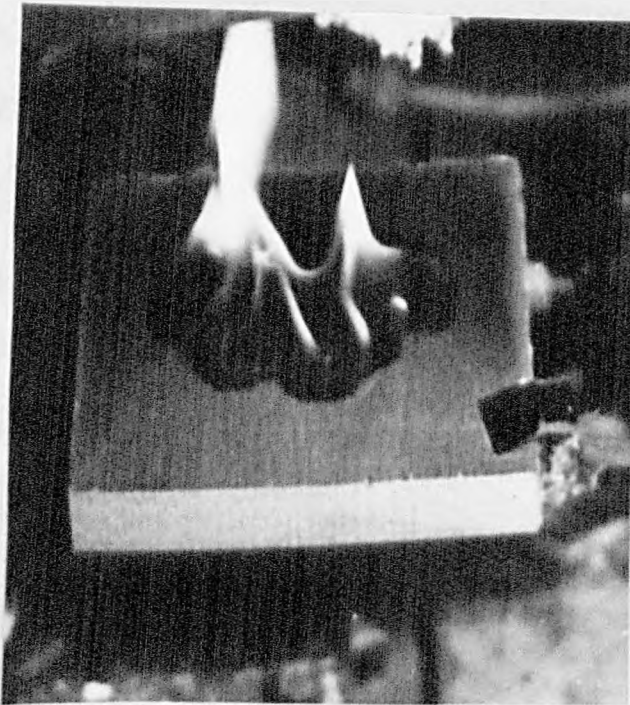


Figure 23.
Photograph of the burning wood.

drawing paper and the burnt area traced round together with the image of the top surface of the wood. The area of the wood was known from its dimensions and hence the area of the burnt surface could be deduced by simple proportion after comparing the respective areas on the tracing by a planimeter. This method did not eliminate errors due to perspective, i.e. the further edge of wood always appeared somewhat smaller than the near edge but as the flame was situated centrally with respect to the wood, this effect was minimised. A typical set of results is shown in Table 11 and Figure 22 shows the type of trace usually obtained, Figure 23 is a photograph of the burning wood.

TABLE 11

Example of the Calculation of the Circular Rates of Spread from the Photographic Negatives

Arbitrary Units

Apparent Area of Wood	Apparent Area of Flame	Real Area of Flame (sq. cms.)	Radius of the Equivalent Circle (cms.)	Time Registered by stopwatch (secs.)
63.9	5.0	15.6	2.23	65
65.5	9.4	28.7	3.02	70
67.2	16.1	47.8	3.90	75
59.5	16.9	56.6	4.24	80
50.3	20.7	82.0	5.10	85
62.3	29.2	93.5	5.45	90

The burning was generally allowed to proceed to a radius of 6 cm.

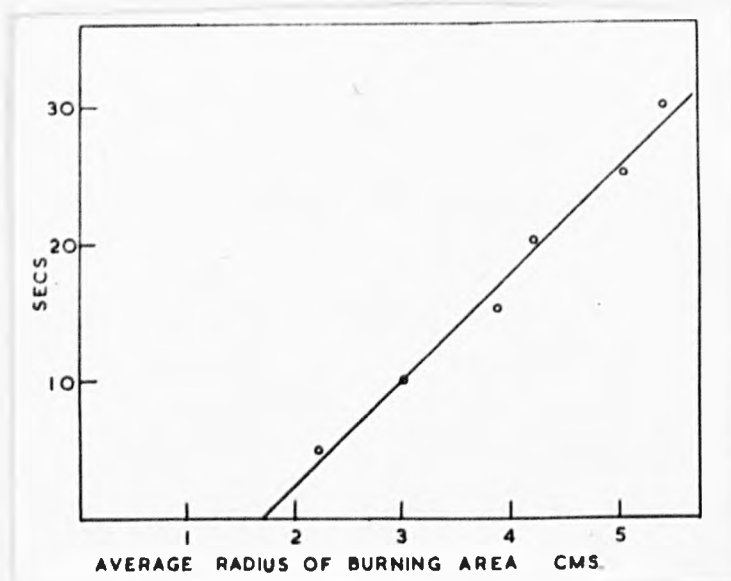


Figure 24.
The average radius of the burning area
at different times.

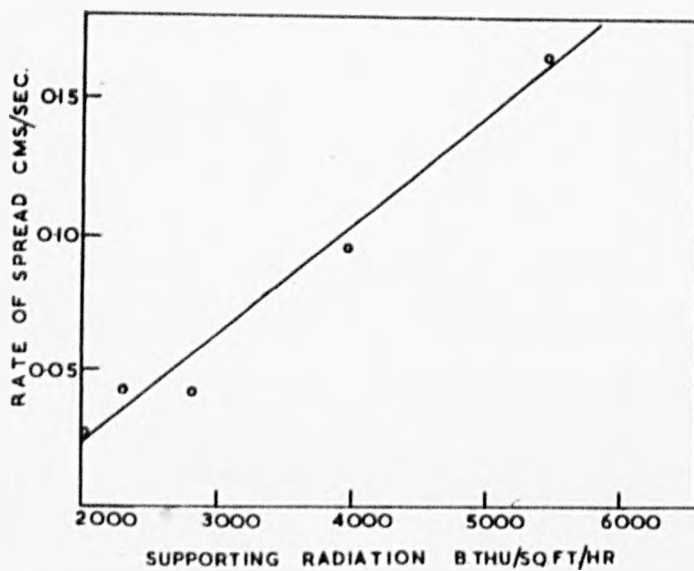


Figure 25.
The variation of the circular rate of spread
with varying radiation intensity.

after which the circular nature of the area became distorted. The results are finally tabulated in Table 12 as the radius of a circle whose area is equal to the area of burnt wood. A plot of this hypothetical radius against time is shown in Figure 24 where it will be seen to be nearly constant, whilst the rest of the results are shown in Figure 25 and Table 12.

TABLE 12

Circular Spread under Radiation

Species of Wood	Radiation (B.Th.U./sq.ft./hr.)	Rate (cms./sec.)
Gurjon	2020	0.027
	2310	0.043
	2830	0.042
	3990	0.096
	5440	0.166
Birch	2130	0.123
	1600	0.060

It was noticed in these experiments that the flame was quite thin and flat in the neighbourhood of the line of discolouration and appeared to be swept back to the centre of the wood where it rose to a conical shape. Moreover, from the results it will be seen that the circular rate of spread is smaller than the linear, just the opposite of the effect observed with paper. These observations support the conclusion that convection currents play a major part in determining the rate of flame spread. For here

there is no convection outwards from the centre of the flame as no hole is burnt in the centre of the wood. Also in the case of linear spread along wood, the burnt material is left in a horizontal plane which should direct air currents in the direction of flame travel.

Turning to the result obtained with a $\frac{1}{2}$ " specimen, it will be seen that the rate of spread is somewhat slower than those along a similar 1" specimen suggesting that a measurable quantity of heat was being lost by conduction into the wood to a depth of at least $\frac{1}{2}$ " as more heat would be lost from the bottom of the $\frac{1}{2}$ " specimen than would be further conducted into a 1" piece of wood.

Physical constants

The more important physical constants for the Birch timber are listed in Table 13.

TABLE 13

Conductivity	C.G.S.Units
Parallel to grain	0.001169
Across the grain	0.000330
Density	0.66
Specific Heat	0.266 0.000116

The figures taken for the conductivity across the grain (it was not obvious whether the plank had been cut radially or tangentially) were determined by Summersgill on material taken

from the stock as was used in the present investigation. It seemed advisable to determine the conductivity of the wood in a direction parallel to the grain, as in general this is much larger than that across the grain. It was also thought that diffusivity and conductivity could be measured by the same apparatus as was used by Summersgill. Briefly this consisted of two brass blocks 9" x 4½" x ¼" between which was sandwiched the specimen of dimensions 9" x 4½" x 1". These blocks were supported horizontally and the lower one was heated electrically, the heat flowing through the wood and escaping from the top brass block. Precautions were taken to ensure a uniform perpendicular flow through the central portion of the specimen whose surface temperatures were measured by fine copper/constantin thermocouples held between the wood and the brass surface. The apparatus has been used for some time to measure the conductivity of refractory materials with low temperature thermal characteristics similar to those of wood.

The conductivity of the material is calculated in a straight forward manner by allowing the apparatus to come to equilibrium, measuring the surface temperatures of the material, and calculating the heat lost from the top plate and hence the heat flow through the wood. The appropriate equation is then

$$\frac{d\theta}{dx} \quad k \quad = \quad \frac{q}{a}$$

where ($\frac{Q}{A}$ is the perpendicular heat flow)
 (per unit area)
 ($\frac{d\theta}{dx}$ is the temperature gradient between)
 (the two surfaces)
 (K is the conductivity of the materials)

The specimen was made from the 6" x 1" planks of birch by cutting strips $4\frac{1}{2}$ " x 1" across the plank and orientating them so that the surfaces which originally made up the 6" surface of the plank now lay face to face. The strips were glued in this manner to form a block 9" x $4\frac{1}{2}$ " x 1", which had the grain running perpendicularly between the two 9" x $4\frac{1}{2}$ " surfaces.

Diffusivity

The attempt to measure the diffusivity of the wood did not yield results which were accurate enough to be of use, but the method is included here as it does not appear to have been suggested before and should be more successful where more violent methods of heating the specimens could be applied.

Diffusivity in one dimension is defined by the following equation:-

$$\frac{d\theta}{dt} = \frac{k}{c\rho} \frac{d^2\theta}{dx^2}$$

where θ is the temperature

x is the distance measured in the direction of heat flow

k is the conductivity

ρ is the density

c is the specific heat

which expresses the assumption that the rate of rise of temperature in a small volume of material is proportional to the rate of change of temperature gradient through that volume. The proportionality constant $\frac{k}{\rho c}$ is defined as the diffusivity of the material. The solution of the above partial differential equation between various boundary conditions has been discussed at some length in the literature. Some formal solutions have been given for the more simple boundary conditions such as a semi-infinite block heated on one face in such a way that the temperature gradient at that surface was proportional to the temperature difference between it and its surroundings, i.e. under Newtonian conditions of heating and cooling. Various methods have also been suggested which involve substituting finite difference ratios for one or more of the differential temperature gradients in space and time, and in particular Hartree and his confederates have applied solutions of this nature to the heating and cooling of ingots¹⁵ and recently a paper has been published in which similar methods are applied to the forced burning of wood. This paper is discussed more fully below (Page 102), but at the moment only the part appertaining to the solution of the diffusivity equation will be considered. The equation to be solved is

$$\frac{d^2 \theta}{dx^2} = \frac{c \rho}{k} \frac{d \theta}{dt}$$

with the boundary conditions

$$\theta = \text{constant for } 0 < x < l \quad \text{for } t = 0$$

$$\theta_{,1} = f(t) \quad \text{and} \quad \theta_{,2} = \phi(t) \quad \text{for } t > 0$$

where l is the thickness of the specimen which is considered to be of infinite extent in the other dimensions, i.e. there is parallel heat flow between the faces of the block.

$\theta_{,1}$ is the surface temperature at the hot surface
 $\theta_{,2}$ is the surface temperature at the cool surface

The manipulation of the equation is considerably simplified by the introduction of new units of space and time defined by

$$\xi = \frac{x}{l} \quad \text{and} \quad \tau = \frac{k}{l^2 c \rho} x t$$

the equation then becoming $\frac{\partial \theta}{\partial \tau} = \frac{\partial^2 \theta}{\partial \xi^2}$ with the corresponding boundary conditions. If now θ_{m-1} , θ_m and θ_{m+1} are the temperature at the points $\xi_{m-\delta\xi}$,

ξ_m and $\xi_{m+\delta\xi}$; then by Taylor's Theorem

$$\frac{\partial^2 \theta_m}{\partial \xi^2} = \frac{\theta_{(m-1)} - 2\theta_m + \theta_{(m+1)}}{\delta\xi^2} \quad \text{approximately and}$$

making a similar substitution for the time derivative, the equation becomes

$$\theta^1_m - \theta_m = \frac{\delta\tau}{2\delta\xi^2} \left[\theta^1_{(m-1)} + \theta_{(m-1)} - 2(\theta^1_m + \theta_m) - \theta^1_{(m+1)} + (\theta_{m+1}) \right] \quad \text{-----3}$$

Where m etc. are values at ξ and m are values at τ

Using the above equations the integration can now proceed in small steps of $\delta\xi$ and $\delta\tau$ and in this particular case it was

found that taking $\delta\xi = \frac{1}{3}$ and $\delta\tau = \frac{1}{9}$ the equations could be

solved in reasonable time and with sufficient accuracy. The experimental procedure was as follows:-

The apparatus was allowed to heat up at a low constant rate of heating and when equilibrium was reached, the temperature of the top and bottom surfaces noted, and the temperature gradient between the surface assumed to be linear. The heat input into the apparatus was then raised to a much higher value, and the temperatures of the top and bottom surfaces taken at intervals of 15 or 30 minutes as the block tended towards equilibrium again. We now know

- (1) The boundary conditions of the block as a function of time.
- (2) The heat transfer from the cold surface as a function of temperature and hence of time.

but the heat transfer at the cold surface is also given by

$$\theta'_0 - \theta_0 = \frac{6r_2}{\delta l} \left[(\theta'_1 + \theta_1) - (\theta'_0 + \theta_0) \right] \frac{2\ell\delta T}{k\delta l} H \frac{(\theta'_0 + \theta_0)}{2} \quad \text{----4}$$

where θ_0 denotes the surface temperature and H denotes the heat transfer from the surface as a function of temperature.

This expression equates the heat transfer at the surface to the conduction in the surface layer.

Also the temperature at $\delta l = \frac{1}{3}$ is denoted by θ_1 , and at

$\delta l = \frac{2}{3}$ by θ_2 .

Values of K and ρ are known and a value for c was assumed and the solution of the equation proceeded in the following manner:-

The values of θ at $\zeta = 0, \frac{1}{3}, \frac{2}{3}$, and 1, were tabulated, the original temperatures at $\tau = 0$ being known. The integration then proceeds down the table.

Values of $\theta_{\frac{1}{3}}$ and $\theta_{\frac{2}{3}}$ at $\tau = \frac{1}{9}$ are estimated taking account of the rises in surface temperature and these estimated values adjusted until they satisfy equation 3. Then values of $\theta_{\frac{1}{3}}$ and $\theta_{\frac{2}{3}}$ at $\tau = \frac{2}{9}$ are estimated and similarly re-adjusted if necessary, the solution proceeding in this way until the temperature changes become small. Now $H(\theta)$ can be calculated from $\theta_{\frac{2}{3}}$ and θ_1 by equation 4 and then tabulated as a function of θ and it was hoped to adjust the assumed value of the specific heat so that the values of $H(\theta)$ calculated as above, coincided with those arrived at, using the usual combination of radiation and convection losses from a black horizontal plate. After preliminary experiments however, it was not found possible to pursue this method further, two difficulties arising. Firstly the wood could not be heated to high temperatures without charring and the emission of volatiles, and these low temperatures made $H(\theta)$ very sensitive to changes in the ambient temperature which could not be estimated accurately. Secondly, as the temperature gradients of the wood did not appear to deviate very greatly from a straight line, any change in C made very little difference to $\theta_{\frac{2}{3}}$ and hence H . It would seem however, that both these difficulties would not arise using refractories where it is possible to use higher temperatures, and it may also

be possible to overcome them by following the temperature changes over the first few minutes of the heating of the wood much more closely. Shortage of time however, did not allow these studies to be pursued further.

Because of the difficulties arising in the above experiments the specific heat was estimated in the rest of the work from a formula developed by Dunlap₁₇ namely

$$C = 0.266 + 0.00116 \theta \quad \left(\begin{array}{l} \text{where } c = \text{specific heat} \\ \text{and } \theta = \text{°C} \end{array} \right)$$

The possible error here is about 5% and this will have its main effect on the calculations involving heat conducted into the wood. However, for other reasons discussed elsewhere, this quantity could not be assessed with great accuracy, so the above equation was assumed to be sufficiently accurate for the purpose under discussion.

Density

Most of the material was oven dried before burning and all the specimens were found to tend towards the density of 0.66 grams/cc, a figure which remained quite constant among the specimens burnt. It was noticed that the wood suffered a considerable contraction on drying and the density had to be determined separately when using air dried material.

Moisture Content

The moisture contents of the timbers were determined by drying 1" cube samples for three days at 100° c, in which time they had reached almost constant weight, further drying

Experimental ProcedureApparatus

The original apparatus was improved by making a larger radiator which covered the area of the specimen with an almost uniform radiation. This radiator utilised seven 600 watt 7" elements of the same type as were used previously. They were supported on a backing of two $\frac{3}{4}$ " thick fire bricks clamped together, giving a total area of 9" x 9". Two $\frac{3}{4}$ " angle pieces were bolted on to the backing and the elements supported between them, their ends fitting into holes drilled in the angle iron. Figure 26 shows the radiator slung on a crossbar between two uprights enabling it to be directed upwards whilst the apparatus warms up. The cross bar was fitted with two pulleys at each end and thus could be run up and down the uprights at the side, and the radiator height quickly adjusted whilst the wood was held horizontally in a shallow 'U' shaped metal support by two wooden wedges so that it did not come into contact with large masses of metal at any point.

It had been discovered in preliminary experiments that a flame started at the centre of the piece of wood, travelled 6 cms. outwards in any time between 30 and 200 seconds, depending on the intensity of the incident radiation and an apparatus had to be designed to measure three quantities of heat in

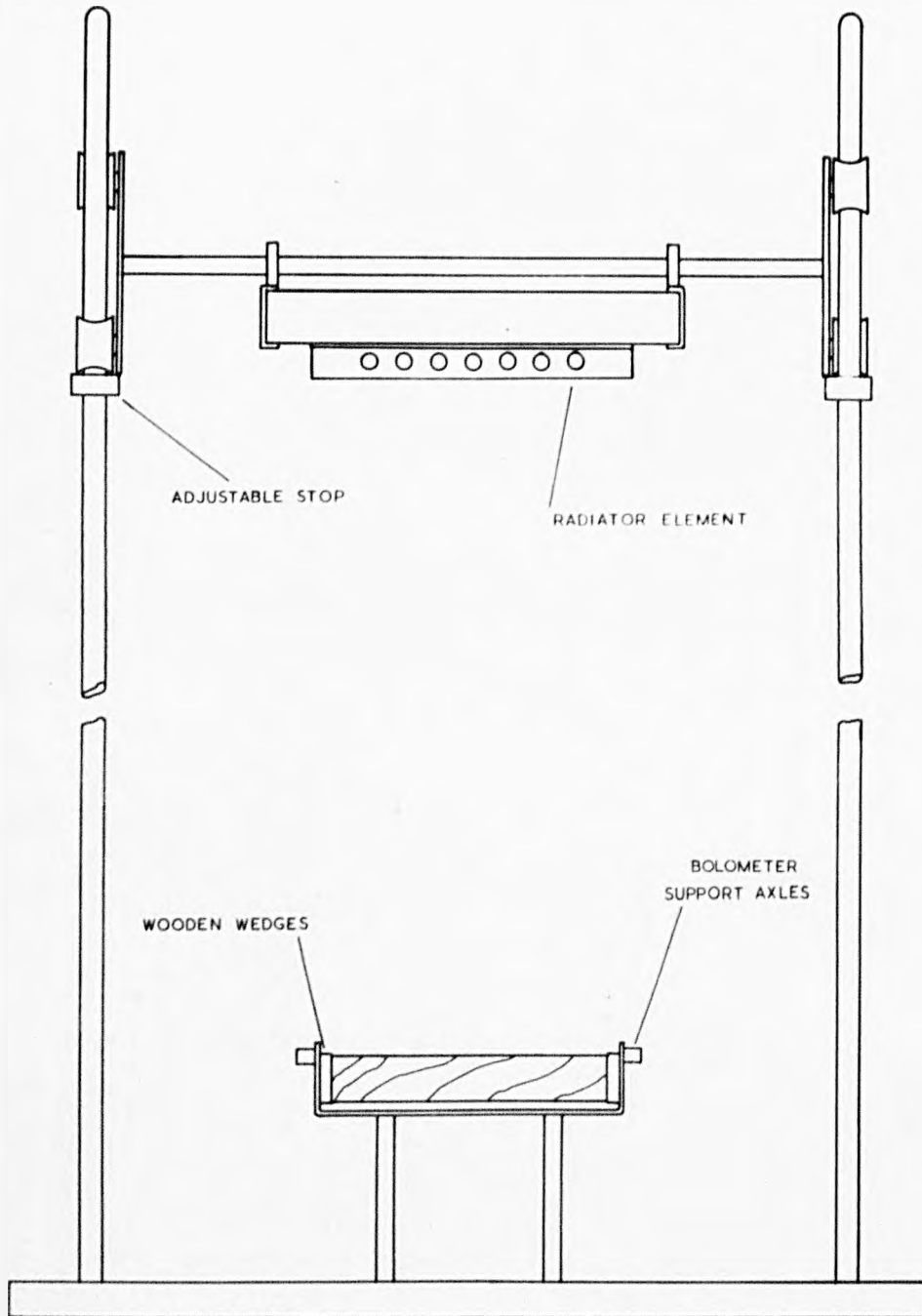


Figure 26.
The construction of the radiator and the support for the wood.

that time.

- (1) The calorific value of the wood destroyed
- (2) The total radiation emitted from the burning wood
- (3) The amount of heat passing into the wood.

(1) The Calorific Value of the Wood Destroyed

The total weight lost by the wood is about 2 grams under the conditions described and this loss in weight is accompanied by a change in calorific value of some partially burnt wood. Thus, in order to calculate the total change in calorific value of the wood, it is necessary to know both the calorific value of the unburnt dry wood and also the calorific value of the remaining partly burnt wood. These figures were obtained using a Scholes bomb calorimeter, which gave results reproducible to within 1%.

Two to three grams of wood in lump form contained in a silica crucible are burnt in a steel bomb under an initial pressure of 30 atmospheres of oxygen. The bomb is submerged in water contained in an adiabatic calorimeter and the temperature rise of the water noted during burning, a temperature correction being derived from Newton's law of cooling. This gave a calorific value of 4710 calories/gram for the unburnt wood, which was constant for all samples taken from twelve different parts of the stock of wood. At first it was attempted to determine the loss of weight of wood by a direct weighing before and after burning, but this could not be done with sufficient

accuracy. The original block of wood weighed approximately 400 grams, and because of absorption of water whilst on the balance, and changes in weight of apparently dry specimens in the drying oven, it was not found possible to guarantee this weight to within 0.05 grams even after uniform drying and cooling times.

In the method finally adopted, the wood was burnt and the charred portion scraped down to the unburnt wood. The mixture of wood and char thus obtained was weighed, and its calorific value found by the Scholes bomb calorimeter. It was found necessary to fit the crucible with a silica grill over the top of the briquetted char, which tended to jump out of the crucible because of its low density. The total weight of wood lost by burning and scraping from the original block was found by taking a wax impression of the cavity in the wood, and weighing the quantity of wax. The surface of the wood was dampened and the wax poured in, and after cooling, the wax was scraped down to the level of the unburnt wood with a straight steel edge. The remaining wax could then be easily peeled off the wood and weighed. It was found possible to duplicate the results to within 1% and as the wax appeared to form a good impression of the wooden surface, the corresponding weight of wood calculated using the measured density of wood and wax, should thus be known with the same accuracy.

From the results of the above procedure, the following

figures could be calculated:-

- (a) The total drop in calorific value of the block as a result of both burning and scraping off of the bulk.
- (b) The drop in calorific value of the burnt block as a result of scraping off the partly burnt surface.

The difference between the two figures gives the heat lost by the wood during the burning time.

(2) The Total Radiation emitted from the Burning Wood

The calculation of radiation from flames depends on their shape, temperature, size and character, and as none of these are known to any degree of accuracy for a flame burning on the surface of wood, it was attempted to make a direct measurement of this radiant heat during the total burning time. Similar measurements have been attempted before on coal and gas fires and in these cases the measuring instruments were either thermopiles, bolometers, water calorimeters or block radiometers. In the case of a source whose intensity changes during the course of the experiment, it is either necessary to completely surround the source with measuring instruments which continually record the radiation during the whole burning time, or else to traverse the whole field of view with one instrument quickly enough to allow extrapolation between readings in space and time.

Because of spacial considerations, (the radiator had to be brought with 25 cms. of the wood in some cases) the latter method was the only possible one, and thus it seemed necessary to use either a thermopile or a bolometer, as these were the only instruments with sufficient mobility. A small 17 element Moll thermopile was examined for suitability, but it was found that radiation which entered the instrument at an appreciable angle to the normal was not measured with the same efficiency as would be expected from a normal cosine rule, as much of it was reflected from the sides of the aperture through which the radiation passed. This meant that the instrument could not measure radiation from any source other than one subtending the same solid angle as the source used in calibration, which made it unsuitable for measurement of radiation from flames. Moreover its response time appeared to be about 0.8 seconds for 70% of the final reading, and this would have been too large to allow the instrument to follow the changes in radiation expected.

Attention was next turned to bolometers and in particular to a small thermister type, of resistance 1.4 megohms. The element measured 2.2×0.23 mms., and was supported in a small copper cavity by two uprights. In series with a load resistance of 1 megohm, such an instrument gives an extremely large and rapid response and because of its small size and rectangular shape, it is not screened by its case and presents a plane area to normal

radiation. The small size of the bolometer was a big advantage because in some positions it had to be interposed between the radiator and the wooden surface, and thus the larger the size of the bolometer, the more radiation would be prevented from reaching the wood. Such instruments have been widely used as detectors of interrupted sources of radiation, a method which has many advantages. The incident radiation is generally interrupted at a frequency of about 25 cycles/second, which allows a good degree of separation from the mains frequency of 50 cycles/sec. and is also low enough to allow a reasonable proportion of the time response curve of the instrument to be used. The output is then fed into a tuned a.c. amplifier which only responds to changes in amplitude of the selected frequency, and this eliminates any difference due to slow changes of ambient temperature. It was not found^{possible} to apply this method in the present case, because any interruption device would have increased the size of the bolometer casing which as stated before, is undesirable, and it was thus decided to use the bolometer as a d.c. instrument.

The problem of measuring the total radiation over the surface of a hemisphere is greatly simplified if it can be assumed that the distribution of intensity is symmetrical about the radius perpendicular to the base of the hemisphere. The apparatus was designed to give a uniform radiation over the surface of the block, and as has been stated before, the flame

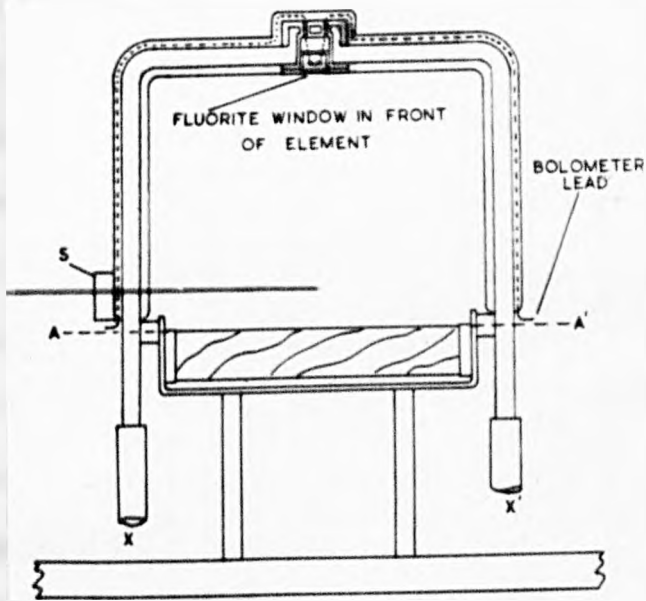


Figure 27.
The construction of the bolometer housing.

in general appeared to spread symmetrically from a point source, and so presumably would radiate in a symmetrical manner. It is understandable that any protruberance of the flame front would not proceed as quickly as its neighbouring sections, for it would not receive the same supporting radiation as they themselves were receiving.

Conversely, any depression in the burning front would accelerate and tend to assume a smooth curve with the rest of the burning zone. From these considerations, measurements of radiation made along one 90° arc of the hemisphere should be representative of the radiation over the whole surface, although the accuracy of this assumption depends on the number of experiments made under any given set of conditions. Figure 27 shows the method used to support the bolometer, which was enclosed in a water cooled brass jacket J lagged on the outside with glass wool, as were the supporting arms, consisting of copper tubes carrying the water supply. The bolometer is shown at the top of its traverse and is capable of being rotated through 90° around AA^1 as axis to a horizontal position. In front of the element was a Fluorite window which excluded draughts, and, as Fluorite is transparent to conduction down to a wave length of about 8μ , transmitted almost all radiation both from a black body at 900°C and from a flame containing carbon dioxide and water molecules. The borders of the Fluorite window had an internal chamfer which reduced reflection to a

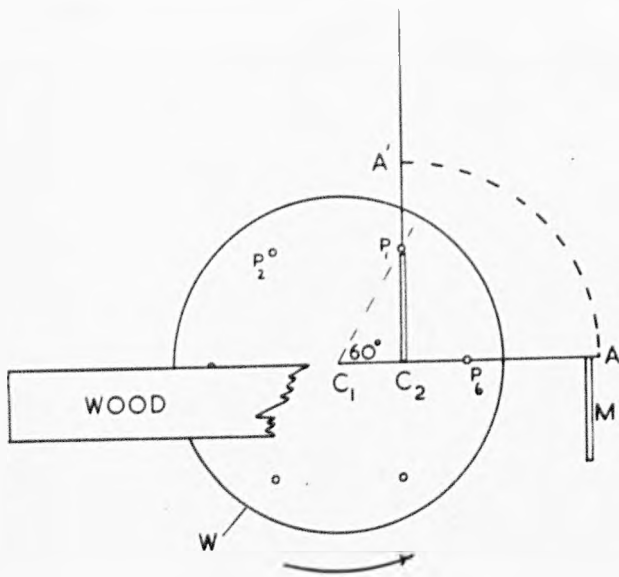


Figure 28.
The bolometer sweep mechanism.

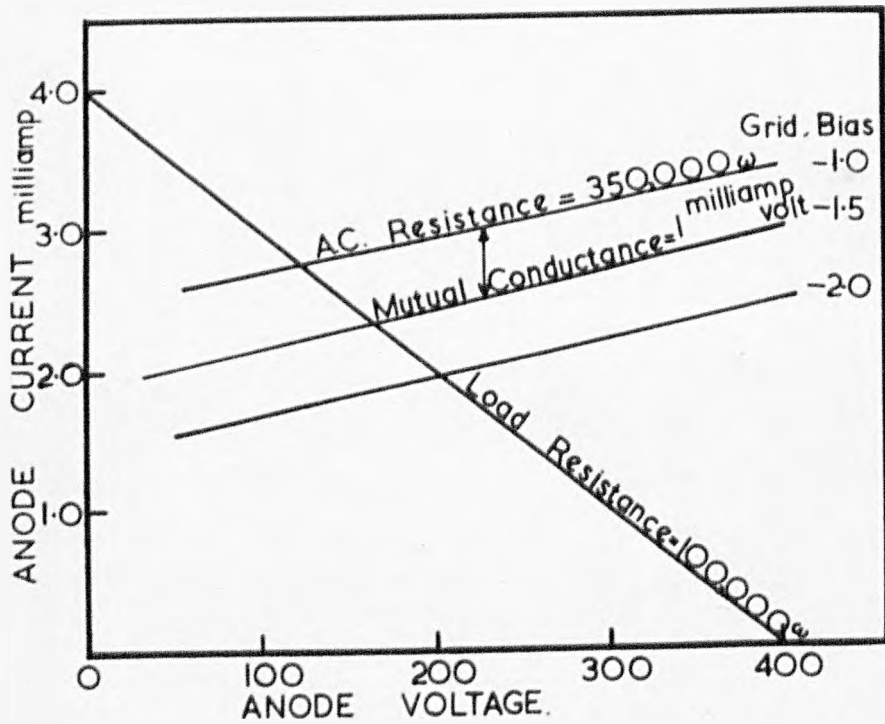


Figure 29.
The load line diagram

minimum, whilst the inside of the copper case of the bolometer was blackened for the same reason.

Now as the experiment proceeds it is desirable to obtain as many readings as is possible at each position on the arc swept out by the bolometer, and a mechanism was devised to raise and let drop the bolometer along this arc every 20 seconds. The essential features of this device are shown in Figure 28. The bolometer supporting arms are represented by the line A^1C_2 and the bolometer travels along the arc AA^1 . The bolometer arm is driven by the pins P_1 and P_6 , fixed to the driving wheel W , which rotates in an anti-clockwise direction. The pin P_1 forces forwards and upwards a metal stop brazed onto the arm of the bolometer and marked in Figure 28 as S . As the wheel rotates C_2A^1 is carried along with it, but not at quite the same rate, as C_1 and C_2 are not coincident. At the same time P_1 slides up the metal stop and reaches the top edges of the stop when A^1C_2 is vertical. The bolometer then slips back to its original position C_2A where it comes into contact with P_6 where the cycle is recommenced. A considerable degree of control of the timing of the cycle can be accomplished by altering the distance between C_1 and C_2 , and it was found desirable for the bolometer to be left at a position slightly below C_2A at the end of each cycle, where its aperture is covered by a water cooled metal screen. This allows a zero reading to be taken every 20 seconds, and corrections can thus be made for drifts due to

temperature changes in the instrument. The bolometer was brought to rest slightly below A by a rubber topped spring stop which minimised the otherwise considerable shock sustained by the element. The movement was also made less violent by the provision of a counterbalance fixed at the other end of the brass arms.

The Apparatus used to measure the heat conducted into the wood

This problem is simpler in one respect than the measurement of total radiation, in so far as the initial and final temperatures of the wood are all that are needed to give the quantity of heat stored in the wood if the specific heat of the block is known. The measurement of temperatures in low diffusivity materials is made difficult because of the large disturbances in the heat flow caused by the introduction of metal measuring instruments such as thermocouples. Any heat flow along a thermocouple in such a block must be greater than the parallel heat flow in its surroundings at roughly the same temperature, and hence as heat is being lost along the couple leads, the introduction of a thermocouple must lower the temperature in the material. Ideally the couple leads should be brought out along isothermals in the wood, thus minimising heat flow, a result which can also be obtained by reducing the diameter of the thermocouple leads.

It was not found possible to drill holes longer than about $1\frac{1}{8}$ " accurately into the 6" block without using a drill of at

least 1/16" diameter. These holes would have to run parallel to the front surface, and so would have to be at least 3" long to reach the centre of the block, and the depth of the end of the hole beneath the front surface of the wood could not be determined very accurately. Holes could be drilled however, to a depth of over 1" by using stainless steel hypodermic tubing of 0.02" diameter, and if these holes were drilled in from the back surface of the wood, their depth was known quite accurately. It was then possible to fit silver soldered copper/constantin thermocouples in such holes, the diameter of the wire was less than 0.005" in both cases, the constantin wire being cotton covered and the copper enamelled. Nine couples were inserted in the block in the following positions.

Position No.	Position in Horizontal Plane	Depth from burning surface (mm)
1	Centre of block	1
2	Centre of block	5
3	Centre of block	10
4	Centre of block	23
5	3 cm. along a diagonal	1
6	3 cm. along a diagonal	5
7	6 cm. along a diagonal	1
8	6 cm. along a diagonal	5
9	6 cm. along a line from the centre of the block and perpendicular to the direction of the grain	5

The temperature was likely to change most violently in the neighbourhood of the top surface, and consequently more couples should be situated near that surface. Also the temperature along a diagonal would best represent temperatures in the body of the wood, and a check on the temperature at a point in a different position but at the same distance from the centre of the wood would tell whether appreciably more heat was travelling along the grain than across it. Considering the higher conductivity along the grain it would seem likely that position 9 would be cooler than position 8, a point which was decided by the results quoted later.

Measurements and recording of the readings

The temperatures were measured by small potential differences between 0 and 10 M.V. at the ends of the thermocouple leads, whilst the bolometer readings were available in a similar form. Now in order to obtain a continuous record of the radiation readings, any recording instrument must follow the change in voltage across the bolometer resistance as quickly as possible. Moreover, this instrument must be suitable for measuring F.M.Fs. from a source of high internal resistance, as the resistance of the bolometer is of the order of 1 megohm and its load resistance varies from 600 to 20,000 ohms. in different experiments. The obvious choice under such circumstances was a Cathode Ray tube and amplifier, the latter needing an amplification factor of about $\times 10^4$ in order to supply the

100 volts needed for full scale deflection. Such amplification factors are not in general possible with D.C. amplifiers in a single stage and a two stage amplifier is inherently unstable unless supplied with a very stable source of voltage. Any change of supply of voltage to the anode of the first stage is immediately communicated to the grid of the second stage and consequently amplified. Moreover, such changes are brought about by varying the current taken by the valves during their normal operation and the change in voltage so produced is in such a direction as to cause a further similar change of anode voltage and hence cause instability.

A.C. amplifiers are not subject to such disturbances as there is no direct connection between various stages, any coupling is done by condensers or tuned circuit which can be adjusted to eliminate all variations except those of a desired frequency. However, as has been stated earlier, many complications arose in converting the signal to A.C. by interrupting the source of radiation and it was decided to use a D.C. amplifier.

The use of a balanced push-pull circuit eliminates many of the difficulties arising with a more normal type of amplifier and such a circuit has been used for Bioelectric recording¹⁶ with amplification up to $\times 10^6$ using battery operation.

Consequently a two stage D.C. push-pull amplifier was built and in the form adopted was supplied from the mains A.C. voltage.

Amplifier Design

The voltage amplification of any valve depends on the A.C. resistance, its mutual conductance and its load resistance. The mutual conductance decides the change in current through the valve for a given change in grid voltage and the change in current decides the change in voltage across the load resistance depending on the value of the A.C. resistance of the valve and of the load resistor. The operation of such an arrangement is best shown by Figure 29 and the load line diagram, which represents the voltage of the anode of a single valve as a function of the current through the valve under various conditions. The actual amplification achieved by such an arrangement can be represented by the change in the voltage of the anode from A to B along the load resistance line, achieved by a grid potential change of one volt. The high tension voltage is represented by the intersection of the load line and the voltage axis, that is, it represents the voltage of the anode when there is no current passing through the valve and hence through the load resistance. Now the voltage drop across A B can be increased both by an increase in the A.C. resistance of the valve and in the load resistance. In practice however, the valve only works efficiently between certain limits of anode current and voltage which in turn effects the value of high tension needed. The high frequency Pentode type of valve is the most suitable for this type of voltage amplification, combining a high A.C. resistance with a good mutual conductance,

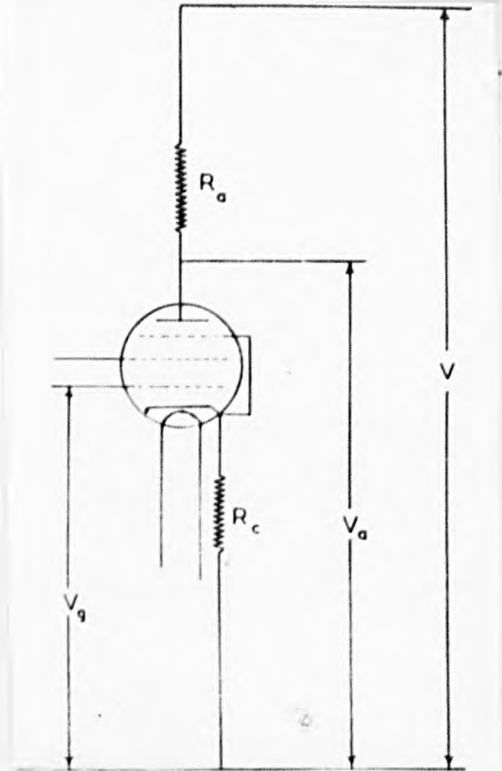


Figure 30.
Amplification circuit with cathode resistance.

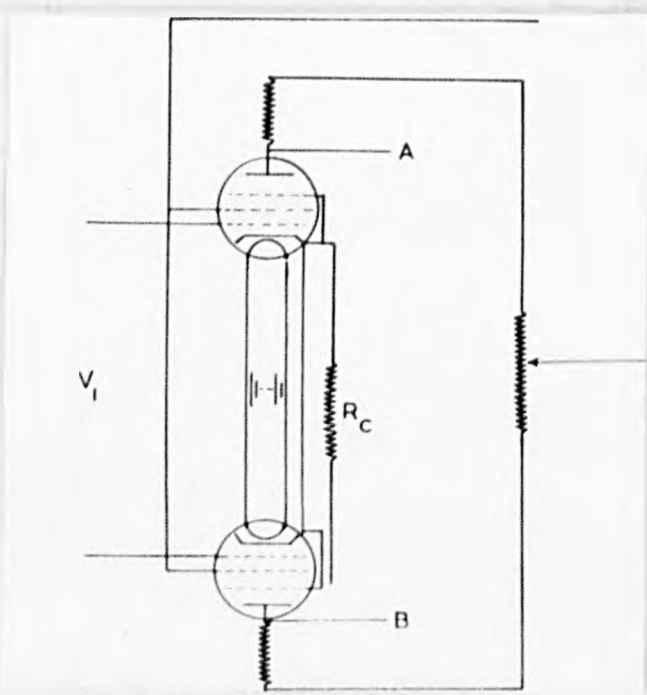


Figure 31.
Push-pull amplification circuit.

together with straight line characteristics over a wide range of conditions and in particular the 6 K.7G valve was chosen. Now Figure 30 shows a circuit containing a cathode resistance R_c and hence any current passing through the valve also passes through R_c and thus affects the voltage of the cathode relative to the grid. Now if V_g is kept at some constant value and V reduced by some small amount, first of all the current through valve and resistors will fall by some amount depending on the resistance of the circuit. As however, the current through R_c drops, so must the voltage of the cathode drop, thus increasing the potential of the control grid relative to the cathode, which in turn tends to increase the current through the valve and thus oppose the reduction in anode voltage. Thus R_c has a stabilizing effect on the circuit with respect to changes in anode voltage which can be made almost completely by increasing the value of R_c . In the above circuit however, this had the effect of nullifying the amplifying properties of the circuit for changes in anode current produced by changes in grid voltage are opposed in almost exactly the same way.

It is here that the advantages in the push-pull amplifier became apparent, for considering Figure 31, it will be seen that changes in V_a are opposed in the same way as before by changes in current through R_c if V_I remains fixed, but if V_I is altered the change in voltage across A B is not affected by R_c because, assuming the circuit to be symmetrical, the same change

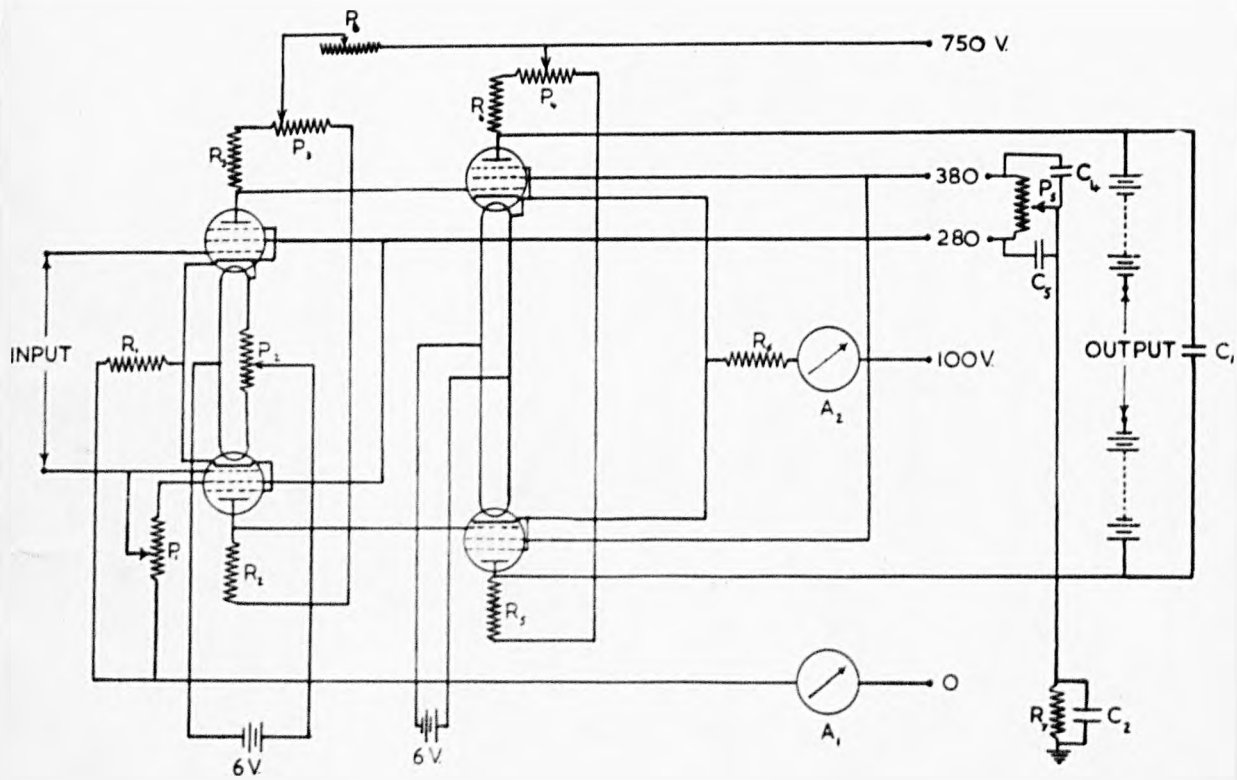


Figure 32.
Two stage amplifier circuit.

is brought about in the voltage of A and B by R_c and hence their relative voltage is unaltered. A change in V_I however, affects the symmetry of the circuit and hence the voltage across AB. The two stage unit is shown in Figure 32 with the following values for the various resistances, condensers and potentiometers.

R_1	20.000 ohms	$C_1 = 0.01$ m.f.d.	$P_1 = 50.000$ ohms
R_2	90.000 "	$C_2 = 5$ m.f.d.	$P_2 = 5$ "
R_3	90.000 "	$C_3 = 2$ m.f.d.	$P_3 = 10.000$ "
R_4	70.000 "	$C_4 = 2$ m.f.d.	$P_4 = 10.000$ "
R_5	70.000 "	$C_5 = 2$ m.f.d.	$P_5 = 10.000$ "
R_6	14.000 "		$P_6 = 1000.000$ "
R_y	1.000.000 ohms		

A_1 and A_2 are 0 - 10 milliameters.

The first stage of the amplifier had to be balanced very carefully, that is, disturbances due to changes in high tension supply had to be almost completely eliminated. The two valves in the first stage were thus carefully matched, as were their load resistors R_3 and R_2 by means of P_3 . P_2 was provided in the heating filament circuit to enable the valve circuit to be properly matched and also to allow their anode potentials to be equalised with no input to the circuit. The second stage was matched in a similar manner except that it was not found necessary to include a potentiometer in the heating circuit of the valves. The values of the grid/cathode voltage in the second stage were adjusted by means of P_6 and as the valves were

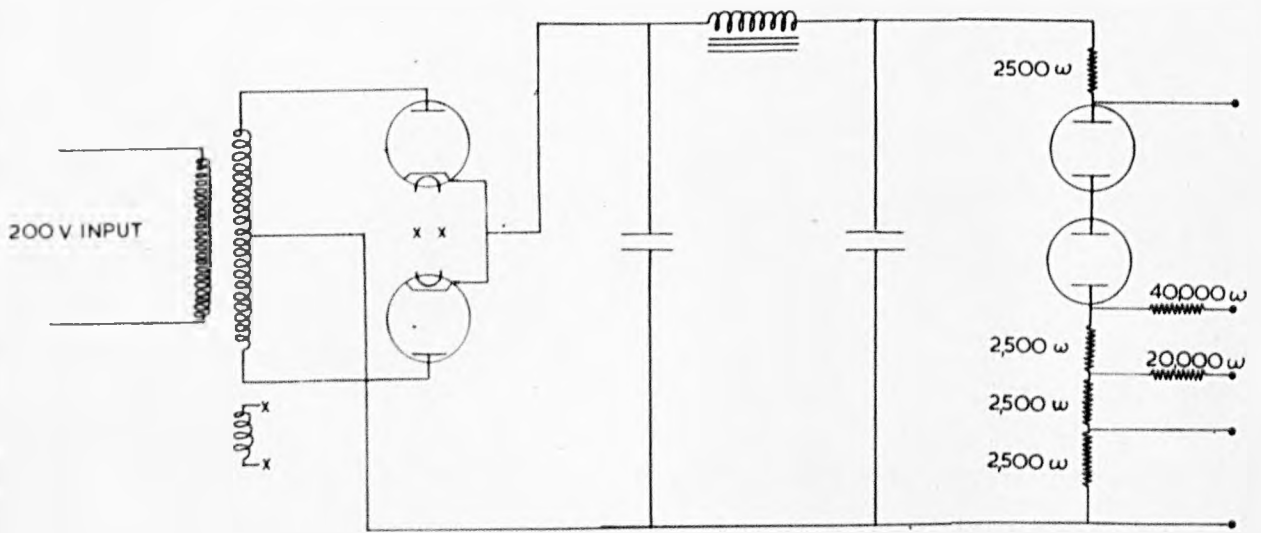


Figure 33.
The amplifier power pack.

variables μ types, this potentiometer also controlled the sensitivity of the system. The amplifier was very sensitive to stray electrical and magnetic fields and hence all leads were shielded by flexible copper sheathing, and, in the case of the amplifier and C.R.Tube, by iron and μ metal screens. It was also essential that these shields should be sufficiently earthed besides the amplifier itself, and a complication arose as the grid leads of the first stage were not at earth potential. This was necessitated because the output voltages had to operate a Cathode Ray Tube and thus had to be approximately at earth potential in order that the spot could be focussed sharply on the screen. For efficient operation of the valves, the anode voltages must be considerably higher than the grid voltages and so the final anode voltage is some 150 to 200 volts above the original grid voltage. This difference was reduced to a large extent by the use of high tension batteries at the output, but as it was considered dangerous to the apparatus to have the possibility of a direct short between grid and ground, the danger was somewhat lessened by earthing through the large resistance R_7 and bypassing the A.C. component through C_2 . This did not eliminate disturbances of mains frequency apparently arising across the input and this was minimised by the condensers C_2 and C_3 , which did not seriously affect the response time of the instrument. High tension power was supplied to the amplifier by a two valve double wave 850 volt rectifier, whose output was smoothed by two 10 m.f.d. condensers and a suitable choke. A stabilizing

current of about 50 milliamps was passed through a potential divider system which included two neon voltage stabilisers in series with the appropriate resistances as shown in Figure 33, and very little A.C. interference seemed to arise from this source. The filament current of the amplifier valves was supplied by separate 6 volt batteries as these had to be at different potentials.

The amplifier was built into a converted Naval radar chassis containing a cathode ray tube, V.C.R.97, and some trouble was experienced at first in eliminating stray fields arising in the C.R. tube, but this was overcome by suitable screening. It was found possible to increase the sensitivity of the C.R. tube by reducing the anode voltage to below 1.000 volts and if deflection was impressed by the X plates the focussing was only affected slightly although it was found necessary to operate the filament from a D.C. source as at the low anode voltages the electron beam was also more sensitive to filament voltage changes. This arrangement proved very satisfactory, the instrument being able to detect 0.1 millivolts input quite easily. Valve noise however, was just detectable and it was realised that the instrument may have been improved by the use of a special low noise valve. The power pack for the C.R. tube was of the normal type with only a moderate degree of smoothing, and supplied by a single wave valve rectifier.

It was possible to feed the thermocouple voltages via a

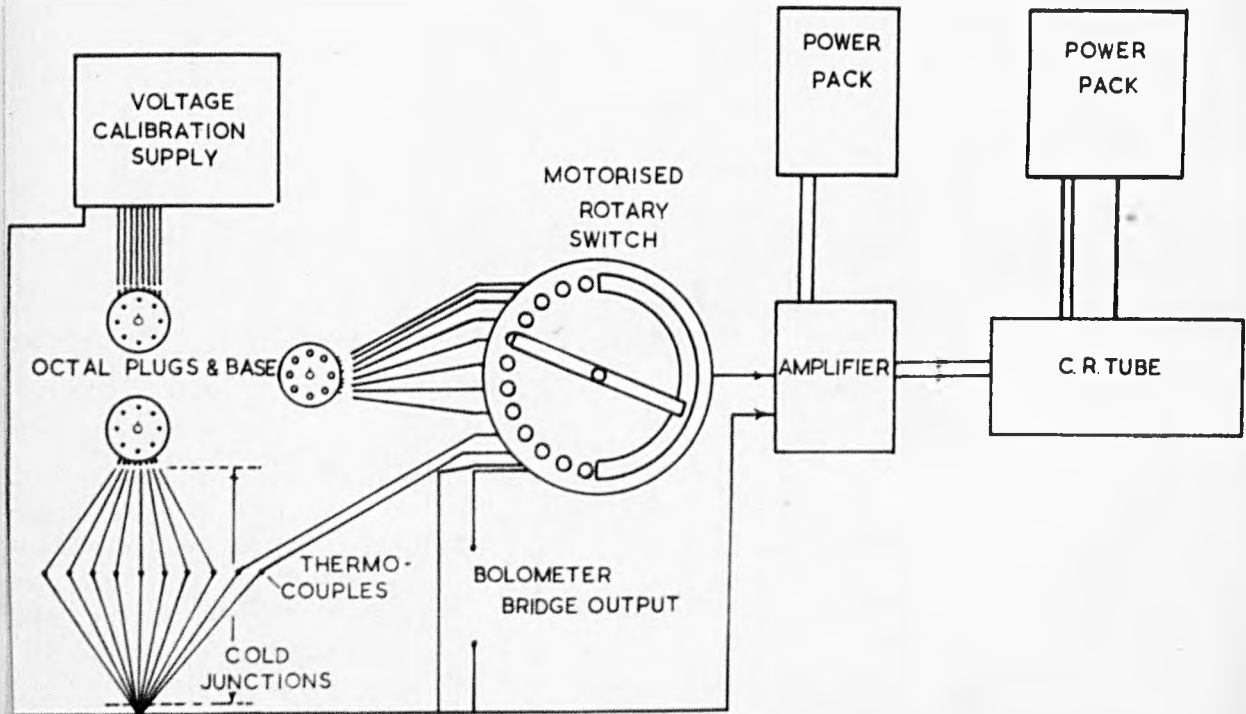


Figure 34.
General wiring diagram.

rotary switch to the amplifier as shown in Figure 34, but a bridge circuit was necessary to operate the bolometer as shown in Figure 35. R_L is the load resistance of the bolometer which determined the sensitivity of the instrument in much the same way as the load resistor circuit. In the present case maximum sensitivity is attained when $R_L = R_B$ (the bolometer resistance).

It is possible to show that the sensitivity of the instrument is very nearly proportioned to R_L for small values of the latter, for, considering Figure 35, we have

$$\frac{V}{R_B} = \frac{V}{R_b + R_L}$$

$$\frac{dv}{dR_b} = V \left[\frac{(R_b + R_L) - R_b}{(R_b + R_L)^2} \right]$$

$$\text{Sensitivity} = \frac{dv}{dR_b} = \frac{V R_L}{R_b^2 + 2 R_b R_L + R_L^2}$$

$$\text{Now } R_b = 1.4 \times 10^6 \text{ ohms}$$

$$\text{and } R_{L1} = 590 \text{ ohms}$$

$$R_{L2} = 1010 \text{ "}$$

$$R_{L3} = 2980 \text{ "}$$

$$R_{L4} = 18850 \text{ "}$$

$$\begin{aligned} \text{and sensitivity (1)} &= \frac{V R_{L1}}{(1.4 \times 10^6)^2 + 2.8 \times 10^6 \times 590 + 5.90^2} \\ &= \frac{V R_L}{(1.4 \times 10^6)^2} \quad \text{very nearly} \end{aligned}$$

$$\text{and sensitivity (4)} = \frac{V R_{L4}}{(1.4 \times 10^6)^2 + 2.8 \times 10^6 \times 18.850 + (18.850)^2}$$

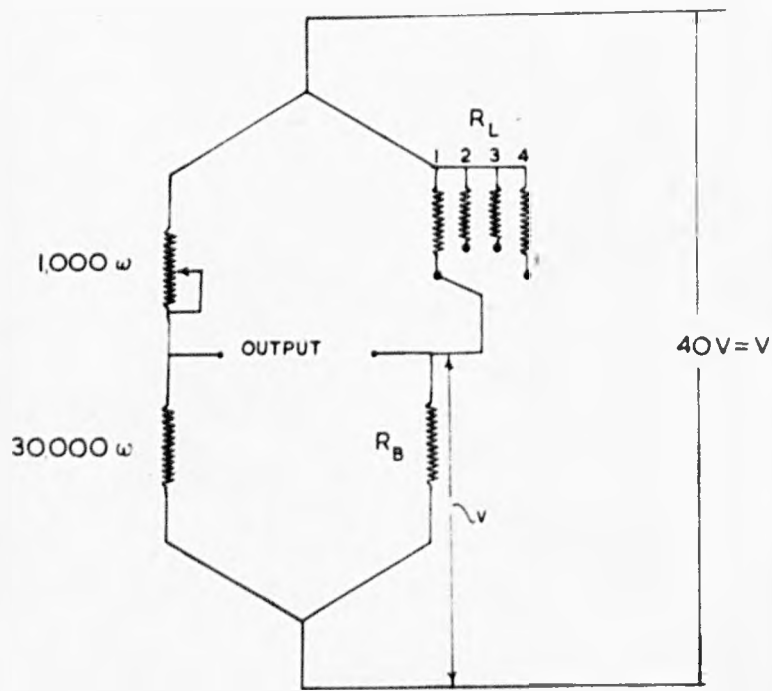


Figure 35.
The bolometer bridge circuit.

$$= \frac{V R_{L4}}{(1.4 \times 10^6)^2 \times 1.025} \quad \text{very nearly}$$

Thus the sensitivity of the instrument is very nearly proportional to R_L but in the case of the higher sensitivity this assumption is in error by 2.5%, a factor which was allowed for in the calculations.

The bridge circuit voltage was supplied from the main H.T. voltage supply to the amplifier and was balanced by the potentiometer P_1 , the output from this circuit being fed to the rotary switch shown in Figure 34. This rotary switch was driven by a synchronous motor which also drove the bolometer sweep mechanism through two sets of reduction gears. A plan of the arrangement is shown in Figure 36. There are twelve contacts on the rotary switch, which are connected as follows -
 Position No.1 - Short circuit and zero voltage reference point.
 Positions Nos.2 and 7 - Bolometer connections.
 Position Nos. 3 - 6 and 8 - 12 Thermocouple connections.

The switch rotates once in 1.95 seconds and thus a bolometer reading is taken approximately once every second and every thermocouple voltage is recorded once every two seconds. The thermocouple leads are led out to cold junctions and then to the rotary switch which worked quite smoothly and did not measurably distort the voltage input to the amplifier.

The Recording of the Cathode Ray Trace

At first the spot was deflected by the input voltage in a vertical direction and moved in a horizontal direction at a constant rate across the screen by a changing voltage across

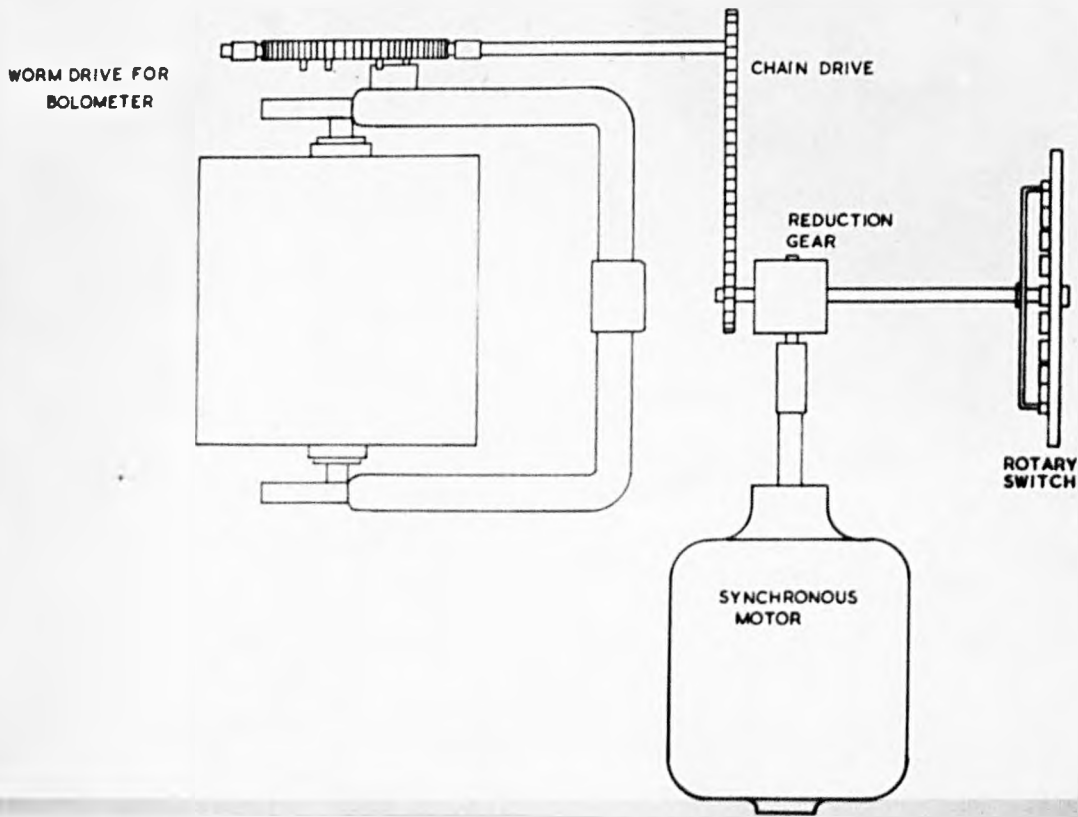


Figure 36.
The gearing of the bolometer sweep and rotary switch mechanism.

the X plate developed by a motor driven potentiometer.

In this way the apparatus produced a trace of 11 dotted lines representing the twelve voltages on the studs of the rotary switch, two of which, the bolometer readings, traced the same line. The trace was at first recorded by an ordinary $\frac{1}{4}$ plate camera, but this method was abandoned because it was not found possible to distinguish individual spots on the negative.

This difficulty was overcome by elongating the trace by means of a 35 mm. rotating drum camera, shown in full detail in Figures 37 and 38. This camera was originally used for measuring flame speeds through gases contained in tubes and incorporated an f 1.8, 5 cm. lens which projected the image of the trace on to an 8 inch length of 35 mm. film supported on a drum, which by adaptation of the driving mechanism, was made to rotate once in four minutes. A typical trace is reproduced in Figure 39, where individual lines can be easily distinguished. Any fast panchromatic film was capable of giving a good exposure with sufficient contrast.

The traces were read by a magnifying inspection glass with an illuminated scale graduated in millimetres and it was found easy to estimate the position of the spot to 0.1 millimeter.

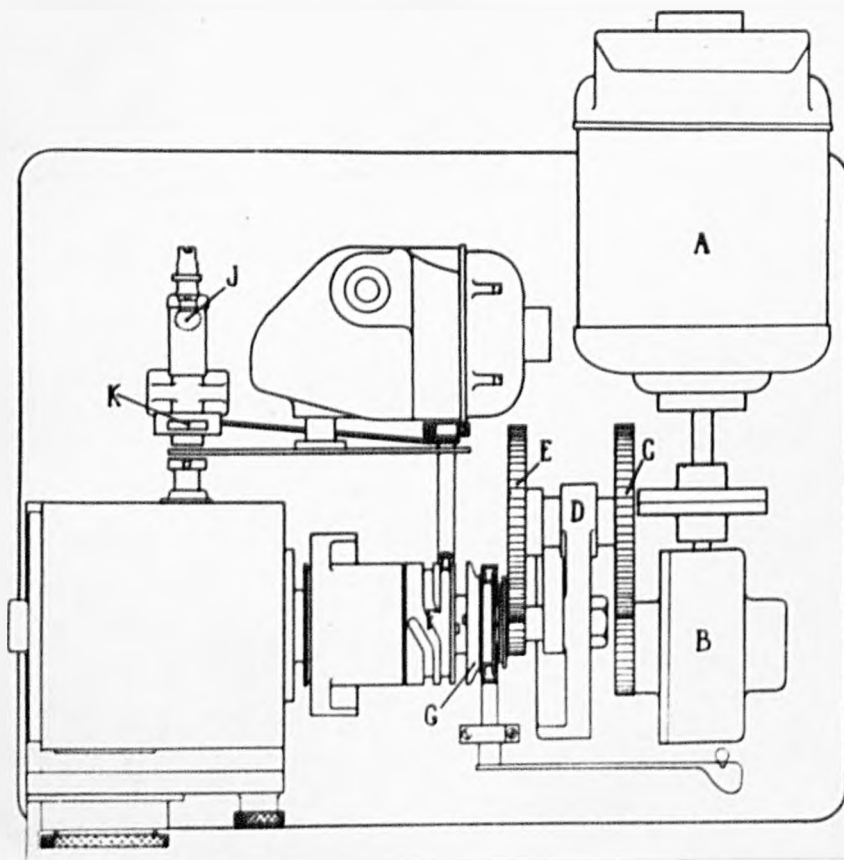


Figure 37.
Plan of the rotating drum camera and drive.

Experimental procedure

Experiments were carried out at varying radiant intensities and also with woods of different moisture content, but the experimental procedure was almost exactly the same in each case.

The piece of wood from the six inch plank was weighed and had the measurements checked and the thermocouples inserted. The amplifier and radiator were then switched on and left to warm up for at least three quarters of an hour with the radiator pointing away from the apparatus, and during this time the wood was fixed in place beneath the radiator and levelled with a spirit level. The thermocouples were connected to the cold junctions and the circuit checked for continuity. The cooling water for the bolometer and metal screen was supplied from a constant head and left running until the water temperature became constant and during this time the rotating drum and normal 35 mm. film cameras were loaded. The second camera was used as in the preliminary experiments to measure the area rate of spread of the flame and was clamped to the top of the radiator upright as was a photoflood lamp and reflector necessary to illuminate the burning wood. After the original warming/^{up}period, the wood was shielded from radiation by a double asbestos sheet and the radiator hung facing vertically downwards. The synchronous motor was set going and the drop back position of the bolometer noted for each of the six pegs on the driving wheel. This was found to be necessary as the driving pegs for raising the bolometer had slight

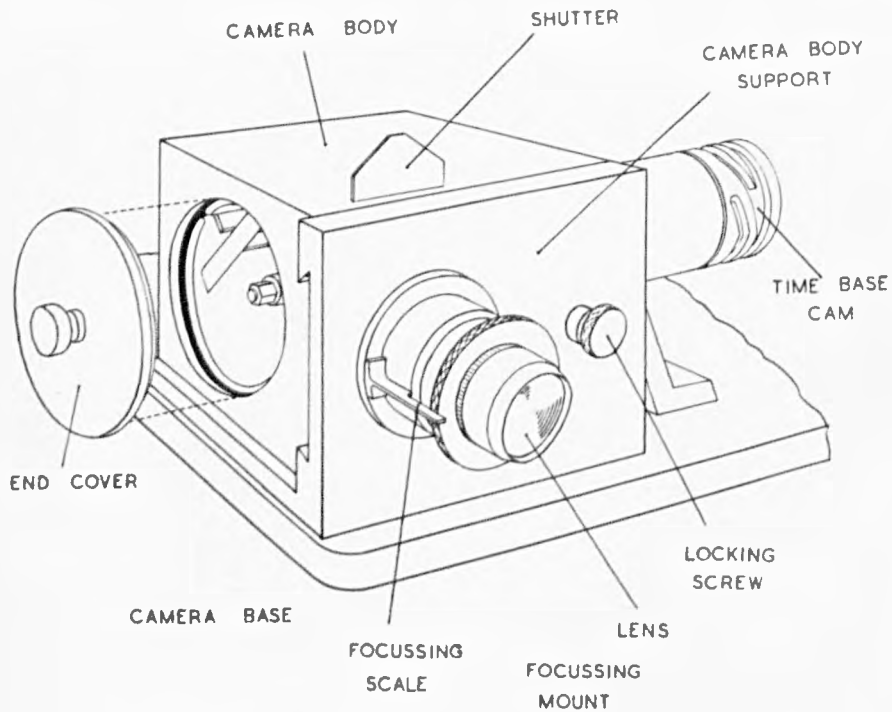
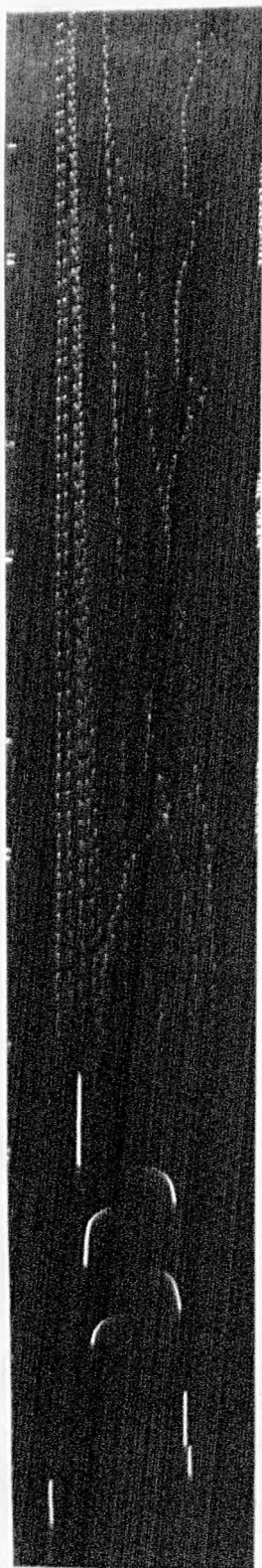


Figure 38.
General view of rotating drum camera.

J.S.Forsyth - Ph.D. Thesis - Leeds -1943.

inaccuracies in placing on the driving wheel. The angle of the bolometer to the wood was read directly on a 90° scale at the side, and in all cases the bolometer first became exposed to the radiation at an angle at 5° to the wood. Next the cathode ray tube was switched on and the spot and both cameras focussed. The spot was adjusted to within 1.5 cms. of the edge of the screen, with no input voltage to the amplifier, and then the bolometer bridge adjusted so that the spot was at the opposite side of the screen with no radiation falling on the bolometer. The electromotive forces developed by the bolometer and the thermocouples were made to be opposite in sign as this separated the thermocouple trace from the bolometer trace until both readings became large enough to overlap. The apparatus was left for some time in this position and final adjustments made to the balance so that a heavy load placed across the mains supply made no difference to the position of the spot on the screen. The spot always tended to drift across the screen as the apparatus warmed up, but after fortyfive minutes equilibrium was almost reached and any further drift was very slow. The cold junction temperatures and the inlet water temperature to the bolometer were taken and the space between the cathode ray tube and the drum camera covered by a black cloth and shield to prevent extraneous light fogging the film. The radiator was then brought down to its final position and the photofloods switched on, the asbestos shield withdrawn from over the wood and the stop watch, placed in the field of view of the second



Radiation from wood.

Radiator radiation.

Reference voltage.

Figure 39.
Print of a typical cathode ray trace.

camera, was started simultaneously. The rotating drum camera was started at some fixed time which would enable it to record all the burning time of the wood and as much of the preheating time as could be fitted on one rotation of the drum, that is, in a period of four minutes. The driving mechanism for the bolometer and rotary switch was started just before the drum camera was opened and the initial position of the mechanism recorded. At a prearranged time at which it was certain that the wood would ignite immediately, a pilot flame was applied to the centre of the wood, and immediately withdrawn when a flame appeared on the wood surface.

Photographs were then taken of the flame as it spread over the surface of the wood at such intervals that from six to twelve exposures were made during each burning. As the flame came within about 1.5 cms. of the edge of the wood, the asbestos shield was inserted over the top of the flame which was extinguished, whilst the time was noted.

The driving mechanism of the bolometer and drum camera was also stopped and the radiator raised to its highest point. The bolometer was then disengaged from the driving mechanism and held vertically underneath the radiator pointing directly along its mid normal. The rotary switch was turned to one of the bolometer positions, the rotating drum camera started and the bolometer exposed for two three-second periods to the radiator.

MILLIVOLTMETER

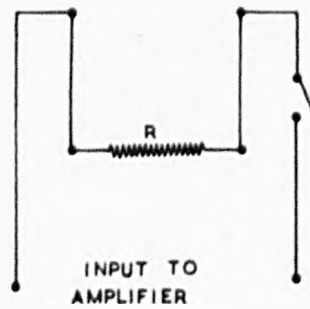
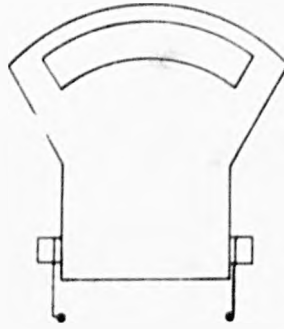


Figure 40.
The input and calibration circuit to the amplifier.

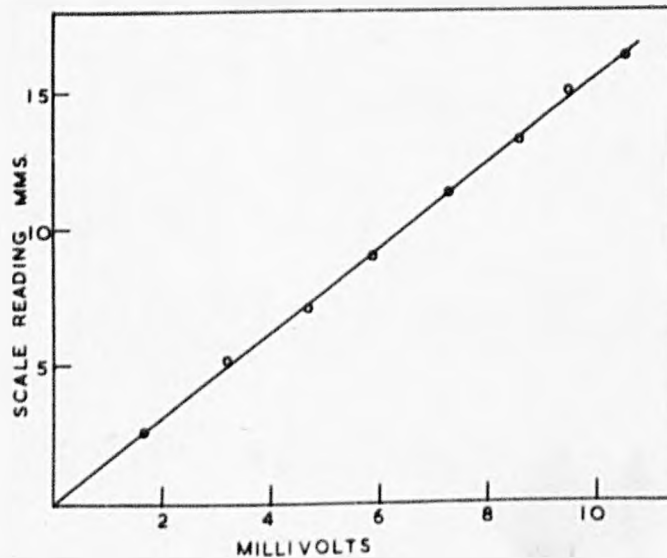


Figure 41.
Response curve of the amplifier and cathode ray tube.

A reliable millivoltmeter was then switched across the input to the amplifier as shown in the circuit Figure 40, and the reading of the millivoltmeter adjusted to about 10 millivolts by the potentiometer provided for adjusting the balance of the bolometer bridge circuit. The drum camera was again started and the resistance R in Figure 40 which was approximately equal to the millivoltmeter resistance was substituted for the millivoltmeter. This was to avoid recording the back E.M.F. generated by the millivoltmeter when changes in input voltages caused the suspension to swing. The rotary switch was now moved to the zero position and thus a record of a known voltage was impressed on the film which was developed, fixed and dried in the normal manner, together with the recording of the flame spread over the wood.

The burnt wood was then treated as described above to discover the loss in calorific value during burning.

Before full calculations could be made of the heat changes during the burning however, several subsidiary experiments had to be performed to determine the sensitivity of the apparatus and to measure the extraneous heat reflected and emitted from the surroundings, these experiments being described below.

The response of the Amplifier and Cathode Ray Tube

In the first few experiments nine different voltages were fed into the amplifier at the end of each experiment by means of the voltage calibration unit marked in Figure 34, and the response of the amplifier recorded. The voltage calibration supply was simply a potential divider system with a millivoltmeter in circuit across the input to the amplifier. The different voltages were first read off on the millivoltmeter and then a resistance equal to that of the millivoltmeter substituted for reasons described above. In all cases it was found that the scale deflection was directly proportional to the input voltage over a range of 10 millivolts. A typical set of figures is shown in Table 14 and Figure 41.

TABLE 14

<u>Millivolts</u>	<u>Scale Reading</u>
0.0	0.0
1.7	2.4
3.1	4.5
4.5	6.3
5.8	8.0
7.0	9.8
8.3	11.8
9.1	13.0
10.1	14.2

This result was unexpected, for the characteristics of the valves have slight curvature as has also the fluorescent screen of the cathode ray tube. However, the grid swing of the second stage probably never exceeds 1 volt, and the expected deviation would not have been very large. As can be seen from the figures just quoted, the system gave a full scale deflection of about 10 m.v.s. with a probable accuracy of reading 0.05 mvs. A smaller change of voltage could be detected by the movement of the spot, but any greater accuracy than that quoted could not be attained because of distortion of the spot partly due to mains hum and sudden changes in the mains voltage. In all the above calibration experiments, an exposure of 3 seconds was given to the bolometer at each intensity, and the reading of the Cathode Ray trace taken before the same interval.

It was found necessary to give a definite time of exposure for although the response of the bolometer was exceedingly sharp over the first 0.4 seconds, after this there was a slow increase in reading as the case warmed up, despite the water cooling system. On shielding the bolometer from further radiation there was again a sharp change in the voltage developed corresponding to 60% change in 0.2 seconds, which was again followed by a slow drift back to the original condition. This defect has been noticed in nearly all other types of bolometer and thermopile, thus making it essential for readings to be taken after fixed heating and cooling times or some other

correction made to account for the temperature drift.

The efficiency of the bolometer response was investigated by the following calculations:-

The equation relating the temperature of the element and time under a given radiation was assumed to be $\frac{d\theta}{dt} = k(a - \theta)$ --- (5)

Where θ is the temperature of the element

and t is the time

and k and a are constants, a actually representing the

equilibrium temperature reached after an infinite time.

Now if we let a be a function of time, this corresponds to varying the incident radiation with time and leads to the following equation :-

$$d\theta + k\theta dt = kf(t)dt$$

Now multiplying by the integrating factor $\frac{e^{kt}}{k}$, the equation becomes

$$\frac{e^{kt}\theta}{k} = \int (f)t \cdot e^{kt} dt + b$$

Assuming 60% response in 0.2 seconds, from equation (5)

$$\log \frac{a}{a - \theta} = kt \text{ whence } k = 4.58$$

Now suppose ' a ' is a function of time such that $a = b + ct$,

we then get

$$\frac{\theta e^{kt}}{k} = \int (b + ct) e^{kt} dt$$

$$\text{whence } \theta = b + c \left(t - \frac{1}{k}\right) + e^{-kt} \left(\frac{c}{k} - b\right)$$

If we let $\theta' = b + ct$, this will represent the temperature

which would have been attained by an instrument with zero response time, and hence

$$\frac{\theta}{\theta'} = \frac{1 - \frac{c}{k} \left(\frac{c}{k} - b \right) e^{-kt}}{b + ct}$$

Under the conditions of the experiment, the rate of change of radiation was never greater than an increase of 25% in 10 seconds, except at the instant of exposure of the bolometer in each cycle, and so by letting $\frac{5b}{4} = b + 10.c$ which represents the above condition, we get $b = 40c$, and hence

$$\frac{\theta}{\theta'} = \frac{1 - \frac{1}{180} - \left(\frac{1}{180} - 1 \right) e^{-4.58t}}{1 + \frac{t}{40}}$$

after 3 seconds we get

$$\frac{\theta}{\theta'} = 0.995$$

i.e. the response is correct to within $\frac{1}{2}\%$ within 3 seconds.

Thus the actual response of the element is highly satisfactory and the slow drift was almost completely accounted for in the following way :-

As stated above, the bolometer came to rest behind a cooled metal screen for 3 seconds at the end of each cycle, and a zero reading taken. Now between each cycle there was also a slow drift due to ambient temperature changes not entirely eliminated by the lagging and water cooling. To account for this, fine lines were scratched on the negative between each of the zero points and the radiation scale reading measured from this line.

This proceeding would tend to minimise any error due to the slow

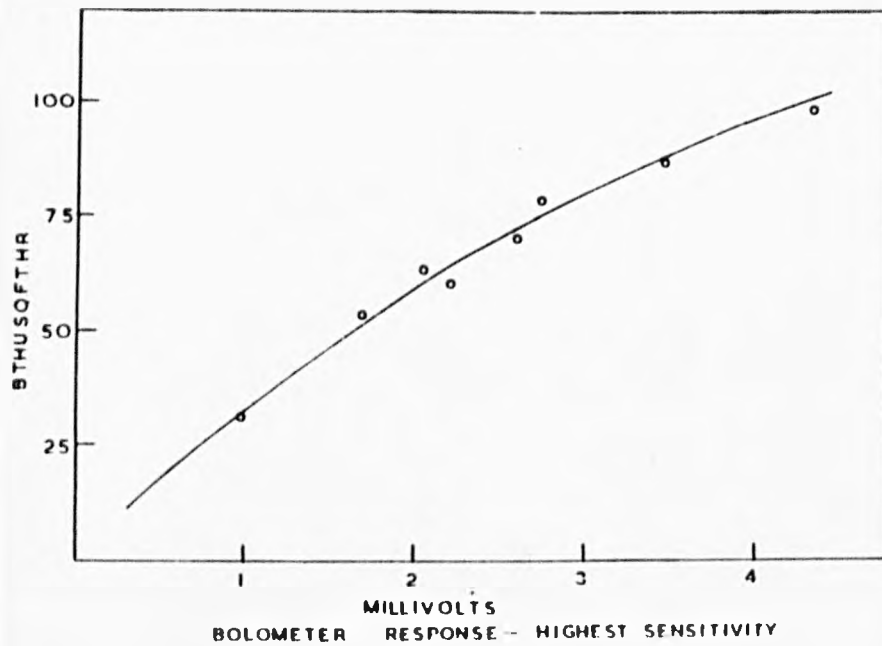


Figure 42.
The bolometer response to black body radiation.

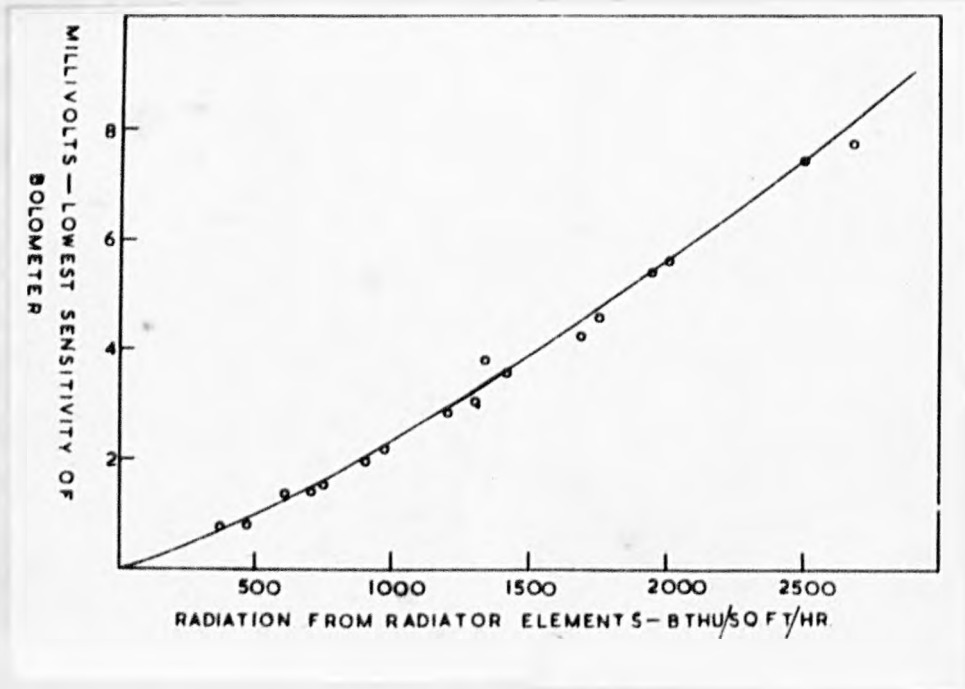


Figure 43.
The bolometer response at high radiation intensities.

warming up of the bolometer case while the element was receiving radiation.

Calibration of the Bolometer

The calibration of the bolometer was very similar to the calibration of the thermopile described in the appendix to the paper work. The absolute sensitivity was found at low radiant intensities using a black body furnace and the relative sensitivity at high intensity using non black sources.

The apparatus for the black body calibration was the same as that used in Figure 11 except that in this case a special slide was constructed to move the bolometer backwards and forwards. The results are shown in Table 15 and Figure 42. The bolometer was used at its highest sensitivity, i.e. with a load resistance of 18.850 ohms.

TABLE 15

Black Body Calibration of Bolometer

Millivolts	Radiation Intensity	Black Body Temperature ($^{\circ}$ K)	Distance from Aperture (cms.)
0.98	30.14	1240	1.2
1.68	53.27	1387	10.3
2.05	64.12	1387	9.3
2.21	59.40	1451	11.7
2.60	71.12	1451	10.7
2.74	78.65	1387	8.3
3.48	86.84	1451	9.7
4.36	98.74	1387	8.3

The above figures were obtained at different temperatures of the black body furnace at different distances from its aperture and it was apparent that the bolometer response did not vary linearly with radiation.

Calibration using the 600 watt Electrical Elements

Two separate experiments were performed to determine the response/incident radiation relationship at the higher intensities of radiation using the lowest sensitivity of the instrument.

Firstly three bars only of the seven bars radiator were connected and the bolometer adjusted vertically beneath them along the mid normal. After allowing the radiator to warm up and reach equilibrium, readings were taken of the bolometer response at different distances under the radiator and the same shape factor as was used for the original three bar radiator was used to calculate the approximate radiation intensity at each distance.

In the second experiment a single 600 watt element was supported in a vertical position and bolometer placed at different distances along the horizontal mid normal to the bar.

The variation of intensity with distance was calculated using the shape factor for a single bar determined in the Appendix to Part I in a similar way to that used for the three bar radiator.

In both cases it was found that the variation of response with intensity could be represented by the expression $I = kv^{0.795}$ where I is the radiation intensity and V is the voltage developed. This is not a dimensionally correct relationship but

represents the best curve which can be drawn through the experimental points.

Now the value of K determines the sensitivity of the instrument which was determined at low intensities by the black body calibration described above. Even at these low intensities the experimental points fitted quite well on to the curve represented by $I = KV^{0.795}$, and using the logarithmic mean of the black body radiation and corresponding voltages, viz 64.42 B.Th.U/sq.ft./hr = 2.31 millivolts, it is possible to calculate a value for K at the relevant sensitivity of the bolometer range. For the lowest sensitivity range corresponding to a load resistance of 590 ohms. we have

$$\begin{aligned} 2.31 \text{ millivolts} &= \frac{2.31}{18.850} \times 590 \times 1.025 \\ (18.850 \text{ load resistance}) & \\ &= 0.074 \text{ millivolts} \\ & \quad (\text{load resistance} = 590 \text{ ohms}) \end{aligned}$$

which on the 590 ohms range gives

$$I = 511 V^{0.795}$$

The experimental points using the radiator elements are given in Table 16 and plotted in Figure 42. In the graph a smooth line corresponding to the calculated curve has been drawn through the experimental points.

Now in the normal experiments on burning wood, the most suitable sensitivity was found to be that using a bolometer load resistance of 2980 ohms. which corresponds to $K = 140.8$, and substituting this in the millivoltage - radiation relationship

TABLE 16

<u>Radiation Intensity (B.Th.U./sq.ft./hr.)</u>	<u>Millivolts</u>	<u>Type of Radiator</u>
2480	7.35	Three Bar
2000	5.57	"
1940	5.33	"
1680	4.18	"
1410	3.53	"
1330	3.81	"
1200	2.71	"
970	2.21	"
750	1.53	"
700	1.40	"
460	0.76	"
2680	7.62	Single Element
1750	4.50	"
1310	3.00	"
900	1.96	"
615	1.41	"
378	0.76	"

the sensitivity of the bolometer during the experimental work was obtained.

The Calculation of the Radiation received by Wood from the Radiator

The radiation intensities at the wooden surface varied between 1,000 and 3,000 B.Th.U/sq.ft./hr. It was difficult to measure the radiation intensity directly as it would involve bringing the bolometer to within 25 cms. of the radiator in some cases. Consequently the ends of the arms supporting the bolometer would have been within 10 - 12 cms. from the radiator, with subsequent damage to the rubber tubing and heating of the water supply. The variation of radiant intensity with distance beneath the radiator was therefore calculated and the radiation intensity measured at a convenient distance away from the radiator at the end of each experiment as described above.

The radiant intensity at any distance from the radiator could thus be deduced. A calculation such as shown in the Appendix to Part I, is somewhat lengthy and the result could have been arrived at much quicker if it had been possible to take the area of the radiator as a plane surface. The radiation from such a rectangular area to a point on its abnormal is given by

$$q = (\theta_1^4 - \theta_2^4) \frac{2AA_1}{\pi} \left[\frac{L_2}{\sqrt{L_1^2 + L_2^2 + 1}} \sin^{-1} \frac{L_1}{\sqrt{L_1^2 + L_2^2 + 1}} + \frac{L_1 \sin^{-1} \frac{L_2}{\sqrt{L_1^2 + L_2^2 + 1}}}{\sqrt{L_1^2 + 1}} \right]$$

where σ = The Stefan Boltzmann Constant

θ_1 is the temperature of the plane area

θ_2 is the temperature of the surroundings

$A A_1$ is a small area receiving the radiation

L_1 is the ratio of half of one side to the distance separating A_1 and the plane

L_2 is the ratio of half of the other side to the distance separating A_1 and the plane.

Now if we assume the plane to be situated along the radiator backing, the variation of radiation with distance is easily calculated. The dimensions of the radiator were taken to be 13.8 x 6.0 cms. and the shape factor found at several distances from the radiator. Table 17 shows the results. The radiant intensity at 25 cms. has been made equal to the intensity previously calculated at that distance in the Appendix to Part I.

TABLE 17

Radiation Intensity	Distance from Radiator backing (cms.)
5640	10
4300	12
2960	15
1778	20
1175	25
823	30
475	40
305	50
216	60

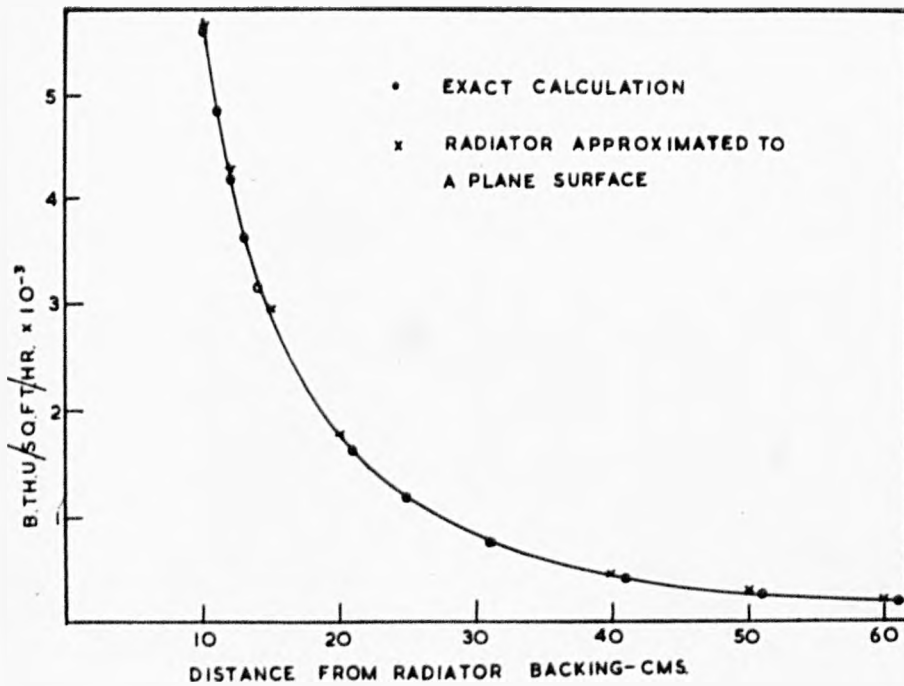


Figure 44.
Calculated radiation intensity from the three bar radiator.

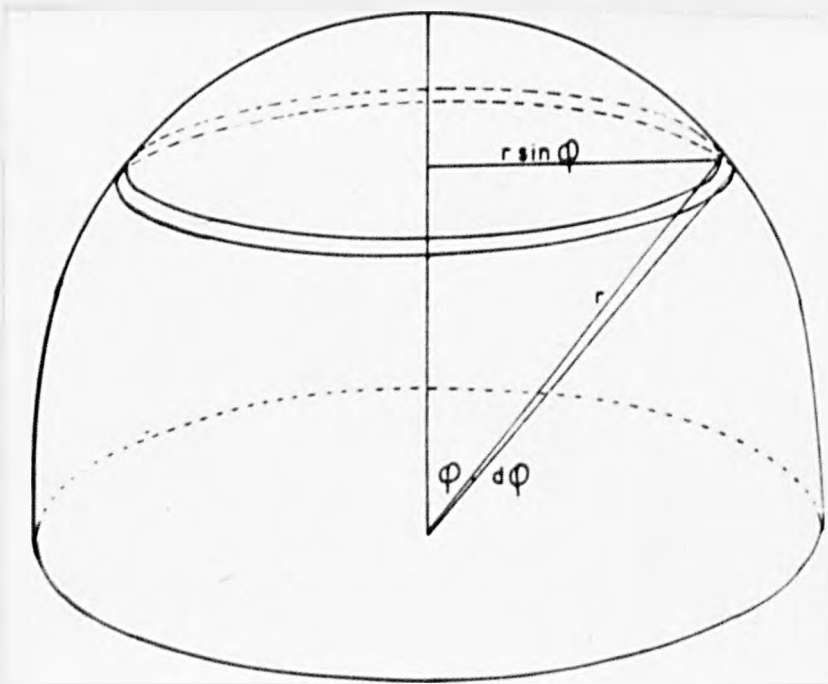


Figure 45.
Integration over the hemispherical surface.

These results are plotted in Figure 44 together with the more exact results previously calculated. The maximum difference is less than 2% and so any similar calculations making similar assumptions about the square radiator should be in error by less than this amount, for this radiator has a more nearly plane surface relative to its overall dimensions. This was considered to be accurate enough for the present purpose and a similar calculation was made for a radiator of dimensions 14.0 x 14.0 ins. square, the results being shown in Table 18.

TABLE 18

Distance from Radiator Backing (cms.)	Radiation (Arbitrary Units
10	8000
11	7250
12	6320
15	4570
20	2820
25	1901
30	1360
40	794
45	631
50	515
55	427
60	362

Measurement of Extraneous Radiation received by Bolometer

At each position of the radiator and bolometer the latter was receiving a certain amount of radiation which was reflected and emitted from the surroundings. This radiation had to be subtracted from the total amount of radiation falling on the hemisphere over which the radiation integration was carried out. This extraneous radiation was measured directly for different distances of the radiator from the wood by substituting a water cooled copper screen, the same size as the original piece of wood, in the position occupied by the wood. In this case of course, no thermocouple readings were taken. The copper surface was blackened by several layers of camphor soot and assumed to have a negligible reflectivity. The procedure followed in the burning of the wood was repeated, with the above modifications, and the radiation received by the bolometer at various positions recorded. This was found to be practically constant over the period of an experiment as was to be expected, as the temperature of the apparatus should have reached equilibrium before an experiment commenced. In some respects, the summation of this radiation is very similar to the integration of the radiation output of the burning wood, and the calculation will be described here as an introduction to the latter.

From the cathode ray trace the bolometer readings at approximately one second intervals were read off, and in order to be able to integrate these readings over the surface of the

hemisphere, it was necessary to know the bolometer reading corresponding to different angles of the bolometer to the wood, and hence it was necessary to know this angular variation with time. This variation is measured directly for each of the bolometer cycles before the experiment. Now the time at which the bolometer becomes exposed to radiation which corresponds to an angle of 5° , and also the time at which the bolometer drops behind a metal screen corresponding to an angle previously noted, can be seen from the C.R. trace. Bearing in mind that the variation of bolometer position with time is known, the reading of the bolometer at any angle to the water cooled screen can be deduced. These readings at nine different angles to the wood were then converted to absolute units by the calibration chart, and this reading could in theory be subtracted from each corresponding reading of the bolometer during the burning of the wood. In practice, however, it was found easier to integrate the extraneous radiation readings over the entire hemisphere and subtract this total of extraneous radiation from the total of extraneous and "relevant" radiation measured during a burning experiment. Here the "relevant" radiation signifies that which arises from the burning wood.

The interpretation of the extraneous radiation is carried out as follows :-

The reading of the bolometer at an angle θ to the mid-normal of the wood is said to be the radiation per unit area falling on a strip of the hemisphere in the form of a ring parallel to the

surface of the wood and of radius $r \sin \phi$, where r is the radius of the hemisphere swept out by the bolometer, Figure 45. The total radiation falling on a strip of width ds is thus $I \times 2 \pi r \sin \phi ds$. Where I is the intensity of the incident radiation which becomes $I.2 \pi r^2 \sin \phi d\phi$ on converting to a form suitable for integration. If now $I.2 \pi r^2 \sin \phi$ is plotted against ϕ , the area under the curve represents the total radiation falling on the hemisphere in unit time. The following is a calculation of the extraneous radiation received by the bolometer with the radiator at a distance of 24.0 cms. from the wood.

Intensity of radiation at the position normally occupied by the wood = 2,700 B.Th.U./sq.ft./hr.

TABLE 19

Bolometer Angle to Mid-normal of Wood (Radians)	Bolometer Reading (B.Th.U./sq.ft./hr.)	Radiation/unit angle falling on the Circular Strip
0.262	125	33.1
0.436	117	50.5
0.611	133	78.0
0.785	133	96.2
0.960	133	111.6
1.135	143	132.4
1.309	180	177.6
1.484	230	234.2

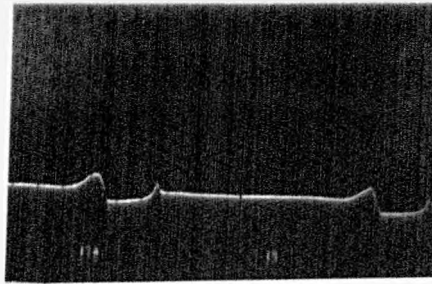


Figure 46.
Cathode ray trace of the extraneous radiation.

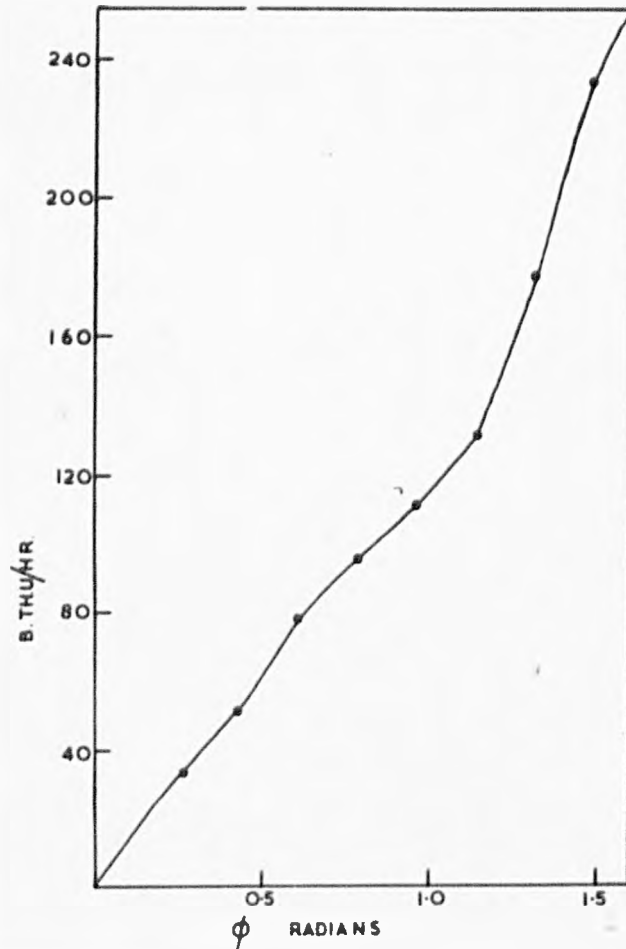


Figure 47.
The extraneous radiation as a function of the bolometer angle.

A reproduction of one cycle of the bolometer is shown in Figure 46 and the plot of radiation/unit angle versus the angle of the bolometer in Figure 47. The area under this curve between $\theta = 0$ and $\frac{\pi}{2}$ is equivalent to 152 B.Th.U./hr. This figure multiplied by the burning time has to be subtracted from the total radiation output registered by the thermopile in a burning experiment in order to obtain the radiation emitted from the wood and flame alone..

With the radiator 28.4 cms. from the position of the wood corresponding to a radiation intensity of 2080 B.Th.U./sq.ft./hr at this position, the extraneous radiation was found to be 102 B.Th.U./hr. whilst with the radiator 34 cms. from the wooden surface, corresponding to 1350 B.Th.U./sq.ft./hr. the extraneous radiation was 20 B.Th.U./hr.

The final calculation of the heat transfers taking place
as the wood is burnt

Heat lost as Radiation

The radiation measured by the bolometer originates in three different ways. Firstly there is the extraneous radiation, whose measurement was discussed above. Secondly there is the radiation reflected and emitted from the hot wooden surface, and thirdly there is the radiation emitted by the burning gases on and above the surface of the wood. It is difficult to separate 2 and 3 because the surface of the wood is not at a uniform temperature, and it is important to recognise that the figures calculated below are composed of radiation from these two sources.

The integration over the hemisphere is similar in principal to that carried out for the extraneous radiation, but is complicated by the variation with time of the intensity of the radiation. In brief, it is necessary to find the total radiation falling on the surface of the hemisphere at certain times, and then to plot these totals as a function of time and integrate the results graphically over the complete burning time. Alternatively, the variation of the radiation at certain angles of the bolometer with time can be plotted and integrated in time. This gives the total radiation during the burning time which falls on certain positions of the hemisphere

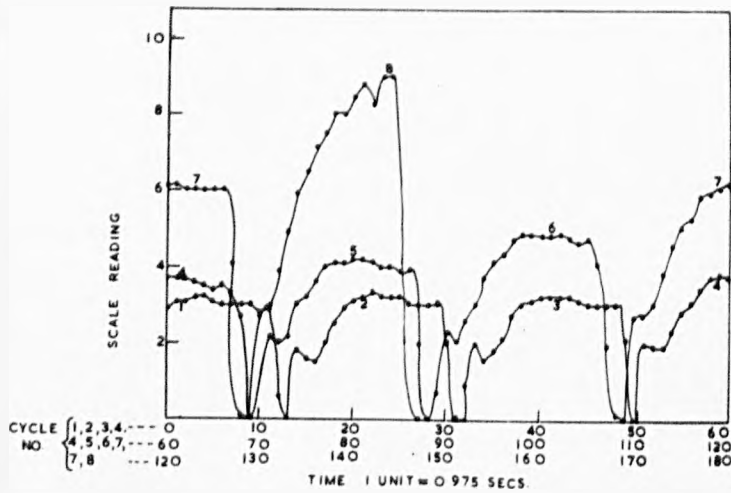


Figure 48.
The variation of radiation intensity from burning wood as measured by the bolometer.

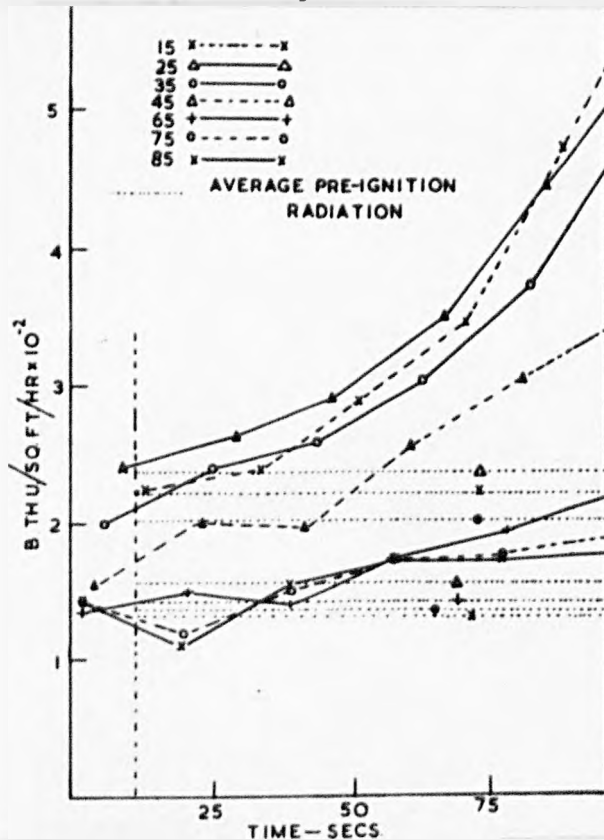


Figure 49.
The variation of radiation intensity from burning wood at a constant bolometer angle, with time.

and these figures when multiplied by $2 \pi r \sin \phi ds$ give the total radiation falling on circular strip s , width ds , around the hemisphere parallel to the surface of the wood, Figure 45. These can then be integrated over the entire surface of the hemisphere as before. The latter method was the one adopted in the present work, and an example under typical circumstances is given below.

The radiant heat emitted by a Birch specimen irradiated at 1.770 B.Th.U./sq.ft./hr. at a distance of 28.4 cms from the Radiator

Time of radiation of wood	= 120 secs.
Time of burning	= 67 secs.
Bolometer sensitivity 92 mvs.	\equiv 17.7 scale divisions.

In this case the drum camera was opened 60 seconds before the wood was ignited, and the plot of the bolometer readings against time is shown in Figure 48. For convenience, the length of the time scale on the graph has been taken at about 3 cycles, and the 4th. cycle is shown as though starting at zero time, similarly with the 7th cycle. As can be seen from the figure, the bolometer performed nearly 8 cycles whilst the camera was open. Now knowing the angular position of the bolometer at any time during the cycle, the bolometer reading for several angles was calculated, and the time at which the bolometer reached these angles noted. It will be seen that for each angle the radiation at that angle is noted once every

TABLE 20

 Angle of Bolometer
to normal

85°	Time of reading	=	51	70	90	110	130
	Reading on scale	=	2.0	1.0	2.3	2.7	2.7
	Reading in B.Th.U.	=	140	110	155	175	175
75°	"		51.4	70.4	90.4	110.4	130.4
			2.0	1.6	2.2	2.7	2.8
			140	120	150	175	180
65°	"		52.0	71.4	91.1	111.1	131.1
			1.9	2.2	2.0	2.7	3.0
			135	150	140	175	195
45°	"		54.1	74.4	93.1	113.3	132.2
			2.3	3.1	3.0	4.0	5.1
			155	200	195	255	305
35°	"		56.1	76.3	95.2	155.5	135.3
			3.1	3.8	4.1	5.1	6.6
			200	240	260	305	375
25°	"		59.4	80.4	98.5	119.0	138.4
			3.8	4.2	4.8	6.0	8.0
			240	265	290	350	445
15°	"		63.8	85.2	102.8	123.5	143.2
			3.6	3.9	4.8	6.0	9.0
			225	240	290	350	485

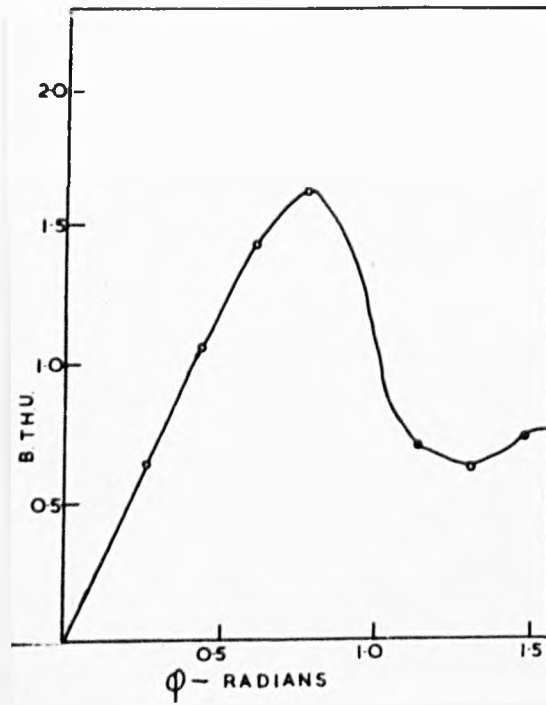


Figure 50.
Graphical integration of the radiation over a hemispherical surface.

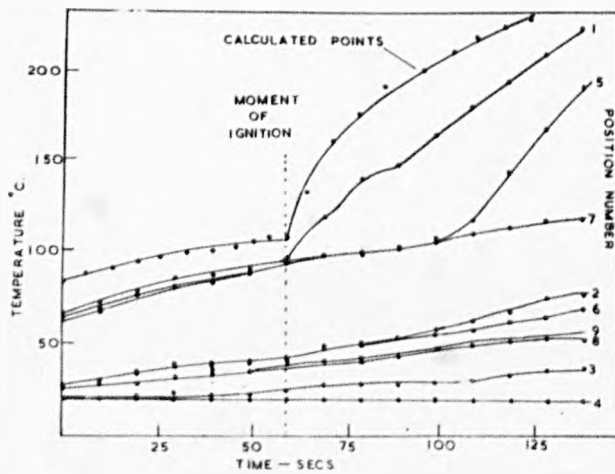


Figure 51.
Temperatures in burning birch.

cycle and thus there are readings at 8 different times for every angle. Only the figures during the last 90 secs. of the bolometer trace appertain to the burning time, these figures being tabulated below in Table 20 and shown graphically in Figure 49.

Now the areas under each curve shown in Figure 50 represent the total radiation falling on the point occupied by the bolometer when at that particular angle to the wood, and in the same way as before the radiation falling on the circular strip shown in Figure 45, is equal to $2 \pi r^2 \sin \phi d\phi$ where ϕ is the angle between the bolometer and the wood, for if the width of this strip is ds , its area is $2 \pi r \sin \phi ds$ and $ds = r.d\phi$. Now the area under the curves in Figure 49 are shown in Table 21, and each of these areas is then multiplied by $2 \pi r^2 \sin \phi$ as shown, and the resulting figures plotted against the angle in radians, Figure 50. The area under this curve taken between 0 and $\frac{\pi}{2}$ is equal to 5.34 B.Th.Us., representing the total output of heat during the burning time. During this time the wood received

$$\frac{1770 \times 87 \times 6 \times 5.5}{3600 \times 2.54^2 \times 144} = 9.8 \text{ B.Th.Us.}$$

as radiation from the radiator.

Calculation of heat conducted into the body of the wood

The following method uses several approximations which may lead to fairly large inaccuracies, but any more accurate calculations would have needed much more experimental data, including the temperature at extra points in the wood, and as stated earlier, a more detailed temperature survey could not be attempted. The temperature time relationship during the same experiment as was used to illustrate the preceding radiation calculation is shown in Figure 51. This is a typical sample of all the rest of experimental results and it was found as in this case, that the temperature distribution in the wood was symmetrical within experimental error, despite the big difference in conductivity along and across the grain. It was found however, that the temperature gradients from the centre of the wood to the edges along the horizontal lines were quite shallow, i.e. very little heat was lost from the edges of the wood, and this largely explains the apparent symmetry of the temperature distribution.

Considering the temperature gradients from the burning surface to the cooled surface of the wood, there is no doubt that at the times when the wood is first exposed to radiation, and later at the instant when flames reach a point on the surface of the wood, the corresponding temperature gradients depart very far from linearity. The most important readings in these experiments however, are taken when equilibrium temperatures are

TABLE 21

Area under curve in B.Th.Us./sq.ft.	Radiation falling on Circular strip in B.Th.Us.	Radiants
0.792	0. 210	0.262
0.834	0.360	0.436
0.741	0.435	0.611
0.602	0.435	0.785
0.419	0.388	1.135
0.396	0.391	1.309
0.393	0.400	1.484

more nearly attained, that is, at the instant before the wood is ignited, and later after the wood has been ignited for approximately 90 seconds. These considerations are of importance in deducing the temperature gradient through the wood from the three or four experimental points available, for in effect, a large amount of interpolation and extrapolation between points is necessary. In particular, the extrapolation to the hot surface is normally one of considerable uncertainty in all problems of this nature, and, as a first step it was decided to calculate the theoretical temperature distribution under conditions similar to those obtaining during the burning time. In this connection the paper by Bamford previously referred to, was of particular importance, and its main features

will now be discussed. This Paper is partly concerned with the solution of the normal diffusivity equation alone, but the major part discusses the solution of the latter, to which had been added a function representing the change in temperature at a point in the wood caused by an exothermic reaction taking place at that point. The equation solved by Bamford and his collaborators is

$$k \frac{d^2 \theta}{dx^2} - q \frac{dw}{dt} = c \rho \frac{d\theta}{dT}$$

where $-\frac{dw}{dt} = k w e^{-E/R\theta}$ and $w(x,t)$ is the weight of the volatile products per c.c. of wood, q is the heat liberated at constant pressure per gm. of volatile products evolved, whilst k is the velocity constant and E the activation of the reaction.

Now as described before, the diffusivity equation can be replaced by a set of simultaneous equations by means of finite difference ratios and Taylor's Theorem. The term $-q \frac{dw}{dt}$ represents the rate of change in temperature at x and t caused by a reaction taking place where rate of the reaction is influenced by θ and w .

On introducing dimensionless units of length and time

$$\xi = \frac{x}{l} \text{ and } \tau = \frac{k}{l^2 c \rho} t, \text{ the equations become}$$

$$\frac{d\theta}{d\xi^2} = \frac{d^2 \theta}{d\xi^2} - \frac{q}{c \rho} \frac{dw}{dT}$$

$$\text{and } \frac{dw}{dT} = \frac{-l^2 c \rho k}{K} \quad w e^{-\frac{E}{R\theta}}$$

Replacing the time and length derivatives by finite difference ratios and substituting $\frac{w' - w}{\delta \tau}$ for $\frac{dw}{dT}$ in the same way. the temperatures at the points $m-1, m, m+1$, in the wood at times τ and $\tau + \delta \tau = \tau'$ become

$$\theta'_m - \theta_m = \frac{\delta \tau}{2(\delta \xi)^2} (\theta'_{m-1} + \theta_{m-1}) - 2(\theta'_m + \theta_m) - (\theta'_{m+1} + \theta_{m+1}) - \frac{q}{c \rho} (w'_m - w_m)$$

where $m-1, m$ and $m+1$ are separated by a small distance, $\delta \xi$

For each step in the integration $(w'_m - w_m)$ is calculated from

$$w'_m = X w_m$$

$$\text{where } X = \exp. \left(\frac{-l^2 c \rho k}{K} \delta \tau e^{-\frac{2E}{R} (\theta'_m + \theta_m)} \right)$$

This function is arrived at by integrating

$$\frac{dw}{dT} = \frac{-l^2 c \rho k}{K} \quad w e^{-\frac{E}{R\theta}}$$

between τ and $\tau + \delta \tau$

Now for the case of a slab of material heated on one side and with the other side following a known variation of temperature with time, the boundary conditions become

$$\theta = \text{constant for } 0 < \xi < 1, \tau = 0$$

$$w = w_0 \quad \text{for } 0 < \xi < 1, \tau = 0$$

$$-\frac{K}{l} \frac{d\theta}{d\xi} = H(\theta) \quad \text{for } \xi = 0, \tau > 0$$

$$\frac{d\theta}{d\xi} = f(\tau) \quad \text{for } \xi = 1, \tau > 0$$

In the present case it was most important to know the temperature distribution in the area closest to the burning face

and a depth of wood of 0.8 cms. from the burning face was considered. At the instant that heat is applied to the upper surface of the wood, the temperature gradients are infinite and this condition would introduce large errors into the finite step integration. Consequently a more rigid solution of the equations was used for the first sixty seconds exposure of the wood to radiation. The equation used gives the variation of temperature with time and position in a semi-infinite slab. That is, in a slab of infinite extent in length and breadth and of such a depth that heat does not reach the back surface during the time of the calculation when the slab is subjected to heat transfer at the front surface. The form of the latter as a function of surface temperature is

$$\frac{d\theta}{dx} = -\alpha + \beta\theta \text{ for } x = 0, \theta = 0$$

and the equation giving temperature difference from the original temperature at $x = 0$ is

$$\bar{\theta} = \frac{\alpha}{\beta} \left(1 - e^{-\beta x + \alpha t} \right) \operatorname{erfc} \left(\frac{x}{2\sqrt{\gamma t}} + \beta t \right) - \frac{\operatorname{erf} \left(\frac{x}{\sqrt{\gamma t}} \right)}{\sqrt{\gamma t}}$$

The various constants used were as follows -

depth of block	= 2.4 mms.
conductivity across grain	= 0.0003704 c.g.s. units
average specific heat	= 0.33 cal/gms.
density	= 0.66 gms/c.c.

Now heat lost due to convection and radiation from wooden surface

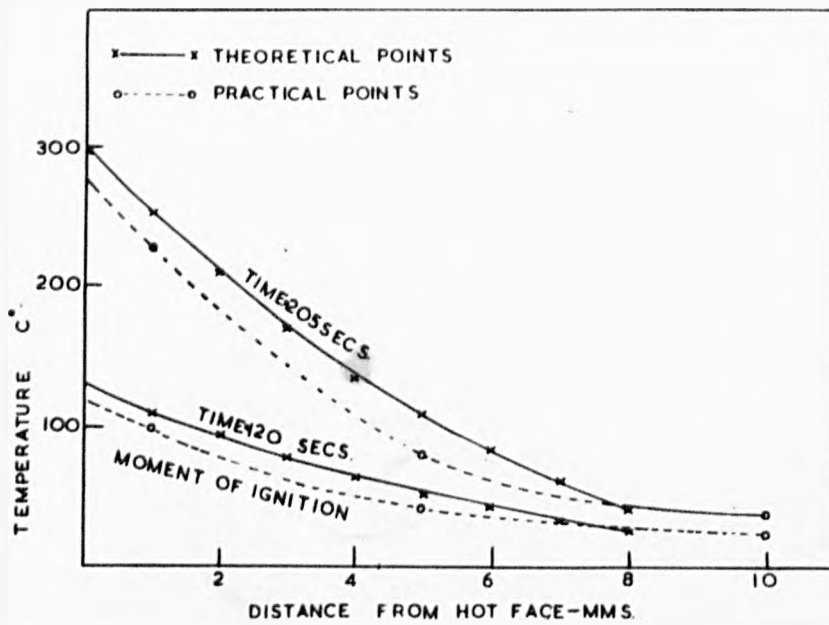


Figure 52.
Temperature gradients in wood heated by radiation.

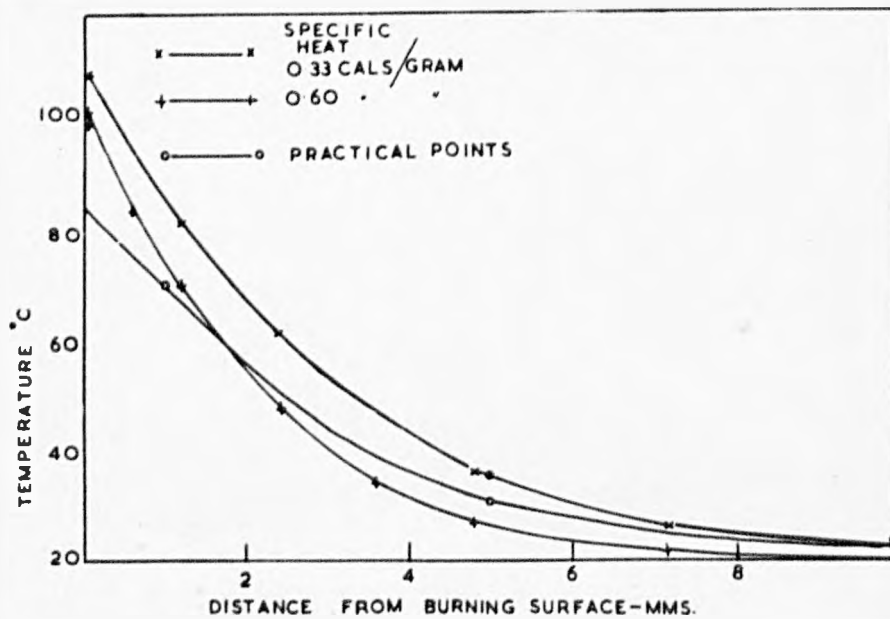


Figure 53.
Temperature gradients in burning birch.

was taken to be

$$Q = 0.81 (\theta_s - \theta_a)^{1.25} \cdot 1.78E \left(\frac{\theta_s}{100} \right)^4 - \left(\frac{\theta_a}{100} \right)^4$$

where θ_s = surface temperature of block)
 θ_a = air temperature) in $^{\circ}\text{K}$.
 E is emissivity of wooden surface)

The emissivity of the wooden surface was taken to be 0.85 which is the figure usually adopted for a planed wooden surface of this nature. This leads to values of α and β of

$$\alpha = 820$$

$$\beta = 2.60$$

$$\text{Now from } \tilde{\gamma} = \frac{K}{l^2} c \rho t \quad \tilde{\gamma} = 0.000263t$$

and hence 60 secs after exposure to radiation the surface temper-

ature ($f = 0$) is given by

$$= 315 (1 - e^{-2.6^2} \times 0.0158 \operatorname{erfc} 2.60 \ 0.0158)$$

$$= 89^{\circ} \text{ c.}$$

The temperature distribution in the wood at the same time is similarly calculated as shown in Figure 52 and Table 22.

The experimental points 0.1, 0.5 and 1.0 cms. from the front surface of the wood are also shown in Figure 52 together with the theoretical temperature distribution calculated, assuming a specific heat of 0.6 and with the heat transfer coefficient adjusted to give approximately the same surface temperature. It will be seen that the difference in curvature caused by the alteration of the specific heat is very noticeable and supports the contention expressed above, that such curves could be used

to find the diffusivity of wood and similar materials.

TABLE 22

Distance from Front Surface (cms)	Temperature (°c)
0	107
0.12	80
0.24	60
0.48	34
0.72	24
0.96	19

The agreement between theoretical and practical points calculated is considered to be satisfactory, as the heat transfer coefficients are not known accurately. The convection losses are probably much higher than those taken above, calculated on the basis of natural convection.

The temperature distribution determined was now used to extend the range of the calculation, first of all to the time corresponding to the moment of ignition of the wood, and then later for a period corresponding to the burning time.

The wood was assumed to be subject to the same intensity of radiation as before and the heat transfer coefficient at the upper surface could now be tabulated as a function of the surface temperature. Only the first 8 mms. depth of the wood was examined and the eight steps in \int in the integration were thus equivalent to 1 mm. intervals.

Now from $\tau = \frac{k}{l^2 c \rho} t$ as $l = 0.8$

$$\tau = 0.002922 t$$

Whence as $\delta \tau = \frac{1}{8}$ and if

$$\left(\frac{\delta \tau}{\tau}\right)^c = 1$$

$$t = 6.6 \text{ seconds}$$

Now knowing the heat transfer coefficient at the hot surface the boundary condition at that surface is now given by

$$\theta_0 = \frac{1}{2} (\theta''_1 + \theta_1) \frac{1}{8 k} H \left(\frac{\theta''_0 + \theta_0}{2} \right) - \frac{q}{2c\varphi} (w^1_0 - w_0)$$

The other boundary condition at 8 mms. depth in the wood was assumed to be the temperature estimated from the practical points obtained in the burning of the piece of wood under discussion.

It was also found that the temperature did not rise high enough to cause appreciable decomposition of the wood and consequently the term involving this function was omitted. The step by step integration is tabulated below, Table 23. The first row of figures are the ones calculated above for $t = 60$ seconds. Subsequent figures are first estimated and then altered first of all to fit the boundary conditions at the hot surface mentioned and then to fit the equation

$$\theta''_m = \frac{1}{2} (\theta''_{m-1} + \theta''_{m+1} + \theta'_{m-1} + \theta'_{m+1})$$

as described in the section on physical constants. The temperature at $\tau = 1$

i.e. 8 mms. depth in the wood was substituted directly in the table from the practical point. Although the method is somewhat tedious, it was found to be quite satisfactory and large

cumulative errors did not appear to rise. The results are tabulated in degrees Kelvin as this is the most convenient form to find the heat evolved by reactions taking place.

TABLE 23

Tabulated in °Kelvin

Time (secs.)	H $\left(\frac{\theta_0 + \theta_0}{2}\right)$ C.G.S.units	θ_0	θ_1	θ_2	θ_3	θ_4	θ_5	θ_6	θ_7	θ_8
6.0		380	357	338	324	313	305	301	297	294
66.6	0.0750	382	361	342	327	316	308	302	298	295
73.2	0.0740	384	364	346	331	319	310	304	299	295
79.8	0.0729	388	367	349	334	322	313	306	300	295
86.4	0.0695	390	370	352	337	325	316	308	301	296
93.0	0.0685	392	372	354	340	328	318	309	302	296
99.6	0.0680	393	374	357	343	330	319	311	303	296
106.2	0.0663	395	376	360	345	332	321	312	304	297
114.8	0.0650	397	379	362	347	334	323	313	305	298
120.0		399	381	364	349	336	324	314	306	298
By extrapolation)										
temp.gradient °c	=	126	108	91	76	63	51	41	33	25

At this instant the wood was assumed to have been ignited and it was found that a heat transfer coefficient corresponding to a radiation intensity of 5640 B.Th.U./sq.ft./hr. gave temperatures which rose at a somewhat greater rate than those actually measured in the wood. The theoretical temperatures were calculated as above and again it was found that the temperatures attained

were not sufficient to start an appreciable reaction.

The average values of the reaction constants using specimens of deal heated by coal gas flames were determined by Bamford as

$$k = 5.3 \times 10^8$$

$$E = 33.160 \text{ cal.}$$

$$q = 86 \text{ cal.}$$

Using these values in the present calculation it is found that a preciable reaction does not take place until about 570°K . This corresponds to the highest surface temperature to be calculated as described below and suggests that only a small amount of exothermic reaction in the body of the wood has taken place at the burning surface although of course, the burning volatiles have given up appreciable quantities of heat. The condition of the burnt surface as examined after burning does indeed suggest that the depth of complete charring is slight, usually less than 1 mm, although this is underlayed by a layer of discoloured material to^a/depth of 2 - 3 mm. It seems likely that over the last mm of charred surface there will be a rise in thermal gradient because of the decrease of conductivity of the char. This decrease appears to be between 10 to 50 per cent of the conductivity of the unburnt specimen₃ and so by this amount the temperature drop over the last mm of wood may be greater than that calculated, ignoring this char, making the surface temperature in error by some twenty degrees centigrade. This, however, only affects the average temperature rise in the

wood by one or two per cent and coupled with the decrease in density of wood on forming charcoal, should not affect the calculation of the heat stored in the wood by more than that amount. The results of the calculation using the increased heat transfer coefficient are given below in Table 24

TABLE 24

Time (secs.)	H $\frac{(\theta_0 + \theta_1)}{2}$										
		0	1	2	3	4	5	6	7	8	
120		399	381	364	349	336	324	314	306	298	
126.6	0.287	480	404	372	353	338	326	316	307	299	
133.2	0.243	494	434	388	361	342	328	318	308	299	
139.8	0.232	513	450	404	370	347	332	319	309	300	
146.4	0.217	522	464	416	381	355	336	322	311	301	
153.0	0.207	533	474	428	391	362	341	325	313	303	
159.6	0.195	540	485	437	399	369	346	329	315	306	
166.2	0.190	545	493	446	407	376	352	333	318	304	
177.8	0.182	551	499	454	415	383	357	337	320	305	
179.4	0.175	557	506	461	422	389	363	341	322	306	
186.0	0.168	560	511	467	428	396	368	344	325	309	
292.6	0.165	564	516	472	434	401	372	348	328	311	
199.2	0.160	566	520	477	439	405	377	352	331	312	
205.8	0.155	570	524	482	443	410	381	356	333	313	

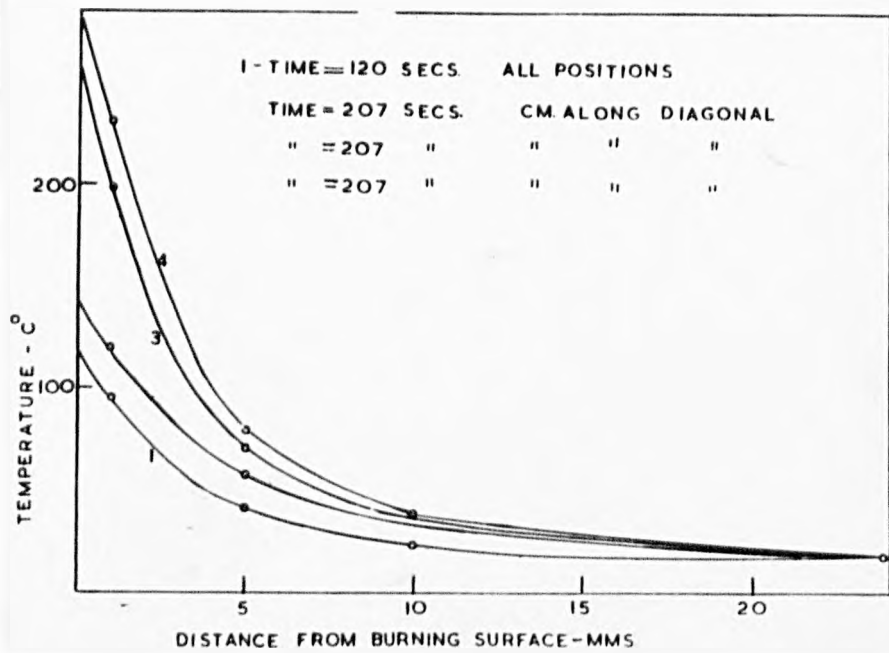


Figure 54.
 Temperature gradients used to find the heat content
 of a birch specimen.

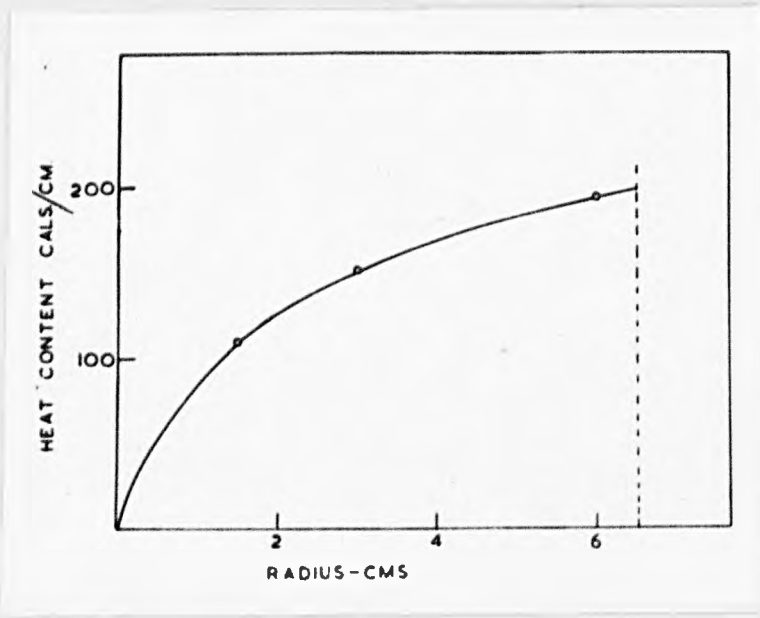


Figure 55.
 Summation of the heat conducted into a birch specimen.

The temperature gradients thus calculated at $t = 120$ and 206 seconds, were plotted in Figure 53, and the points actually measured included on the same graph. The curves were very smooth and it would appear that extrapolation and interpolation could be carried out with very little loss in accuracy. The straight portion of the lower temperature of the theoretical curves are no doubt due to the boundary temperatures being taken too low corresponding to a rather greater heat transfer at the 8 mm. boundary than would normally take place into a further thickness of wood.

As a result of the above calculations it was decided to determine the heat conducted into the wood in the following way:- From Figure 51 a plot of the temperature at the nine positions in the wood against time, the temperature gradients from the front to the back of the wood at three points were plotted:- (a) at the instant of ignition of the wood and (b) at the instant of extinction of the flame. The three points mentioned were the three positions of the thermocouples along a diagonal of the wood, i.e. at the centre, three cms. and six cms. along the diagonal. These curves are shown in Figure 54.

Now considering a cube of wood of sides dx , dy and dz , the heat required to raise the temperature of the cube by a small amount

$$q = c \int dx. dy. dz.$$

where c = specific heat

and ρ = density

and the heat required to raise it from 0 to θ° is

$$q = c \rho dx dy dz \text{ assuming a constant specific heat.}$$

Now considering a strip of wood, sides dy , dz and x , the heat content of this strip is

$$q' = dydz \int_0^x c \theta dx$$

where c is a function of θ and θ is a function of x .

Now for the moment assuming c to be constant, if we know θ as a function of x then $\int_0^x dx$ can be found in the usual manner by graphical integration. The result of this integration then provides an average value of θ which in turn decides the specific heat to be taken in calculation.

Now considering Figure 55, it was found that curve 1 was representative of the temperature at all points in the block within a radius of 6.5 cms..

The area under this curve represents the heat contained in a strip of unit area cross section, through the wood. Now the area under the curves 2, 3 and 4 represent the heat in similar strips situated at their respective positions in the block. The difference in area between curves 1 and 2, 1 and 3 and 1 and 4, thus gives the heat input during the burning time and these areas were measured as usual with a planimeter. Assuming as before, a symmetrical distribution of heat, the heat contained in a ring of radius r , width dr and depth, the full depth of the block is then $2 \int r Q dr$ where Q is the heat content of a strip

of unit cross sectional area through the block r cms. from the centre. Now as the radius at the centre position is zero, it is necessary to find the heat contained in a ring of wood of some small finite radius in order to utilise the figures at the centre position. This was done for a radius of 1.5 cms. by extrapolation between the figure found for the area at the centre position and that at the 3 cm. position. The figures found in this way from Figure 54 are shown in Table 25 and Figure 55. If now these figures giving the number of cal./cms. at three radii are plotted against the radii, the final area taken between 0 and 6.5 cms. gives the rise in heat content in a cylinder of that radius at the centre of the block. It is here assumed that no heat from the burning wood penetrates outside that cylinder. The temperatures obtained during the experiments support this view, any temperature rise outside the cylinder underneath the burning zone being only that which would be expected to arise from the radiation of heat from the radiator. The figure finally arrived at from the integration under the curve shown in Figure 55 was, in this case 3.57 B.Th.U.s..

TABLE 25

Heat conducted into a Birch Specimen burning under a Radiation Intensity of 1770 B.Th.U./sq.ft./hr.

Area under Curve No.1 (°C x C.ms.)	Area under Curves No. (°C x C.ms.)	Specific Heats
	2 163	
86.0	3 125	0.316
	4 111	0.314
°C x Cm at = 1.5	= 145	0.320

The drop in Calorific Value of the Birch Specimen under Radiation intensity of 1770 B. Th.U./sq.ft./hr.

This calculation has been described above (Page 59) and only a brief account will be given here.

Weight of char scraped off block = 2.925 grams.

Calorific value of char = 4940 cal./gram

∴ Total calorific value of the material scraped off the surface. = 14410 cal.

Weight of wax impression of the cavity in the surface of the wood formed by burning and then scraping off the char = 6.94 grams

Density of wood = 0.66 grams/cc.

Density of wax = 0.906 grams/cc.

∴ Weight of unburnt wood originally occupying the cavity = 5.06 grams.

Calorific value of unburnt wood = 4710 cal's per gram

.. Total calorific value of materials scraped and burnt off the surface of the block = 23850 cal's.

Now the calorific value lost during burning is thus the difference between the calorific value of the material scraped and burnt off the surface of the block and the calorific value of the material scraped off the block which equals in this case 9440 cal's.

= 37.47 B.Th.U's.

It is convenient here to summarise the results already obtained and to discuss the desirability of further calculations.

Considering the piece of wood just discussed, two quantities of heat released during its burning time have been calculated. First the total amount of radiation falling upon a hemisphere of the same radius as the arc swept out by the bolometer arm. Secondly the increase in heat content of a cylinder of wood over which burning has taken place. This amount of heat is largely due to the burning of volatiles on the surface of the wood, but some no doubt, arises from the radiator, and yet another quantity is probably due to some exothermic reaction taking place in the wood near the surface. The total amount of heat arising from the destruction of the wood is volatiles and char is also known. Taking into account the extraneous radiation arising from the surroundings, it is now possible to summarise the known and unknown quantities in the heat

balance as follows:-

Total heat input during the burning time is:-

Q_R = The total radiation falling on a central disc of wood of radius 6.5 cms. during the time of burning, plus

Q_W = The heat evolved as a result of the decomposition of the wood.

The quantities of heat transferred during the experiment which are known are :-

- (1) Q_R
- (2) Q_W
- (3) The total radiation falling on the hemisphere formed by the rotation of the arc swept out by the bolometer.
- (4) The rise in heat content of a cylinder of wood situated centrally in the wood underneath the burning zone.

Considering each of these quantities in turn, paying attention to their origin and final distribution, it is known that the quantity Q_R is divided at the wooden surface in such a way that a certain quantity is reflected and the rest is absorbed into the body of the wood. The proportion of each of these figures to the whole is given by the reflectivity of the wood which is about 0.15 to 0.10, for the wood, and somewhat less for the charcoal surface.

Of the quantity Q_W a certain proportion is emitted as radiation by the flame. Some of this radiation reaches the bolometer, some is absorbed and reflected by the wood, whilst some is lost by convection in the hot burnt gases and surrounding air.

The rest is evolved in the body of the wood as an exothermic

reaction which raises the temperature of the surrounding wood and char.

In the calculation of the radiation falling on the hemisphere surrounding the burning surface it was assumed that the radiation falling on the arc swept out by the thermopile was representative of the radiation at similar positions over the hemisphere.

This assumption is not strictly correct. First, with regard to the extraneous radiation from the surroundings, this quantity is not likely to be absolutely symmetrical about the centre of the wood, because of the unsymmetrical nature of the surroundings. However, as the total quantity of extraneous radiation is not required, the figures for this radiation obtained over the arc swept out by the bolometer, could have been subtracted from each reading taken during a burning experiment before integration and in this way the unsymmetrical component eliminated. Nevertheless as stated before, the same final result can be achieved by integrating both the extraneous and "relevant" radiation together and later subtracting the integrated extraneous radiation.

This can be simply expressed mathematically by

$$\int_0^t \int_0^{\theta} Q + Q^1 d\theta dt = \int_0^t \int_0^{\theta} Q d\theta dt + \int_0^t \int_0^{\theta} Q^1 d\theta dt$$

where Q and Q^1 are the relevant and extraneous radiations.

Now in the figures previously taken as "relevant" there is another unsymmetrical component, namely the radiation arising from the wood as a result of the radiation falling on it from the radiator. Because of the square shape of the wooden surface the

radiation received by the bolometer will not be representative of the radiation over the rest of the hemisphere, but only of that received at similar positions opposite the mid point of each edge of the wood. The radiation from this source at the start of the burning time is known however, from the preliminary readings of the bolometer but its assessment over the burning time is complicated by its changing intensity with time.

If it could be assumed constant with time, the difference between the readings registered before burning commenced and the later readings obviously would give the radiation due only to the burning of the wood. The surface temperature of the unburnt wood was however, found to vary over the burning time by the methods previously outlined. In the case of a radiation intensity of 1770 B.Th.U./sq.ft./hr. this rise in temperature was about 14°C . over the period of a minute.

This corresponds to a rise of from two to three per cent of the total radiation output before burning. The latter is also composed of radiation from the surrounding, and about 15% of reflected radiation from the wood, these two quantities remaining almost constant during the time of burning.

Now the bolometer readings were noted before the start of each experiment and these readings were used to differentiate between the radiation output from the wood during burning and the radiation arising from the hot unburnt surface. This was done simply in each experiment by extrapolating the original

bolometer readings over the whole time of burning as shown in Figure 49. The area between this line and the curve for the corresponding angle then gives the increase in radiation intensity during the time of burning at that angle. The figures for each of the angles can then be integrated over the whole hemisphere in the usual way and the total increase in radiation found. This figure can be regarded as arising almost entirely as a result of the burning of the wood, although of course, the amount of radiation evolved in the burning is influenced by the previous heat treatment of the specimen. This procedure was followed in evaluating the heat lost as radiation as a result of the burning of the wood.

The rise in heat content of the cylinder of wood considered before, is similarly considered to be partly a result of the heat liberated by the burning wood and partly due to radiation absorbed from the radiator. The latter figure is easily obtained if one assumes a figure for the absorptivity of the burning and unburnt wooden surface and also that a negligible amount of heat flows out of the cylinder to the outer edge of the wood and through the back face.

From the literature the best approximation would seem to be about 85% for the wood and 90% for the char, and as the area of the charred wood is approximately proportional to the square of time, the heat average figure is 87%. From the variations in the range of figures quoted by Summersgill₈ for the relative

reflectivities of pine, gurjon, oak and birch, it would seem that a maximum variation of 4% would cover possible error.

Considering the heat lost by conduction into the edges of the wood, the temperature gradient across the wood seems to be negligible, even considering the larger conductivity across the grain. Similarly, the heat lost from the back face where temperature remains very nearly constant in all the experiments can be ignored.

The heat absorbed by the wood from the radiator is calculated in this way below, using the same example as in the above radiation calculations.

Intensity of incident radiation = 1770 B.Th.U./sq.ft./hr.

Area considered = $(6.5)^2$ sq.cms. = 0.1428 sq. ft.

Average absorptivity = 0.87

Time of radiation = 87 seconds.

.. Total radiation absorbed = 5.31 B.Th.U's.

From the above calculations it will now be seen that the distribution of the heat evolved during the burning of a piece of timber under a given radiation is now known in the form of

- (1) Heat radiated by the hot wood and flame
- (2) Heat conducted into the body of the wood
- (3) By subtraction of (1) and (2) from the total loss in calorific value of the wood, we know the proportion of heat lost as convection, that is, in the form of hot gases. Some of the heat contained in these gases will be further

radiated outside the hemisphere over which radiation has been measured but most of their heat will pass along the flow stream of the gases being dissipated at some distance from the burning zone in a way which will depend on the nature of the surroundings.

The above classification of the various heat losses is sufficient for many calculations, but in some cases it is desirable to subdivide the radiation terms into:-

- (a) The radiation emitted by the flame
- (b) The radiation emitted by the hot surface of the wood.

As previously stated (a) cannot be calculated with a reasonable degree of accuracy. Nearly all calculations of total radiation from flames involve many assumptions regarding the shape, temperature, and composition and even under most rigorous experimental conditions, there is still some doubt as to the accuracy with which the composition of the flame is known.

The calculation of (b) is also inaccurate, again because of the uncertainty of the emissivity of the surface and even more so, of the value of the surface temperature. Moreover the radiation from the surface depends on the fourth power of the surface temperature, thus magnifying any error in the latter.

The calculation was carried out however, for the present case in order to provide some basis for the solution of any problem which may demand a separation of (a) and (b).

The Radiation emitted by the hot Wooden Surface

The surface temperature during the burning time were found for the central position of the block at about six different times by extrapolation of the internal block temperature gradients. These temperatures were then taken to approximate to the average surface temperatures of the burning wood. Considering the low density of the charcoal and its decreased conductivity this approximation is probably the best one to make from the available results.

The area of the burning surface at any time was then found from the known rate of spread of flame and thus, knowing the area, temperature and emissivity of the surface, its radiation output can be calculated at the various times that the surface temperatures are known. Thus the total radiation Q from a plane area A at a temperature θ is given by

$$Q = \sigma E A \theta^4$$

where E is the emissivity of the surface
and $\sigma =$ the Stefan Boltzman Constant.

The figures found in this way for a piece of birch burning under a supporting radiation intensity of 1770 B.Th.U./sq.ft./hr. are given below, Table 26. These figures can now be graphically integrated over the time of burning, leading to a figure of 0.68 B.Th.U's. in the present case.

TABLE 26

Surface Temperature (°c.)	Time measured from the start of burning (secs.)	Area of burnt surface (sq.ft.)	Radiation Output (B.Th.U./hr.)
120	0	0.000	0
150	10	0.00081	0.5
175	20	0.0034	2.3
190	30	0.0076	5.8
200	40	0.0136	11.2
230	50	0.0212	22.1
245	60	0.0305	36
290	87	0.0641	104

Experimental Conditions

The effects of the following variables were measured

- (a) The intensity of supporting radiation
- (b) The time of pre-radiation of the wood
- (c) The moisture content.

The radiation intensity was altered by adjusting the height of the radiator above the wood and measurements were made at three distances of the radiator backing from the wooden surface, namely 23.8, 28.4 and 34.1 c.m. Both the resistance of the radiator and the supply voltage varied considerably between experiments and consequently there were some differences of radiation intensity at the same distance from the radiator in different experiments. The radiation from the radiator was always measured directly by the bolometer as described previously.

At each distance an experiment was made at at least two values of the pre-heating time. The lowest value was the smallest at which it was certain that the flame would travel over the surface of the wood.

Most of the above experiments made use of oven dried birch timber. However, four more similar experiments were performed on birch of a moisture content of 11.6% calculated on a dry weight basis. The temperature/time and radiation/time relationships were all plotted in the same way as

in Figure 51 and Figure 48, whilst the heat transfer by radiation and conduction was found by graphical integration in the manner already described. The surface temperature was estimated by extrapolation of the temperature gradients in the body of the wood. All the final results are shown in Table 27 and are discussed together with the experimental observations in the next section.

TABLE 27

Radiation from Radiator B.Th.U./sq.ft./hr.	Rate cms./sec.	Preheating time sec.	Burning time sec.	Heat evolved in reaction B.Th.U.	Heat conducted into B.Th.U.
1860)	0.0610	345	81	65.1	8.35
1860) 8%	0.0283	330	101	53.8	5.29
1950) moisture	0.0430	315	73	34.9	4.21
2460)	0.0590	210	74	36.8	6.45
2740 Oven Dried	0.1430	150	30	25.1	1.84
2890 " "	0.1280	105	50	23.9	3.76
2680 " "	0.0750	105	57	15.2	4.03
2040 " "	0.0612	180	79	27.8	3.41
2100 " "	0.0995	180	51	44.8	3.61
1920 " "	0.0604	120	79	36.5	4.32
1770 " "	0.0500	120	87	37.5	3.57
1470 " "	0.0750	480	89	42.3	1.77
1250 " "	0.0415	240	138	52.3	6.73
1270 " "	0.0336	240	131	52.3	5.01

Measured Increase in Radiation during burning time B.Th.U.	Surface Temperature at moment of ignition °c	Calculated increase in radiation from hot burning surface alone B.Th.U.	Radiation received during burning time B.Th.U.	Heat lost by surface at temperature at the start of burning B.Th.U.
1.89	103	0.78	5.98	0.99
2.34	112	0.33	7.46	1.36
1.50	107	0.26	5.64	0.94
2.81	100	0.56	7.23	0.88
1.51	152	0.16	3.26	0.60
1.63	137	1.03	5.74	0.97
2.47	110	0.36	6.08	0.75
2.51	140	1.03	6.40	1.42
2.31	150	0.50	4.25	1.01
1.05	115	0.79	6.03	1.09
1.42	103	0.68	6.11	1.07
2.42	150	1.58	5.20	1.76
4.91	125	3.28	6.85	2.11
2.73	100	1.14	7.13	1.56

Results and Experimental ObservationsSummary of typical set of results

In this example the birch sample was oven dried and irradiated at an intensity of 1770 B.Th.U./sq.ft./hr. the pre-heating time being 120 secs. Considering now the central cylinder of wood of radius 6.5 cm. during the time of burning this cylinder receives and subsequently evolves the following quantities of heat:-

- (a) The radiation from the radiator = 6.11 B.Th.U.
- (b) The heat evolved by the burning wood = 37.5 B.Th.U.

The following quantities of heat are also known:-

- (1) The increase in heat content of the cylinder during the burning time = 3.57 B.Th.U.
- (2) The increase in radiation from the top of the cylinder during the burning time = 1.42 B.Th.U.
- (3) The proportion of 2 due to the hot wooden surface = 0.68 B.Th.U.
- (4) The radiation from the top of the cylinder at the start of the burning time = 1.07 B.Th.U. taken over the time of the experiment.

From the above the total heat input is 44.01 B.Th.U. during the burning time. During this time the wood and flame radiates 2.49 B.Th.U. and 3.57 B.Th.U. is conducted into the wood. This leaves a total of 37.95 B.Th.U. to be accounted for by convection.

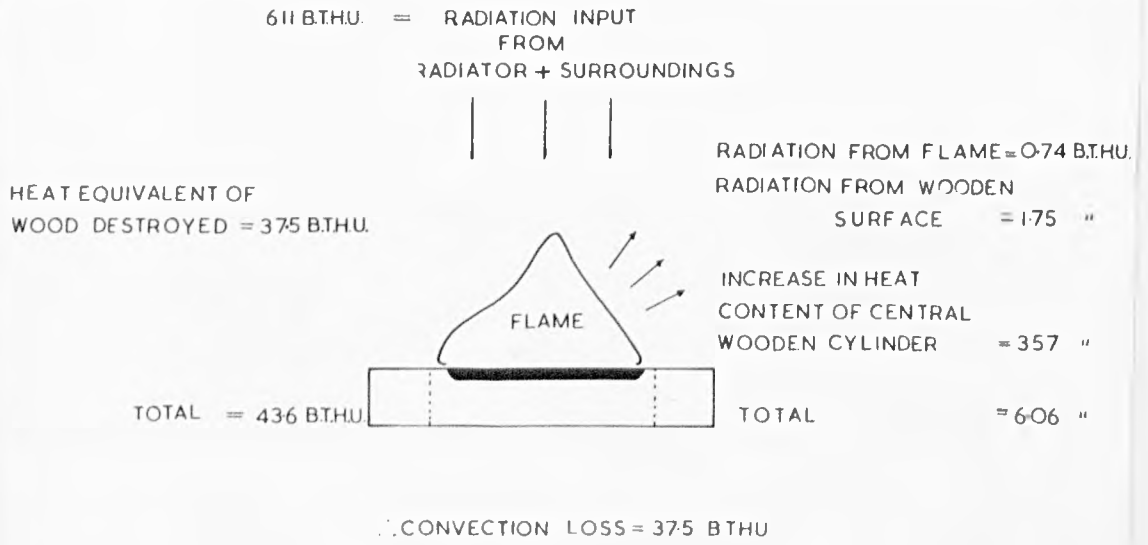


Figure 56.
Summary of the heat transfers in burning birch timbers

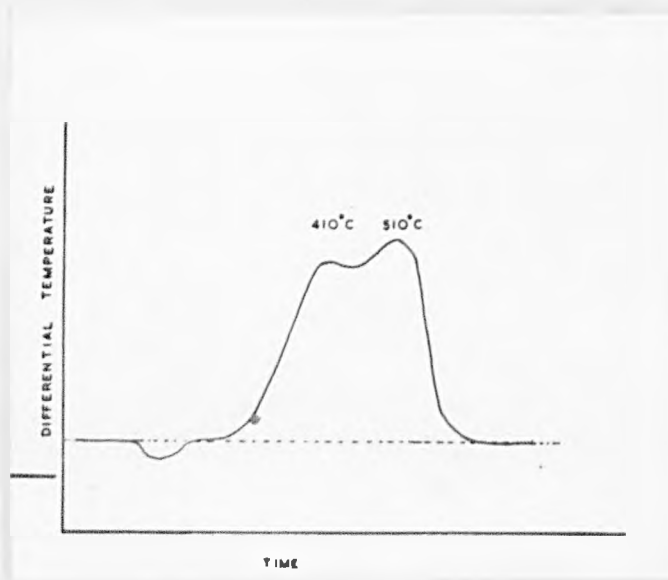


Figure 57.
The differential thermal analysis of birch.

The calculation of the convection figure by subtraction is dependant on the assumption that all the volatiles are completely burnt, the validity of this assumption depending on the size of the flame and the quantity of air available. In the present experiments there was a plentiful supply of air and very little smoke appeared to be evolved, but under conditions such as obtain in conflagrations of large masses of material there may be considerable amounts of volatiles unburnt.

It is important to realise that the proportions of heat transferred in different ways depends on the history of the specimen such as its initial heat content and it cannot be rigidly asserted that any quantity of heat arises from any one source once it has entered the wood. Thus the heat radiated from the wood arises as a result of its surface temperature which itself is a function of its previous heat treatment, supporting radiation intensity and the quantity of wood burnt. Thus the heat changes are best expressed in the form just quoted if they are to be used in a further calculation, note being taken of the experimental conditions. Consequently the figures obtained in a similar way for the rest of the pieces of wood burnt are expressed in the above form. The above results are summarized diagrametically in Figure 56.

The Temperature/time relationships in the wood

The results obtained using the dry wood were all found to be very similar in form. Important points which were noted were that no consistent differences would be detected in the readings of the thermocouples at positions 8 and 9, confirming that the heat content of the wood was distributed symmetrically. It was also noted that the temperature at position 5 rose quicker than those at position 1 after the flame had reached those positions, suggesting that the heat transfer to the burning wood had increased during the spread of flame over the first three cms. radius. Considering the calculation of the temperatures in the wood, assuming constant heat transfer to the surface (Page 108), it would seem that a better agreement would have been found if the heat transfer coefficient had been assumed to be a function of both temperature and time. This increase in the heat transfer coefficient agrees with the tendency towards an increase in the rate of spread as the area of wood burnt increases, which had been noticed when calculating the rates of spread previously.

There was one feature of the temperatures at position 1 which seemed to need further explanation. It will be seen from Figure 51 that immediately after ignition there is a fairly large rate of rise in temperature, which drops to a smaller value and then again increases to a rate which seems to remain almost constant over the burning time. This kind of inflection

although of slightly varying shape and size, was noticed in all of the results, and is almost certainly due to some extra heat input at that part of the experiments. Three possible sources of this extra heat were considered.

- (1) An exo-thermic reaction at that point
- (2) A greater heat transfer from the flame at the moment of ignition.
- (3) The heat input from the pilot flame.

In view of the slight reaction at low temperature previously noted, it was decided to investigate further the possibility of a considerable reaction taking place. The technique of differential thermal analysis which has been used for the examination of refractory clays at Leeds for some time, is a very convenient way of carrying out such investigations. The specimen under examination is mixed in the proportion of about 10% with some inert refractory material, and this specimen is heated together with another of similar shape and size, the latter being composed entirely of the inert refractory. If the two are heated under identical conditions, the differential temperature between them is a measure of any heat change which takes place as a result of a reaction in the specimen under examination. In practice the temperature is controlled to rise at a steady rate, and a recording made of the differential and absolute temperatures. This method was applied in the present

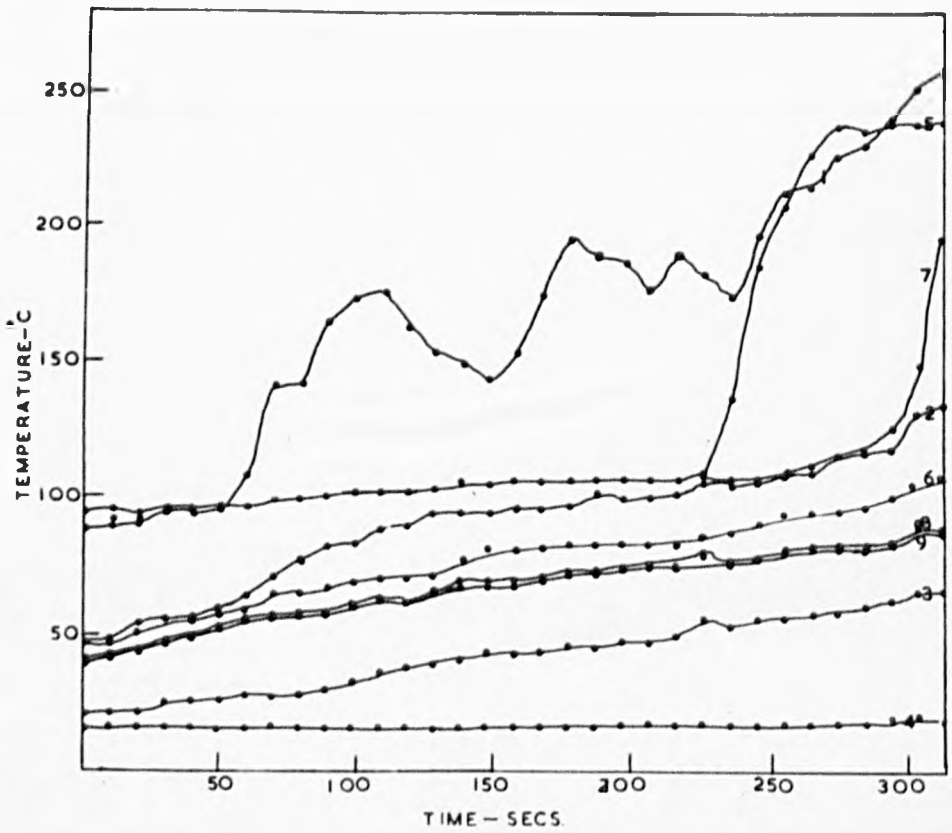


Figure 58.
 Temperatures in burning air dried birch.

case to the birch wood in the form of a fine sawdust taken from an air dried specimen, and the experiment carried out by Dr. R. W. Grimshaw in the Refractories Department at Leeds. The shape of the curve produced is shown in Figure 57. The only heat change taking place below 200°C is endo-thermic and can be attributed to the loss of water from the specimen. An exo-thermic reaction however, does become appreciable at about 270°C giving peaks at about 410 and 520°C , though the effects at the higher temperature are somewhat suspect as the apparatus was known to contain a certain amount of oxygen and its effect could not be measured. As has been stated previously in the work, using the figures given by Bamford for the activation energy and reaction constantm appreciable reaction does not seem to take place below 300°C , and thus these two sources of information both confirm that there is no appreciable exo-thermic reaction in the body of the wood below 200°C . Thus the original postulate (1) above was disproved, as was further confirmed by the lack of similar affects at position 5. This latter observation also seems to invalidate (2) above for similar reasons. This being so, it seems that the extra heat input can be ascribed to the pilot flame, which in general was left in contact with the wood for two or three seconds. This flame was always less than $\frac{1}{2}$ " long, and the heat transferred to the wood must have been very small.

The shape of the temperature/time curves obtained for the air dried specimens were also of interest. It had been noticed

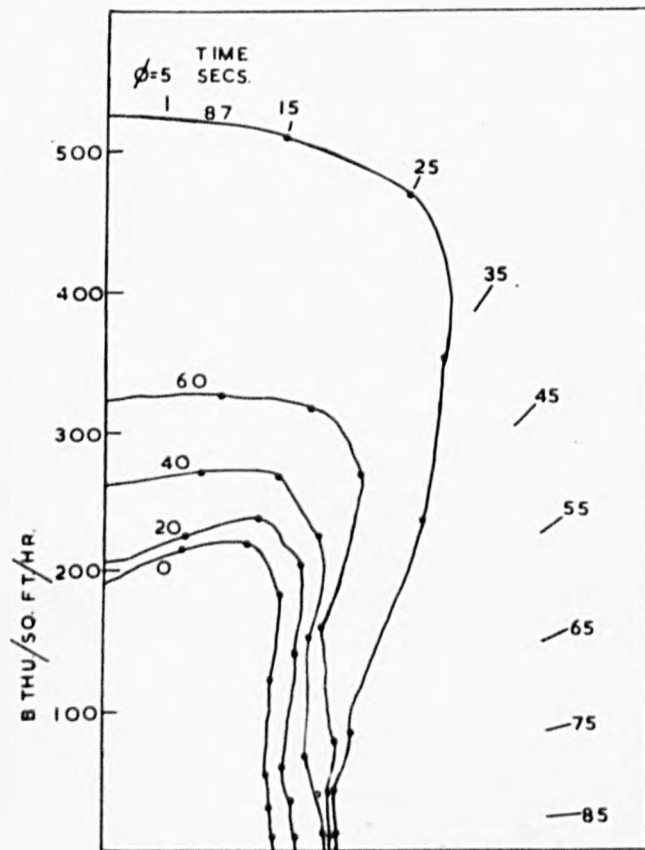


Figure 59 .
 The radiation from a piece of burning birch presented as
 a polar diagram.

by previous workers that when a piece of wood of definite moisture content was heated from one side, the temperatures in the wood tend to rise to just over 100°c , and there remain comparatively steady until presumably all the water has been distilled from the neighbourhood of the thermocouple. This effect was quite marked in the results under discussion as shown in Figure 58, and suggests that the water distills off at a fairly constant low pressure. The most striking differences in the form of the temperature relationship is however, shown at position 1. It will be seen that above 100°c . the temperature oscillates over a range of some 50°c , an effect which was never noticed in the oven dried specimens. It is considered that this is a result of the distillation of slightly super-heated water in the neighbourhood of the thermocouple, and the oscillations are really periods of cooling of the thermojunction due to the sudden expansion of the water, and the absorption of its latent heat.

The Radiation Intensities emitted by the Burning Wood

The results are best presented for discussion in the form of a polar diagram such as Figure 59. The direction of maximum intensity lies at an angle of about 15° to the normal of the wood, and in the case shown the maximum intensity corresponding to an area of burning of 59 sq.cms. is 540 B.Th.U./sq.ft./hr.. The supporting radiation in this case was 1770 B.Th.U./sq.ft./hr., and hence this area of burning wood is not sufficient for self

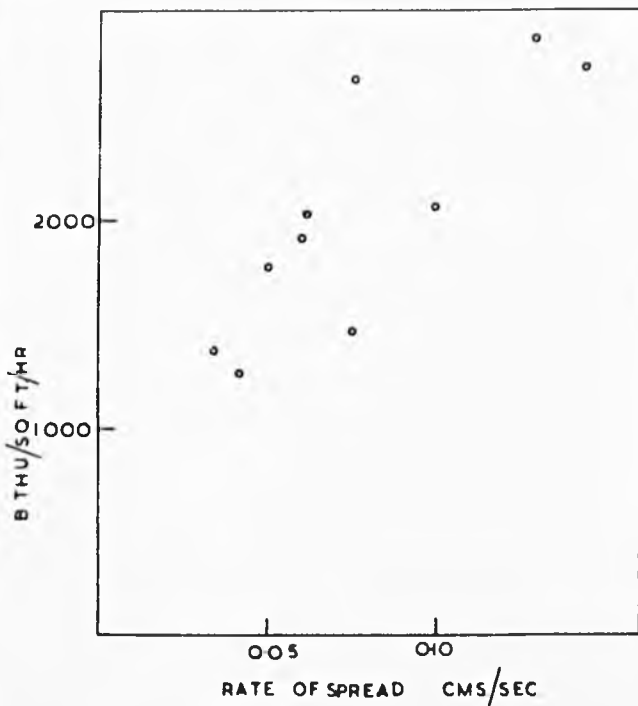


Figure 60.
The rates of spread at different radiation intensities.

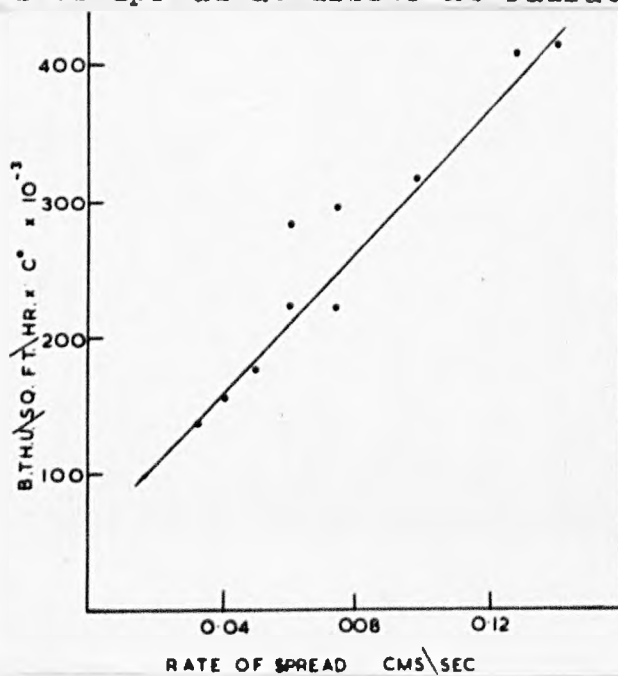


Figure 61.
The rates of spread as a function of radiation intensity x the initial surface temperature.

supported propagation between two surfaces separated by a distance of 12.3 cms. (the radius of the bolometer arm) under the conditions governing this experiment. These arguments can not be applied straight away to practical cases, because under such circumstances at least one piece of wood must be inclined to the horizontal in order to receive appreciable radiation, thus affecting both the rate of spread and the heat transfer. However, it would seem safe to say that two surfaces arranged at right angles to each other would spread flame further if each had an adjacent area already burning of about 200 sq. cms. and was preheated in the same way as the wood described above.

The Rates of Spread

The effect of radiation upon the rate of spread of flame has been discussed in Part I and in the introduction to Part II, where it was shown that flames travelled with a speed which was proportional to the supporting radiation intensity under certain conditions which tended to give a constant initial surface temperature of the material.

In the present experiments the surface temperatures at the moment of ignition were deliberately varied by altering both the pre-heating time and the intensity of the supporting radiation. Consequently, if the rate of spread of flame is plotted against radiation intensity, a large amount of scatter is evident in graph (Figure 60). If however, the radiation intensities are

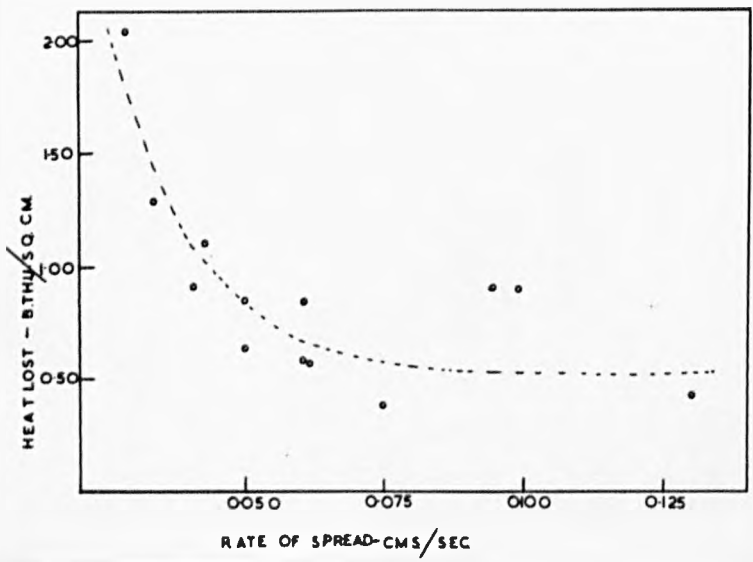


Figure 62. The heat evolved per unit area of surface during the burning time at different rates of spread.

multiplied by the surface temperature at the moment of ignition, a much better degree of correlation is obtained, as will be seen from Figure 62.

This result is important in that it indicates that the increased rate of spread is due to the increased temperature of the wood and hence the increased rate of distillation of volatiles. It is possible that the radiation affects the combustion of the volatiles in the flame, but very little is known about such effects.

The above results suggest that it may be possible to deduce an expression relating the rate of spread with the supporting radiation and the surface temperature of the material, and Figure 61 is utilised to attempt this later in the Theses.

The heat transfer during the burning time

It has been stated earlier in the Thesis that heat transferred at the wooden surface by any one of three mechanisms considered, cannot be attributed to any one source of heat, but rather the heat balance must be looked at as a whole. The dependence of each individual heat transfer on a large number of variables makes correlation of results very difficult. Moreover, because of the deviation of the shape of the burning area from a circle, it was not possible to stop the burning after a constant area of wood had been burnt. Thus although it is possible to derive the amount of heat emitted per square cm. of wood during the time of burning, Figure 62, these results obviously depend on the area of wood burnt. This effect follows from the saucer

shaped nature of the reaction zone, and hence the different edge effects of different areas. Thus the points in Figure 62 show a large amount of scatter, although there does seem a definite trend to increased depth of reaction at slower rates.

DISCUSSION

The large number of variables which govern the rate of spread of flame make it necessary to obtain results concerned with the alteration of one variable only. Because of the variability found amongst pieces cut from the same plank each experiment should be repeated with several samples to obtain satisfactory accuracy. This procedure was followed in the experiments described in Part I and in the introduction to Part II. Because however, of their complex and time-consuming nature, the later experiments could not be carried out in duplicate, and this, as has been pointed out, made their correlation difficult. However, if attention is confined to one experiment much light is thrown on the mechanism of propagation, and it is possible to give an approximate mathematical treatment which shows clearly the relationship between the supporting radiation zone and the rate of spread.

From the evidence supplied by the differential thermal analysis experiment, it would seem that the rate of distillation of the volatiles from the surface of the wood can be represented approximately by the equation

$$-\frac{dq}{dt} = Kwe^{-\frac{E}{R\theta}}$$

as used by Bamford and also that the activation energy assumed in this paper, is representative of the reaction under consideration. The above constants were taken as average values based on the assumption that the reactions taking place can be represented by

a single unimolecular reaction and have been adjusted to fit the experimental results found by Bamford. In these experiments 1" sheets of deal were heated on both sides by large luminous gas flames and the central temperature of the block measured. This temperature was also deduced from the heat transfer coefficient at the surface, (found in a subsidiary experiment) by using the finite difference method of solution of the equations quoted earlier.

The effect of the supporting radiation on the burning of the volatiles in the flame is neglected in the present treatment and the following assumptions made :-

- (1) That at a certain depth of wood reaction stops, and that after the passage of flame the reaction is complete to that depth.
- (2) That in the reacting zone of the wood the average rate of distillation corresponds to an average reaction temperature $\bar{\theta}$ with an average amount of unreacted wood \bar{w} .
- (3) That the average temperature of the material as determined by its total heat content approximates to $\bar{\theta}$.

Proceeding on the above, a strip of flame of unit length is considered to be moving at a constant rate over the surface of the wood at an average temperature $\bar{\theta}_0$ in the depth dx . If now the reaction is considered to be taking place in a length l , then the average rate of destruction of wood is

$$-\frac{dw}{dt} = k\bar{w} e^{\left(-\frac{E}{R\bar{\theta}}\right)} \quad \left(\text{where } w \text{ is the amount of wood which will react if the wood burns to completion without ignition of the char. ---10}\right)$$

Fresh wood has to be supplied at the same rate as it is being

destroyed and now it is supposed that of the initial quantity of wood a proportion z of the reaction zone will be destroyed. Thus the rate of destruction of volume is

$\frac{-dw}{dt} \times \frac{1}{z} \times \frac{1}{p}$ Where p is the density.
and hence the rate of linear destruction is

$$\frac{-dw}{dt} \times \frac{1}{zp} \times \frac{1}{dx} = \text{rate of spread} = v. \quad \text{----- 3}$$

If now, the total overall heat input into the wood is $q/\text{cal.}/\text{sq.cms}/\text{sec.}$ the rate of heat input into the burning zone is $q_1/\text{cal.}/\text{sec.}$

Now the rate of heat input must be such as to raise the quantity of wood that is being destroyed per unit of time to the average temperature $\bar{\theta}$ i.e.

$$\begin{aligned} Q_1 &= \frac{-dw}{dt} \frac{c}{z} (\bar{\theta} - \theta_o) && \text{where } \theta_o \text{ is the initial} \\ &= \frac{c}{z} \rho v z dx (\bar{\theta} - \theta_o) && \text{temperature of the wood} \\ &= cv \rho dx (\bar{\theta} - \theta_o) && \text{assumed constant.} \\ \therefore \bar{\theta} &= \frac{Q_1}{cv \rho dx} + \theta_o && \text{-----4} \end{aligned}$$

From (2), (3) and (4)

$$\text{and this leads to } vz \rho dx = \frac{k \bar{w}}{e} - \frac{E/R}{e} \left(\frac{Q_1}{cv dx} + \theta_o \right) \quad \text{-----5}$$

that is, under the above circumstances, the rate of spread would be

$$v = \frac{k \bar{w}}{z \rho dx} \exp - \left(\frac{E}{R \left(\frac{Q_1}{cv \rho dx} + \theta_o \right)} \right) \quad \text{-----6}$$

where the following are known approximately

$$\begin{array}{l}
 k = 5.3 \times 10^8 \quad) \\
 E = 33160 \quad) \\
 z = 0.375 \quad)
 \end{array}
 \begin{array}{l}
) \\
) \\
) \\
) \\
)
 \end{array}
 \begin{array}{l}
) \\
) \\
) \\
) \\
)
 \end{array}
 \begin{array}{l}
 = 0.66 \quad) \text{ from} \\
) \text{ previous} \\
 c = 0.35 \quad) \text{ work} \\
) \\
) \\
)
 \end{array}$$

$$\text{whence } v = 2.14 \times 10^9 \frac{\bar{w}}{dx} \exp\left(-\frac{16580}{\left(\frac{Q_1 + \theta_0}{0.231 \rho v dx}\right)}\right) \text{ -----7}$$

The equivalence of pre-heating time and supporting radiation under the above conditions is plain, both influencing the average reaction temperature. Indeed it was found possible by carefully heating a 6" block of birch on the top surface, so as to char it as little as possible, to raise it to such a temperature that flame would spread over the surface of the block, although such a flame is doomed to die out without a supporting source of heat. This point needs further consideration, for here it is necessary to make some distinction between supporting radiation and initial "surface temperature". In the above discussion no account was taken of the heat lost by the various possible mechanisms, an overall heat transfer into the wood being assumed. Now if the heat transfer cannot be sustained by the flame itself, the reaction must slow down and eventually cease. As wood will not burn in air without supporting heat, more energy must be lost from a burning surface than is transferred back by the flame alone, and thus the temperature of the surface layers will drop and slow down the reaction until the burning ceases. The function of the supporting heat is thus to maintain the surface temperature so that reaction will take place there at an

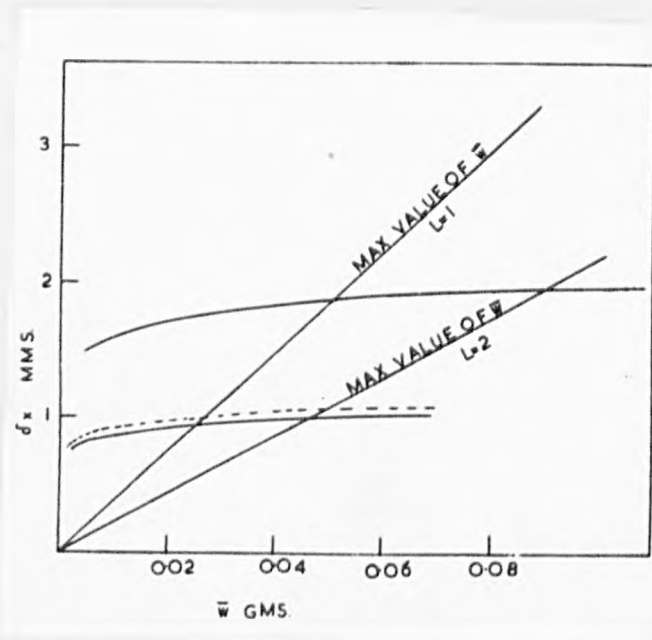


Figure 63.
The relationship between the average length of burning zone, depth of combustion and the average amount of reactant.

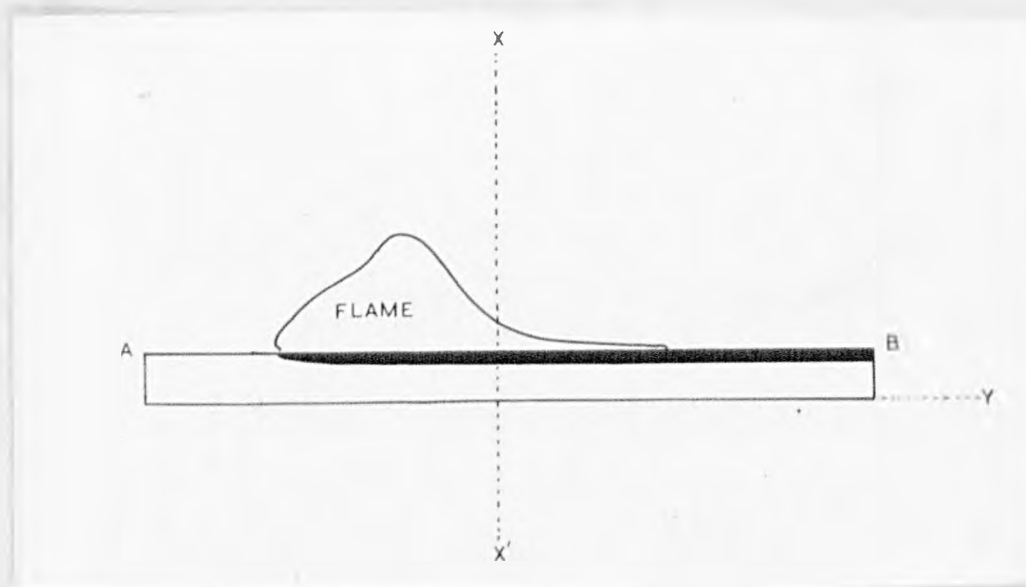


Figure 64.
Suggested further experiment.

appreciable rate when extra heat is liberated by the flame.

Although the relationship deduced above is primarily intended as a qualitative demonstration of the mechanism of the flame spread, it is possible by using the known constants to deduce feasible relationships for the unknowns. Besides the known constants listed above it was also found when considering the thermal gradients in the wood, that the rises in temperature could be approximately explained by assuming that heat was being transferred into the burning zone at a rate of 0.360 cal/sq.cm/sec and the surface losing heat at a rate which depended on its temperature. Under equilibrium conditions for flame spreading linearly at a steady rate, there will be some constant overall heat transfer into the burning zone, which will probably be about an average of the heat transfer at the hottest and coldest part of the burning surface. In the present calculations a figure of 0.27 cal./sq.cm./sec. was taken to be representative of the rate of spread of flame of 0.050 cm./sec. over a surface pre-heated to a temperature of 100° c. substitution of these values in equation 7 leading to:-

$$0.05 = 2.14 \times 10^9 \frac{\bar{w}}{dx} \exp - \frac{16580}{\left(\frac{23.41}{dx} + 373 \right)} \quad \text{----- } \theta$$

From this expression relationships for l , \bar{x} and dx can be deduced which are shown in Figure 63. The quantities \bar{w} , dx and l are inter-related as l and dx determine the volume for which \bar{w} is calculated. Now a maximum value for \bar{w} is that which represents

wholly unburnt material, this value being represented in Figure 63 for different values of l by the straight lines and is calculated from a figure quoted by Bamford.

A check on this calculation is afforded by the relationship between the rate of spread, initial surface temperature and supporting radiation, Figure 61. From this graph it will be seen that over the range of figures considered, the rate of variation of v with θ at a constant supporting radiation is

$$\left(\frac{dv}{d\theta} \right)_{\theta_0} = 7.3 \times 10^{-4}$$

But from equation 7

$$\left(\frac{dv}{d\theta} \right)_{\theta_0} = 2.14 \frac{\bar{w}}{dx} \frac{16580 e}{(23.41 + 373)^2} \frac{16580}{dx} - \frac{(23.41 + 373)}{dx} \text{ ----}$$

and from this relationship the variation between \bar{w} , dx , and l can again be calculated using separate experimental evidence. The relationship so deduced is also shown in Figure 63 as a dotted line.

The striking points about these curves include the critical effect of dx at any one value of l and the surprisingly good agreement in dx between the values calculated by 3 and 4. Thus a variation of about 10% in dx covers nearly the whole of the possible range in \bar{w} which obviously cannot be less than 0.

Conclusions and suggestions for further work

It is considered that the success of equation 6 in correlating some of the more important variables affecting the rate of flame spread, warrants a fuller and more rigid treatment of the problem based on similar assumptions.

For a flame spreading at a uniform rate over a surface these assumptions can be listed as follows:-

- (1) The rate of destruction of wood determines the rate of flame spread because the amount of wood consumed at any point after reaction has ceased must be constant in any plane parallel to the surface.
- (2) The total heat input into the reaction zone, taking into account the heat released in chemical change and any heat lost to the body of the wood, is responsible for maintaining the temperature at all points in the reaction zone, and so determines the rate of destruction of wood at any point.

In expressing the above assumptions in equation 6 however, it is necessary to make many approximations which can be avoided by a more rigorous approach and by using more suitable experimental results in calculating the constants involved. Because the rate of spread can only be considered when equilibrium has been reached, that is, when the flame is spreading at a constant rate, it is desirable to consider a

reasonably wide flame front spreading as a straight line, and it is also essential for the treatment to cover the entire reaction zone, both in depth and length. Thus the hypothesis demands that the practical results be obtained under circumstances which have previously been called linear spread. It is as well to note here that although the rate of circular spread appeared to be almost constant over the radius considered, it seems quite likely that a change in the rate of spread would take place as the radius of the circular flame front increased until, at an infinite radius, the rate of spread would be equal to the rate of linear spread. The model considered in the following treatment is represented in Figure 64. The direction of flame spread is from B to A and the reaction is supposed to have ceased at some point between C and B. The linear flame front extends in a direction perpendicular to the plane of the paper. It is intended to compute the heat transfer to the reaction zone together with the temperature and hence the rates of reaction in that zone.

The heat transfer at the surface of the wood can be deduced from the measured temperatures inside the wood. The temperatures parallel to the flame front are assumed to be constant and thus the two dimensional heat flow equations are applicable when combined with the term representing the heat released by chemical reactions in the wood i.e.

$$\frac{d\theta}{dt} = K \left(\frac{d_2\theta}{dx^2} + \frac{d_2\theta}{dy^2} \right) - q \frac{dw}{dt}$$

where $-\frac{dw}{dt} = k w e^{-\frac{E}{R\theta}}$ as previously

x is the coordinate perpendicular to the surface

y is the coordinate parallel to the surface

and $\frac{dw}{dt}$ is the rate of change in the weight of wood capable of reacting in the small element of volume considered.

As before, the above equation can be represented in dimensionless units by letting

$$T = \frac{K}{l^2 cp} t, \quad X = \frac{x}{l} \quad \text{and} \quad Y = \frac{y}{l}.$$

where l is some length greater than the length of the reaction zone.

$$\text{Hence } \frac{d\theta}{dT} = \frac{d^2\theta}{dX^2} + \frac{d^2\theta}{dY^2} - \frac{q}{cp} \frac{dw}{dT}$$

$$\text{also as before } \frac{d^2\theta}{dX^2} \approx \frac{\theta_{(m-1)1n} - 2\theta_{m1n} + \theta_{(m+1)1n}}{X^2}$$

$$\text{and } \frac{d^2\theta}{dY^2} = \frac{\theta_{m1n-1} - 2\theta_{m1n} + \theta_{m1n+1}}{Y^2}$$

and if $\delta X^2 = \delta Y^2$ replacing $\frac{d\theta}{dt}$ with a finite difference ratio

$$\theta'_{m1n} - \theta_{m1n} = \frac{\delta T^2}{2\delta X^2} \left[(\theta_{(m-1)1n} + \theta_{(m-1)1n}) + (\theta_{(m+1)1n} + \theta_{(m+1)1n}) + (\theta'_{m1(n-1)} + \theta_{m1(n-1)}) + (\theta_{m1(n+1)} + \theta_{m1(n+1)}) - 4(\theta'_{m1n} + \theta_{m1n}) \right]$$

Where m is the X coordinate and n the Y coordinate.

If in considering conditions at the boundary it is assumed that the heat transfer is such that it can be represented by extending the wood outside the boundary and assigning to it temperatures which would give the required heat transfer.

$$\text{then } H_{\theta} = \frac{K}{l} \frac{d\theta}{dx}$$

$$\text{or } H_{\theta} \theta_{o,ln} = \frac{K}{l} \frac{\theta_{1,n} - \theta_{o,-1,n}}{2\delta X}$$

$$\text{and } \theta'_{o,ln} - \theta_{o,ln} = \frac{\delta T^2}{2\delta X^2} \left[(\theta'_{o,(n-1)} + \theta_{o,(n-1)}) + (\theta'_{o,(n+1)} + \theta_{o,(n+1)}) \right. \\ \left. (\theta'_{1,n} + \theta_{1,n}) - 4(\theta'_{o,n} + \theta_{o,n}) \right. \\ \left. (\theta'_{1,n} + \theta_{1,n}) - H_{\theta} \frac{\theta_{o,-1,n} - \theta_{o,n}}{2} \frac{\delta X_1}{K} \right]$$

($\theta_{1,n}$, $\theta_{o,n}$ and $\theta'_{1,n}$) represent the temperatures at $Y = n$ and $X = -X_1$ and X respectively.

Given the necessary boundary conditions, the above equations can be used to calculate the resulting temperatures in the wood and also the amount of wood which had reacted at any one point at any time.

It is suggested that the following practical experiment should be performed. The flame should be allowed to spread over some suitable timber such as birch, of such a width and length as to satisfy the assumptions that temperatures are constant over the central portion of the flame front, in a

direction parallel to the flame, and that there is sufficient length to include the complete reaction zone. The flame travelling over this horizontal surface should be sustained by weak radiation so that the depth of reaction will not be too great and the length of reaction zone kept short, whilst the equilibrium temperature of the wood under this radiation should be attained before it is ignited. The back face of wood should be kept at a constant temperature by means of a water cooled metal block or some similar device and the temperatures along the longitudinal vertical central plane in the block measured by thermocouples. It will be appreciated that the temperatures through the depth of the block at one point in this plane, such as along the line $x x^1$ in Figure 64, will be representative of all the temperatures in the reaction zone if a complete record of their magnitude is kept throughout the experiment. It is also suggested that the thermocouples be inserted, if at all possible, parallel to the front surface of the wood.

From the complete record of the temperatures in the wood it would now be possible to deduce by trial and error, the heat transfer at the top surface which would give the surface temperatures, by solving the equations as has been demonstrated earlier in the Thesis.

Once obtained, a satisfactory solution would not only provide the heat transfer coefficient at all points over the surface, but also define the amount of any unreacted wood at

any moment at any point in the wood. From these figures the total heat transfer at the surface could be found, as well as the total overall rate of reaction. This overcomes the difficulties previously encountered in the assumption that the average temperature measured by the effect of the heat input into a certain amount of wood was the same as the average temperature as calculated by the average rate of reaction. Moreover, the figures obtained as above, would allow the observed rate of spread to be compared with the rate of spread calculated from the rate of destruction of wood.

In addition to the work suggested above, a further investigation of the reaction taking place when wood is distilled would be profitable and in particular, the differential thermal analysis technique carried out in an inert atmosphere would seem to be especially valuable. The main aim of the work would be to represent mathematically the dependence of the rate of reaction on temperature. Although further work into the nature of combustion in the luminous flame and into the method of diffusion of unburnt volatiles to the burning surface is fraught with difficulty, the two researches postulated above may lead to further practical methods of attack of the problem.

ACKNOWLEDGMENTS

The author is widely indebted to members of the Department of Fuel at Leeds and to other Organisations connected with the research, and in particular, the help and encouragement always available from Dr.J.E.Garside has continually sustained the investigation. Much help has also been received from Mr.S.H.Clarke, Director of the Fire Research Organisation of D.S.I.R., which Organisation has made the work described possible.

In conclusion I am deeply grateful to all members of the Combustion School at Leeds, who have helped in the preparation of the diagrams of the Thesis.

BIBLIOGRAPHY

1. Destruction Distillation of Maple Wood - D.F.Othmer and W.F.Schurig - Ind. and Eng.Chem. 33, 188, - 41
2. C.R.Palmer - Ind. and Eng.Chem. 10, 262 - 18
3. M. Midgely - Dept. of Botany, Leeds - Private Communication.
4. The Measurement of Thermal Conductivity - E.Griffiths and G.W.Kaye - Proc.Roy.Soc. A. 104. 71, - 23.
5. Method of Finding the Conductivity for Heat - C.Niven Proc.Roy.Soc. A - 76, 34, - 05.
6. Combustible Properties of Treated Wood by the Crib Test Method. - Amer.Soc.Test.Mat. E. 160 - 46
7. Combustible Properties of Treated Wood by the Fire Tube Method - Amer.Soc. Test. Mat. E. 69 - 46
8. K.Summersgill - B.Sc.Thesis. Leeds 1945.
9. Fire Extinguishing Effects of Chemicals in Water Solution - H.D.Tymer - Ind. and Eng.Chem. - 33, 60 - 41
10. The Combustion of Wood - C.H.Bamford, J.Crank and D.H.Malan - Proc. Camb. Phil. Soc. - 62, 166 - 46
11. Fire Fighting and Prevention - G.I.Finch - Journal of the Royal Society of Arts XCIV - 1946
12. Analysis of Fire Growth - G.I.Finch - Ministry of Home Security Bulletin - B.14.
13. Note on Specific Surface - Inc.Bomb Test Panel - 45
14. Radiant Heat Transmission Between Surfaces Separated by Non-absorbing Media - H.C.Hottel - Trans.Amer.Soc. Mech. Eng. - 53, 265 - 31
15. R.E.Eyres, D.R.Hartree and others - Phil.Trans. A. 240, 1 - 41
16. A High Gain D.C. Amplifier for Bioelectric Recording- Goldberg - Trans.Amer.Inst.Elec.Eng. 59, 60 - 40
17. Dunlap - U.S. Dept. Agric. Forest Serv. Bull. 110 - 12